

# **Optimization of retroviral packaging cells for scale-up of vector production**

Von der Naturwissenschaftlichen Fakultät der  
Gottfried Wilhelm Leibniz Universität Hannover

zur Erlangung des Grades  
Doktorin der Naturwissenschaften (Dr. rer. nat.)

genehmigte Dissertation

von

Yasemin van Heuvel, M. Sc. RWTH

2023

Referent: Prof. Dr. rer. nat. Thomas Scheper

Korreferent: Prof. Dr. phil. nat. Jörn Stitz

Korreferent: Prof. Dr. rer. nat. Sascha Beutel

Tag der Promotion: 13. September 2023

# I ABSTRACT

Retroviral vectors (RVVs) are the key players for somatic gene therapy. However, the large-scale production is very time- and cost-intensive due to the production in adherent cell lines and transient plasmid transfections. To facilitate large-scale RVV production, the bioprocess engineering procedures need to be optimized. In this thesis, ecotropic murine leukemia virus (MLV)-based viral packaging cells (VPCs) were generated and procedures for the rapid and stable production of viral vectors in suspension were developed and improved. For this purpose and as a proof-of-concept (POC), suspension human embryonic kidney cells growing in serum-free media, were employed. In addition, a hybrid technology based on the *Sleeping Beauty* (SB) vector system and MLV donor vector components was applied for an efficient and rapid cell transfection. After stringent selection, a stable polyclonal VPC was generated within only three weeks. The resulting cells were able to produce the ecotropic MLV-based vectors at high levels and for months. The viral functional titers measured in murine fibroblasts and murine myeloblasts exceeded previous published titers generated with adherent or suspension VPCs, reaching tenfold higher titers of up to  $1.4 \times 10^7$  transducing units per mL (TU/mL). Efficient gene transfer was also demonstrated in pre-clinically relevant murine hematopoietic stem and progenitor cells (HSPC). To further increase the production volume, as well as to advance the transposition technology, the transposase gene was *in vitro* synthesized to mRNA and co-transfected with the respective transposon-MLV vector components. Thus, no relevant genes for MLV vector production could be remobilized from the VPC genome any longer by a possibly genetically resident transposase, securing VPC stability. The stable suspension VPCs also proved to be highly efficient and viral titers were improved tenfold as compared to simple plasmid-based transfection or plasmid-based transposase transposition, exceeding  $5 \times 10^7$  TU/mL. Finally, the VPC was successfully cultivated in a stirred-tank bioreactor (STR) with a 500 mL culture volume, continuously producing functional vectors during a ten-day process. This technology will enable future generations of stable VPCs and clinically relevant viral vector productions in fully automated STRs.

**Keywords:** bioprocess technology, retroviral vector, transposon, bioreactor, gene therapy

## II KURZFASSUNG

Retrovirale Vektoren sind die Hauptakteure in der somatischen Gentherapie. Die Produktion in großem Maßstab ist jedoch aufgrund der Produktion in adhärennten Zelllinien und transienten Plasmid-Transfektionen sehr zeit- und kostenintensiv. Um die RVV-Produktion in großem Maßstab zu ermöglichen, müssen die bioprozesstechnischen Verfahren optimiert werden. In dieser Arbeit wurden ecotrope virale Verpackungszellen (VPZs) auf Basis des murinen Leukämievirus (MLV) generiert und Verfahren zur schnellen und stabilen Produktion von viralen Vektoren in Suspension entwickelt und verbessert. Zu diesem Zweck und als Proof-of-Concept (POC) wurden humane embryonale Nierenzellen in Suspension verwendet, die in serumfreien Medien wachsen. Zusätzlich wurde eine Hybridtechnologie auf der Basis der *Sleeping Beauty* (SB) Transposase und MLV Donorvektoren für eine effiziente und schnelle Zelltransfektion eingesetzt. Nach entsprechender Selektion wurde innerhalb von nur drei Wochen eine stabile polyklonale VPZ erzeugt. Die resultierenden Zellen waren in der Lage, die ecotropen MLV-basierten Vektoren in hohen Mengen und über Monate hinweg zu produzieren. Die viralen funktionalen Titer mit  $1,4 \times 10^7$  transduzierenden Einheiten pro mL (TU/mL), welche in murinen Fibroblasten und murinen Myeloblasten gemessen worden sind, übertrafen um ein Zehnfaches bisher veröffentlichte Titer von adhärennten und Suspensions-VPZs. Ein effizienter Gentransfer wurde zudem auch in präklinisch-relevanten hämatopoetischen Stamm- und Vorläuferzellen (HSVZ) der Maus nachgewiesen. Um das Produktionsvolumen weiter zu erhöhen und die Transpositionstechnologie zu optimieren, wurde das Transposase-Gen *in vitro* zu mRNA synthetisiert. So konnten im Genom der VPZ keine für die MLV-Vektorproduktion relevanten Gene durch eine möglicherweise genetisch residente Transposase mehr remobilisiert werden, was die Stabilität der VPZ sicherstellte. Die erzeugten stabilen Suspensions-VPZs erwiesen sich ebenfalls als hocheffizient, und die viralen Titer waren im Vergleich zur einfachen plasmid-basierten Transfektion oder plasmid-basierten Transposase-transposition um das Zehnfache verbessert und überstiegen  $5 \times 10^7$  TU/mL. Schließlich wurde die VPZ erfolgreich in einem Rührkessel-Bioreaktor (STR) mit einem Kulturvolumen von 500 mL kultiviert, wobei während eines zehn tägigen Prozesses funktionale Vektoren kontinuierlich produziert wurden. Diese Technologie wird künftige Generationen stabiler VPZs und klinisch relevanter viraler Vektoren in vollautomatisierten STRs ermöglichen.

**Schlagwörter:** Bioprozesstechnologie, Retroviraler Vektor, Transposon, Bioreaktor, Genetherapie

### III PUBLICATIONS INCLUDED IN THIS CUMULATIVE THESIS

1. **van Heuvel, Y.;** Berg, K.; Hirsch, T.; Winn, K.; Modlich, U.; Stitz, J. Establishment of a novel stable human suspension packaging cell line producing ecotropic retroviral MLV(PVC-211) vectors efficiently transducing murine hematopoietic stem and progenitor cells. *J. Virol. Methods* **2021**, 297, 114243, doi:10.1016/j.jviromet.2021.114243.
2. **van Heuvel, Y.;** Schatz, S.; Hein, M.; Dogra, T.; Kazenmaier, D.; Tschorn, N.; Genzel, Y.; Stitz, J. Novel Suspension Retroviral Packaging Cells Generated by Transposition Using Transposase Encoding mRNA Advance Vector Yields and Enable Production in Bioreactors. *Front Bioeng Biotechnol* **2023**, 11, doi:10.3389/fbioe.2023.1076524.
3. **van Heuvel, Y.;** Schatz, S.; Rosengarten, J.F.; Stitz, J. Infectious RNA: Human Immunodeficiency Virus (HIV) Biology, Therapeutic Intervention, and the Quest for a Vaccine. *Toxins (Basel)*. **2022**, 14, doi:10.3390/toxins14020138.

## IV ACKNOWLEDGMENT

First, I would like to thank my supervisor Prof. Dr. Jörn Stitz for giving me the opportunity to start and finalize my PhD projects in his laboratory at the technical university of applied sciences cologne. His great knowledge and support throughout the whole PhD process helped me building up my scientific skills within the fields of virology, biotechnology, laboratory management and the supervision of students.

I would especially like to thank Prof. Dr. Thomas Scheper for being my supervisor and for taking the time and consideration to evaluate my thesis. Great thanks also to Prof. Dr. Sascha Beutel for declaring his additional readiness to be my second expert.

A big thank you to my dear colleagues, Stefanie, Natalie, Jamila, Karen, Henrik, Nils, Stefan, Anna, Danka and Janine and Pauli for making the past years a very special, nerdy and fun time that I will never forget!

Without the support and love of my family and friends, nothing would have worked out so smoothly! Thank you, Mum, Miguel, Selçuk, Kemal, Thúy, Rémi, Hartmut, Ines, Tanja, Anastasiia, Jhonatan, Polina and Ayse for always believing in me without any doubt. All that I have achieved is because of you!

Special thanks to my best friends for keeping up my strength, walking all the way with me as well as always supporting me in every second of my life. Thank you, Janina, and Max, you are super special to me, I love you!

Clemens, thank you so much for always believing in me, being there in good and bad times, always supporting me and sharing my passion! I love you!

A big thank you to all other friends and people whose names I have not written down, who have supported me in all matters, who paved the way to get where I am now and who gave me strength just by being part of my life.

# CONTENTS

I	Abstract .....	III
II	Kurzfassung.....	IV
III	Publications Included in this Cumulative Thesis.....	V
IV	Acknowledgment.....	VI
V	List of Figures .....	X
VI	List of Tables.....	XI
VII	Abbreviations .....	XII
1	Theoretical background .....	1
1.1	Retroviral vectors in gene therapy.....	1
1.1.1	Clinical applications.....	3
1.2	Principles of retroviral vector technology.....	5
1.2.1	Retroviral vectors (RVVs) .....	7
1.2.2	Retroviral packaging cells.....	10
1.3	Transposon-viral vectors.....	11
2	Aim of the Study .....	14
3	Publication I.....	15
3.1	Introduction.....	17
3.2	Materials and methods .....	18
3.2.1	Cells and plasmids .....	18
3.2.2	Establishment of stable VPCs and recombinant target cells .....	20
3.2.3	Viral vector titration.....	20
3.2.4	Detection of replication-competent retroviruses (RCRs) and recombination of the transfer vector with the gag gene of the packaging construct .....	21
3.2.5	Detection of the transposase gene in VPC-MSCV-EGFP packaging cells.....	22
3.2.6	Murine HSPC isolation and culture.....	23
3.2.7	Transduction of HSPCs .....	23
3.3	Results.....	24
3.3.1	Establishment of the packaging cell line VPC-MSCV-EGFP and vector titration	24
3.3.2	Detection of the transposase gene in VPC-MSCV-EGFP cells.....	28
3.3.3	Preparation of frozen high-titer MLV(PVC-211) vector stocks.....	29
3.3.4	Transduction of murine bone marrow-derived hematopoietic stem cells.....	30
3.4	Discussion.....	31
3.5	Conclusions .....	34

3.6	References.....	36
4	Publication II.....	40
4.1	Introduction.....	42
4.2	Materials and methods .....	43
4.2.1	Cells.....	43
4.2.2	Plasmids.....	44
4.2.3	Establishment of stable ecotropic MLV-based vector packaging cells MuPACK.e 44	
4.2.4	MLV vector productions in shake flasks and STR.....	45
4.2.5	Viral vector titration and flow cytometry .....	46
4.2.6	Quantification of retroviral vectors using an anti MLV p30 immunoassay .....	47
4.2.7	Quantification of transfer vector transcripts in vector particles using RT-qPCR.....	47
4.2.8	Detection of replication-competent retroviruses (RCRs): GFP marker rescue assay and reverse transcriptase (RT) assay.....	48
4.2.9	Statistics .....	49
4.3	Results .....	49
4.3.1	Generation of stable MuPACK.e based VPCs.....	49
4.3.2	Functional titers of generated MLV-based vectors.....	51
4.3.3	Physical titer assessment using p30 capsid-specific ELISA.....	52
4.3.4	Detection of transfer vector transcripts in vector particles using RT-qPCR .....	53
4.3.5	Production and functional titer of MLV vectors in STR .....	54
4.3.6	Discussion.....	56
4.3.7	References.....	61
5	Publication III .....	66
5.1	Introduction.....	68
5.2	HIV-1 Structure and Replication Cycle .....	69
5.2.1	Genome and Virion Structure .....	69
5.2.2	Receptors and Cell Entry.....	72
5.2.3	Nuclear Entry, Reverse Transcription and Uncoating.....	74
5.2.4	Genome Integration .....	75
5.2.5	Transcription, Splicing and Protein Expression.....	75
5.2.6	Assembly, Budding and Virion Maturation.....	78
5.2.7	Cytotoxicity of HIV Infection.....	80
5.3	Antiretroviral Therapy (ART).....	84
5.4	Vaccines .....	87
5.4.1	Interplay of HIV and Immune Response—Implications for Vaccine Development.....	87



5.4.2 HIV Clinical Vaccine Trials.....	89
5.5 Outlook .....	92
5.6 References.....	94
6 Summary & Outlook .....	113
7 References .....	117
8 Conferences & poster .....	126
9 Curriculum Vitae .....	127
10 List of publications.....	128

## V LIST OF FIGURES

Figure 1: An excerpt of the Retroviridae Phylogeny based on full-length polymerase protein.....	2
Figure 2: Illustration of a mature retrovirus and the retroviral genome with the engineered three plasmid components for the production of replication incompetent retroviral vectors. ....	7
Figure 3: Illustration of the DNA transposition process.....	12
Figure 4: Schematic illustration of the constructs used in this study and experimental design of cell line establishment and retroviral vector- mediated gene transfer.....	25
Figure 5: Detection of gag gene sequences in genomic DNA of transduced COS-7mCAT target cells.....	28
Figure 6: Detection of the transposase gene in genomic DNA of VPC-MSCV-EGFP cells. ....	29
Figure 7: Genetic organization of expression cassettes.....	50
Figure 8: Titers of MLV-based vectors in NIH/3T3 target cells of VPC MuPACK.e.SB-LEGFP-N1mRNA. ....	52
Figure 9: Median fluorescent intensities (MFI) of the three VPCs. ....	53
Figure 10: Physical titers of transfer vector transcripts in vector particles measured by real-time RT-qPCR. ....	54
Figure 11: Stirred-tank bioreactor vector particle production over 10 days with VPC MuPACK.e.SB-LEGFP-N1mRNA.....	55
Figure 12: HIV-1 genome and virion structure.....	71
Figure 13: Schematic overview of the HIV-1 replication cycle.....	73
Figure 14: HIV-1 mRNA transcripts and splice sites. ....	77
Figure 15: The cis-acting RNA regulatory elements of HIV-1.....	81
Figure 16: HIV Tat bystander toxicity. ....	82

## VI LIST OF TABLES

Table 1: Summary of viral pseudotypes, their host cell receptors and host range.....	9
Table 2: Transduction-competent vector particles harvested from the packaging cell VPC- MSCV-EGFP. ....	27
Table 3: Transduction efficiencies in target murine lineage-negative hematopoietic stem and progenitor cells (HSPCs) using ecotropic MLV(PVC-211) pseudotype particles produced by VPC-MSCV-EGFP.....	30
Table 4: Operating bioreactor production parameters. ....	46
Table 5: Overview of plasmids and mRNA employed to generate polyclonal viral packaging cell lines. ....	50
Table 6: Functional titers in TU/mL and physical titers in ng/mL (ELISA) of vector particles harvested from the stable VPCs. ....	51
Table 7: Selected examples of cellular HIV restriction factors, mechanism of action, and viral counter measures.....	72
Table 8: Overview of FDA-approved antiretroviral medicines including their mechanism of action, generic names, and approval year. ....	85
Table 9: Overview of HIV vaccine phase III clinical trials in the past 10 years with more than 100 participants.....	92

## VII ABBREVIATIONS

AAV	Adeno Associated Virus	CoV DAPI	Corona Virus 4',6- Diamidino-2- phenylindol
AIDS	Acquired Immunodeficiency Syndrome	DENV DNA	Dengue Virus Deoxyribonucleic Acid
Ad	Adenovirus	EBOV	Ebola Virus
AdV	Adenoviral Vector	EGFP	Enhanced Green
ADA	Adenosine Deaminase deficiency	FBS	Fluorescence Protein Fetal Bovine
ART	Anti Retroviral Therapy	FCS	Serum Fetal Calf Serum
BM	Bone Marrow	FrMLV	Friend Murine Leukemia Virus
bnAb	Broadly neutralizing Antibody		
CAR	Chimeric Antigen Receptor	GaLV	Gibbon ape Leukemia Virus
CCND2	G1/S-specific cyclin-D2	HAART	Highly Active Anti Retroviral Therapy
CHO	Chinese Hamster Ovary	HIV	Human Immunodeficiency Virus
cHS4	Chicken hypersensitive site four insulator	HSC	Hematopoietic Stem Cell
CMV	Cytomegalovirus	HSPC	Hematopoietic Stem and

	Progenitor Cell	MLV	Murine Leukemia Virus
hygroR	Hygromycin Resistance	MOI	Multiplicity of Infection
ICTV	International Committee on Taxonomy of Viruses	MoMLV	Moloney Murine Leukemia Virus
In	Intron		
IRES	Internal Ribosomal Entry Site	MSCV	Murine Stem Cell Virus
LMO2	LIM domain Only 2	MWCO	Molecular Weight Cut-Off
Lin-	Lineage negative	neoR	Neomycin Resistance
LTR	Long Terminal Repeats	NF-κB	Nuclear Factor-κB
LV	Lentivirus	ORF	Open Reading Frame
LVV	Lentiviral Vector	PCR	Polymerase Chain Reaction
mCAT	Murine Cationic Amino acid Transporter	PEI	Polyethylenimine
mAb	Monoclonal Antibody	puroR	Puromycin Resistance
MACS	Magnetic Cell Separation	PV	Poliovirus
MCS	Multiple Cloning Site	PVDF	Polyvinylidene difluoride
MERS	Middle east respiratory syndrome	RCR	Replication Competent Retrovirus
MeV	Measles Virus	RPM	Rotation Per Minute
		RV	Retrovirus

RVV	Retroviral Vector	VSV-G	Vesicular stomatitis virus
SARS	Severe acute respiratory syndrome		glycoprotein
SIN	Self- Inactivating	WAS	Wiskott- Aldrich- Syndrome
STR	Stirred-Tank- Bioreactor	WPRE	Woodchuck Posttranscript ional
TE	Transposable Element		Regulatory Element
TIL	Tumor Infiltrating Lymphocytes	X-SCID	X-linked severe combined immunodefic iency
TIR	Terminal Inverted Repeats		
VCD	Viable Cell Density	YFV	Yellow Fever Virus
VPC	Viral Packaging Cell	ZIKV	Zika Virus

# 1 THEORETICAL BACKGROUND

## 1.1 RETROVIRAL VECTORS IN GENE THERAPY

Worldwide, more than 7000 rare human genetic diseases are affecting about 300 million people. Therapeutic treatments with commercially available drugs are not curative and do only treat the symptoms. Somatic gene therapies targeting those mutations harbor great potential for long-term curation [1]. Gene therapy is defined as the treatment or cure of a genetic, infectious, or degenerative disease by the introduction of a therapeutic gene into a living organism. The therapeutic gene can be delivered *in vivo* or *ex vivo*. For the latter, stem cells or other cells (e.g., lymphoblasts) are taken from the patient or donor and cultivated *in vitro*. Cells are then genetically modified and re-infused into the patient (reviewed in [2]). There are four different approaches in gene therapy: gene replacement, -silencing, -addition and gene editing [3]. To achieve this, a gene-carrying viral or non-viral vector is employed. Non-viral vectors include for example plain or formulated DNA or RNA delivery into the nuclei of the target cells by electroporation, needle injection, gene gun, sonoporation or other techniques. The transgene can then be integrated into the genome by the help of engineered targeting nucleases, e.g., Cas, transcription activator-like effector nucleases (TALEN), zinc-finger nucleases (ZFN) or meganucleases (MN) (reviewed in [1]). The gene transfer efficiency to stably deliver transgenes into the target cells, however, is very low [4].

The most promising vector to deliver heterologous genes at very high efficiencies into target cells are viral vectors. These viral vectors mainly derive from adenoviruses (Ads), adeno-associated viruses (AAVs) or retroviruses (RVs). Depending on the application, viral vectors are characterized by different immunogenic characteristics, packaging capacities as well as cellular integration patterns. Adenoviral vectors are mainly used for short-term transgene expressions (weeks to months) and can induce, as AAV-vectors, the innate and adaptive immune system of the host *in vivo*. The frequency of stable chromosomal integration events of adenoviral- and AAV-vectors is very low with less than 0.1 % of vector-transduced target cells [5–7]. Retroviral vectors (RVVs), however, are used for long-term transgene expressions and do not elicit strong immune responses of the host. Nevertheless, most viral vectors are commonly applied *ex vivo* [8–10]. Key players for long-term gene expression within the last four decades are the  $\gamma$ -RVVs. In the early 1980s the first successful stable gene transfers were achieved in a broad range of mammalian cells [11–14]. Replication-incompetent or helper-free RVVs have been extensively used as gene delivery vehicles

in human gene therapy. They offer many advantages for the delivery of therapeutic genes, as they offer the ability for stable long-term gene expression, individual cell, and tissue tropism as well as large transgenic insert capacities ( $\geq 8$  kb) with controllable copy numbers within the target cell genome [15–17]. According to the International Committee on Taxonomy of Viruses (ICTV), the *retroviridae* family is divided into seven genera: the alpha-, beta-, gamma-, delta-, epsilon retrovirus, spumavirus and the more complex lentivirus, as illustrated in **figure 1** [18].

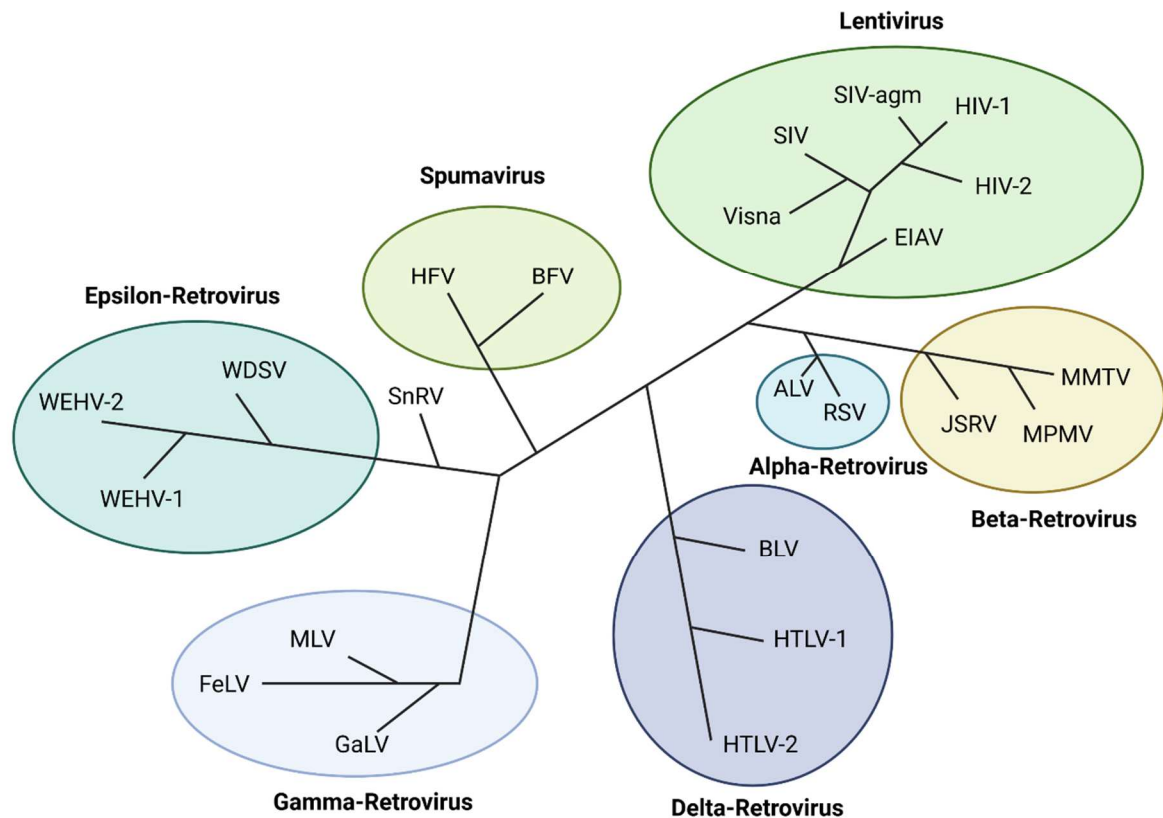


FIGURE 1: An excerpt of the *Retroviridae* phylogeny based on full-length polymerase protein. The phylogeny is divided into seven main genera, the Spuma-, Alpha-, Beta-, Gamma- Delta-, Epsilon-Retrovirus and Lentivirus. Not all species are represented. **Alpha:** Avian leukosis virus (ALV), Rous sarcoma virus (RSV); **Beta:** Jaagsiekte sheep retrovirus (JSRV), Mouse mammary tumor virus (MMTV), Mason-Pfizer monkey virus (MPMV); **Gamma:** murine leukemia virus (MLV), Feline leukemia virus (FeLV), Gibbon ape leukemia virus (GaLV); **Delta:** Bovine leukemia virus (BLV), Human B lymphotropic virus type 1 and type 2 (HTLV-1, HTLV-2); **Epsilon:** Walleye dermal sarcoma virus (WDSV), Walleye epidermal hyperplasia virus type 1 and type 2 (WEHV-1 and -2), **Intermediate Epsilon-like:** Snakehead retrovirus (SnRV); **Spumavirus:** Bovine foamy virus (BFV), Human foamy virus (HFV); **Lentivirus:** Maedi-visna virus (Visna/Maedi/MVV), Equine infectious anemia virus (EIAV), Simian immunodeficiency virus-/isolate from African green monkey (SIV-/agm), Human immunodeficiency virus type 1 and type 2 (HIV-1 and -2). Adapted from [19]. Illustration was created with Biorender.com.



The two most important genera of RVVs in clinical gene therapy today are the  $\gamma$ -RVVs stemming from the murine leukemia virus (MLV) and the lentiviral vectors, (LVVs) stemming from the human immunodeficiency virus type 1 (HIV-1). The main difference is that the  $\gamma$ -RVVs only allow stable gene transfer into proliferating cells. LVVs however, mediate stable gene transfer into proliferating and non-proliferating cells [20].

### 1.1.1 CLINICAL APPLICATIONS

The first human gene therapy proof-of-concept trial took place on May 22, 1989 [21]. Gene-marked immune cells, specifically tumor-infiltrating lymphocytes (TILs), were injected into advanced cancer patients. In this case, the marker gene was the *neomycin resistance* gene (*neoR*) that was stably introduced into the TILs utilizing an MLV-derived retroviral vector *ex vivo*. The marked TILs were used as genetic markers within continuous blood samplings. Gene-marked TILs were detected within the blood as well as within tumor biopsies up to day 189 post-transfusion. The outcome was thus positive, it was safe to transfer a traceable transgene into a patient with no side effects or toxicity [22]. The way for human gene therapy was paved. In the 1990s, the first clinical trial for the treatment of two children with adenosine deaminase-deficient (ADA) severe combined immunodeficiency (SCID) was conducted. Culture-expanded autologous T cells were extracted by leukaphoresis from the patients, and were *ex vivo* transduced with MLV-derived retroviral vectors transferring a functional human *ADA*- and *neoR* gene. Cells were shortly expanded and re-infused into the patient. The patients showed remission and a significant increase in recombinant T cell numbers reaching nearly 25 %. This T cell amount was stable for up to 6.5 months without repetitive treatments. The trial ended after two years, but *ADA* gene expression persisted [22,23]. Gene therapy proved to be safe and efficient for this kind of monogenetic immunodeficiency disorder.

The risk of serious adverse events was rather low, however in 2002, the first insertional mutagenesis events in mice and 2003 in humans were communicated [24,25]. The research group of Hacein-Bey-Abina et al., (2003) reported serious adverse events (SAEs) that happened in a gene therapeutic clinical trial utilizing retroviral vectors for the treatment of X-linked severe combined immunodeficiency syndrome (X-SCID, SCID-X1 or also called gamma-chain deficiency ( $\gamma$ c-deficiency)). A total of twenty patients were treated with genetically modified autologous bone marrow-derived hematopoietic stem cells (HSCs). These cells were *ex vivo* transduced with MLV-derived retroviral vectors transferring a functional  $\gamma$ c-cytokine receptor chain. Two to six years post treatment, five patients showed an uncontrolled clonal proliferation of

mature T cells with characteristics of leukemia. No overexpression of the  $\gamma$ c-chain was observed within the T cells and no replication competent retroviruses (RCRs), or retrotransposons were identified as possible causes. Thorough analysis of the cause revealed an insertional mutagenesis in chromosome 11 close to the LIM domain only 2 (LMO2) promoter locus. LMO2 is necessary for normal hematopoiesis [25]. Additional insertional mutations were identified: integrations near two proto-oncogenes BMI1 a polycomb-group oncogene and cyclin D2 (CCND2), as well as deletions within a tumor suppressor gene finally lead to aberrant T cell proliferations. The patients with T cell immune lymphocytic leukemia (T-ALL) underwent chemotherapy and four of the five patients, as all other 15 patients without SAEs, were cured from SCID-X1 thereafter, showing a normal hematopoiesis and full immune reconstitution [26–28].

These findings initiated intensive research aiming at the development of safer viral vector components. Vector-mediated genotoxicity is defined by two distinct characteristics: (1) The design of the integrating transfer vector and (2) the chromosomal integration sites of the transfer vector. In the first case, the so-called self-inactivating (SIN) long terminal repeats (LTRs) of RVVs and LVVs were introduced to reduce the risk of insertional mutagenesis. Here, the enhancer element of the U3 region within the 3'LTR is removed preventing the 3'LTR downstream transcription and thus the risk of proto-oncogene activation [29,30]. A follow-up clinical study of the group of Hacein-Bey-Abina et al., (2014) assessed the safety and efficacy of an MLV-derived SIN-vector in nine X-SCID patients. All patients were cured from SCID-X1 after SIN-MLV treatment and remained healthy thereafter. Less clustering of insertion sites in proximity of proto-oncogenes as LMO2 was observed [31,32].

Due to the side effects observed, the more complex LVVs were more intensively used in gene therapy. LVVs also prefer transcriptionally active sites for transfer vector integration, however, they do not preferentially integrate close to promoter and enhancer elements. LVVs utilized today were instrumental in many successful clinical trials to cure or improve monogenic or infectious diseases [2]. Nonetheless, even SIN-vector-based LVVs led to activations of neighboring genes, to the formation of chimeric gene fusions as well as to aberrant splicing events in host cell gene transcripts [33–35]. Some studies evaluated the risk of insertional mutagenesis and assumed that the enhancer and promoter elements of the transfer vector driving the transgene expression play a major role [36–38]. Novel transfer vector design strategies, apart from SIN vectors, such as tetracycline genetic switches, recombinase-mediated gene transfer, insulator elements, tissue-specific weak promoter and enhancers and

integrase retargeting strategies are urgently needed to further improve future clinical trials (reviewed in [2,9,38,39]).

Today more than 3600 gene therapy clinical trials were already conducted, and 33 gene therapeutic drugs are already clinically approved [1,40]. Most trials relate to cancer gene therapy with 68.2 %, followed by monogenic diseases with 12.6 %, infectious diseases and cardiovascular diseases with 5.2 %, each. Neurological diseases account for 1.7 %, ocular diseases for 1.5 % and inflammatory diseases for 0.4 %. The remaining trials address gene markings as well as healthy volunteers [40]. Until 2022, a total of 538 gene therapy clinical trials were performed alone with  $\gamma$ -RVVs (14.6 % of clinical trials worldwide) and 364 trials with LVVs (9.9 % of clinical trials worldwide) [40]. Most clinical trials conducted with RVVs aim at the treatment of monogenic diseases such as ADA-SCID; [23,41,42]; SCID-X1 [28,31,32,43] or Wiskott-Aldrich syndrome (WAS; [44–47]). Retroviral-based therapeutics that are already on the market are Rexin-G® (treatment of metastatic pancreatic cancer [48]), Strimvelis® (treatment of ADA-SCID [49]), Yescarta®, Kymriah® and Tecartus™ also known as *ex-vivo* chimeric antigen receptor (CAR) T cell therapy (treatment of non-Hodgkin lymphoma and B cell ALL, B cell lymphoma and follicular lymphoma [50]) and Zynteglo® (treatment of beta thalassemia [51]). Novel viral vector technologies and production at large-scale are currently being tested in pre-clinical and clinical studies and give hope for the development of future curative therapeutics (reviewed in [52]).

## 1.2 PRINCIPLES OF RETROVIRAL VECTOR TECHNOLOGY

The mature RV particle is spherical, membrane-enveloped and has a diameter of 90-140 nm containing two copies of single stranded, positive sense genomic RNA (ssRNA+) of about 8.3 kb with a 5'cap and a 3'poly adenine tail (poly (A) tail). The simple ssRNA+ contains three main open reading frames (ORFs) encoding for the viral structural, catalytic and envelope proteins Gag, Pol and Env necessary for viral assembly and replication, illustrated in **figure 2** [53]. For MLV, these ORFs are sufficient for viral replication and pathogenesis. For the more complex LVs however, additional ORFs and genes are needed for their pathophysiology, described in detail in chapter 5.2. [39]. The envelope glycoproteins Env consist of a heterodimer complex build out of a surface- (SU) and a transmembrane- (TM) unit. Those heterodimers form trimeric complexes spiking the viral outer membrane. The N-terminal SU contains the receptor-binding function and interacts with the host cell receptor, TM then mediates fusion and cell entry. Inside the cell, the ssRNA+ is reverse transcribed by the multifunctional viral reverse transcriptase (RT) into double stranded DNA (dsDNA)

with the help of a DNA polymerase activity as well as a ribonuclease H activity. Thereby the promoter located at the 3' end of the RNA is juxtaposed upstream of the coding sequence. Linear DNA is then chromosomally integrated during mitosis, with the help of the viral integrase and host cell proteins, into the host cell genome. At that point the integrated viral genomic DNA is called the provirus. Only one promoter within the viral long terminal repeats (LTR) drives transcription of the provirus. The LTRs have a size of approximately 600 nucleotides (nt) and are divided into three distinct parts, the U3, the R and the U5 element. The U3 region in the 5'LTR mainly acts as an RNA Pol II promoter and the 3'LTR, at which the p(A) is added, as the terminator of transcription. Partial splicing of the simple retroviral mRNA generates two RNAs. (1) The full-length mRNA translates to a Gag protein and a Gag-Pro-Pol fusion protein precursor by a mechanism called "readthrough suppression". Gag initiates the particle formation, assembling 10-20 Gag molecules with one Gag-Pro-Pol precursor at the inner host cell membrane. (2) The spliced mRNA is translated to Env which is cleaved by host cell proteases into the heterodimers SU and TM. For immature particle formation, Gag, Gag-Pro-Pol, Env and the viral genomic full length RNA are assembled at the inner host cell membrane, budding into the extracellular compartment. The retroviral particle then converts into a mature and infectious particle by the help of the viral protease cleaving the Gag and Gag-Pro-Pol precursor into the reverse transcriptase (RT), the integrase (IN), the protease (PR), the matrix (MA), capsid (CA) and nucleocapsid (NC) proteins. The MA is associated with the lipid envelope building the outer protein shell, the CA forms an inner protein shell harboring the viral genomic RNA and the Gag-Pro-Pol viral enzymes and the NC finally forms a complex with the genomic viral RNA. The viral particle now is finally processed and able to infect bystander cells [20,53–55].

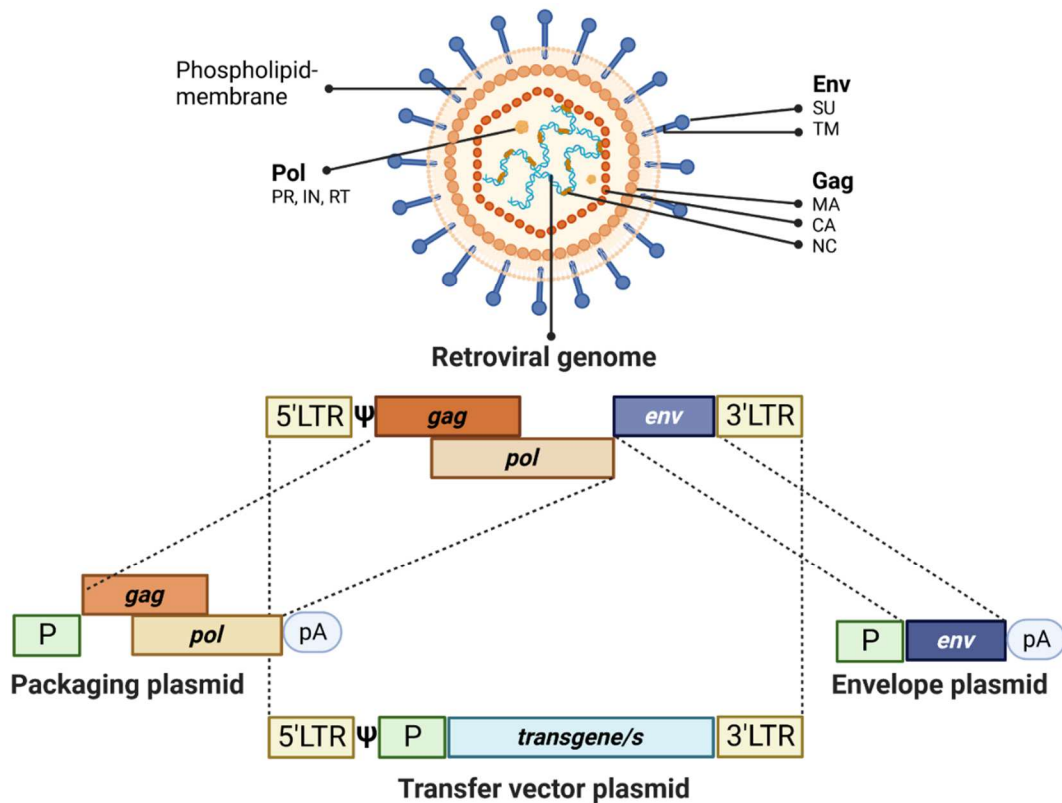


FIGURE 2: Illustration of a mature retroviral particle and the retroviral genome with the engineered three plasmid components for the production of replication incompetent retroviral vectors. The spherical retrovirus is enveloped by a phospholipid bilayer stemming from the host cell. The membrane is spiked with the envelope glycoproteins Env. Env consists of two subunits the surface- (SU) and transmembrane unit (TU). Below the membrane, the structural and catalytic proteins Gag and Pol are located. Mature Gag is divided into the three proteins, matrix (MA), capsid (CA) and nucleocapsid (NC). Pol stands for the catalytic proteins: protease (PR), integrase (IN) and the reverse transcriptase (RT). Inside the CA, two copies of single stranded, positive sense RNAs are located, that are stabilized by the NC. The retroviral genome consists of 5'- and 3'- long terminal repeats (LTRs) flanking the retroviral genes *gag*, *pol* and *env*. The 5'LTR mainly acts as an RNA Pol II Promoter and the 3'LTR as the terminator of transcription. A *cis*-acting packaging signal psi ( $\Psi$ ) is located downstream of the 5'LTR. The three plasmid components for viral vector production contain the same represented genes and genetic elements split on three plasmids containing heterologous promoters (P) and a heterologous polyadenylation signal (pA)). The transfer vector uses next to the viral LTRs and  $\Psi$  an additional P as well as individual cDNA transgene sequence(s). Created with BioRender.com.

### 1.2.1 RETROVIRAL VECTORS (RVVs)

From the early 1980's, until today, three generations of retroviral vector systems have been developed to massively reduce the risk of undesired RCR generation. In the first generation, the packaging signal of the provirus was simply deleted, however RCRs were detected within the infected target cells [11,56]. In the second generation, a p(A) of the simian virus 40 (SV40) instead of the 3'LTR was implemented, the packaging signal was removed and the 5' end of the 5'LTR, containing the tRNA primer binding site essential for reverse transcription, was deleted to prevent further reverse

transcription, integration and packaging of the transcribed RNA [57]. Within the third generation, the full-length provirus was split into three plasmids separating the coding regions Gag, Pol and Env and the *cis-acting* elements from each other. The packaging construct with *gag-pol*, the envelope construct with the *env* gene and the transfer vector [58]. All plasmids were equipped with heterologous promoters and the packaging and envelope plasmid received a heterologous p(A), as depicted in **figure 2**. The split genome finally offered the highest biosafety standard, eliminating RCR formations caused by homologous recombination events (reviewed in [59,60]).

For the generation of replication-defective retroviral vectors today, the split genome approach is exclusively used. The packaging plasmid, encodes the viral Gag and Pol proteins. The second plasmid encodes the viral Env protein, called the envelope plasmid. The *gag*, *pol* and *env* genes are driven by heterologous promoters (P), e.g., of the cytomegalovirus (CMV), the Rous sarcoma virus (RSV) or of the human elongation factor 1 alpha (EF1 $\alpha$ ) and terminate with a heterologous p(A) mostly deriving from the bovine growth hormone (BGH). The third plasmid encompassing the transfer vector, harbors the viral identical LTRs flanking one or several genes of interest (GOI). The 5'LTR is followed by a *cis-acting* packaging signal *psi* ( $\Psi$ ), initiating the encapsidation of the transfer vector transcripts. Next to the LTRs and  $\Psi$ , the transfer vector utilizes an additional heterologous promoter as well as individual cDNA transgene sequences (e.g., the therapeutic gene or a reporter gene) [20,55,59,61]. Usually, to co-express two GOIs with the same transfer vector, a *cis acting* RNA sequence, called the internal ribosomal entry site (IRES) is utilized and implemented between two genes. The IRES promotes an internal initiation of protein synthesis by a cap independent recruitment of a 40S ribosomal subunit [62]. Another *cis-acting* element, the posttranscriptional regulatory element of the woodchuck hepatitis virus (WPRE), is commonly implemented upstream of the 3'LTR leading to an enhanced transgene expression and inhibiting readthrough transcription [63].

The retroviral envelope protein defines due to its specificity the viral host range and can be substituted by envelope proteins of other viruses that use different host cell receptors (called pseudotyping). By pseudotypisation, the viral host range can get expanded or limited, depicted in **table 1** [64].

TABLE 1: Summary of viral pseudotypes, their host cell receptors and host range.

<b>Pseudotype</b>	<b>Host cell receptor</b>	<b>Host range</b>	<b>References</b>
MoMLV Env, Friend MLV Env	SLC7A1 (mCAT)	Mouse and Rat cells	[65]
Xenotropic MLV Env, Xenotropic MLV-related virus (XMRV) Env	Xenotropic retrovirus receptor 1 (XPR1)	Mammalian cells including human cells, but not mouse cells	[66,67]
GaLV Env	SLC20A1 (Pit1) and orthologue SLC20A2 (Pit2)		[68,69]
FeLV C RD114 Env	SLC1A4, SLC1A5	Mammalian cells including human cells but no mouse and feline cells	[70]
1504A-MLV Env, 4070A-MLV Env	SLC20A2 (Pit2)		
10A1 MLV Env	SLC20A1 (Pit1) and SLC20A2 (Pit2)	Mammalian cells including human cells	[71-74]
VSV Env	Low-density lipoprotein receptor (LDL-R)	All mammalian cells and some types of non-mammalian cells	[73,75]

Abbreviations: MoMLV: Moloney murine leukemia virus; MLV: Murine leukemia virus; SLC: Sodium-dependent phosphate transporter; GaLV: Gibbon ape leukemia virus; FeLV C RD114: Endogenous feline type C virus isolated from human rhabdomyosarcoma; VSV: Vesicular stomatitis virus.

During evolution, different strains of MLV evolved, mainly differing in their envelope proteins, leading to altered host ranges. The tropisms of MLV Env were thus classified into three distinct subclasses. The ecotropic envelope binds to a receptor present only on mouse and rat cells, called the murine cationic amino acid transporter (mCAT), whereas the xenotropic envelope proteins bind to a xenotropic retrovirus receptor (XPR1) expressed on most mammalian cells, including human cells but excluding mouse cells. The amphotropic envelope protein is able to bind to a type III inorganic sodium-dependent phosphate transporter represented on a wide range of mammalian and non-mammalian cells, including human cells [60]. In addition, MLV vectors can get pseudotyped with envelope proteins of different viral species, for example with the envelope glycoprotein of the vesicular stomatitis virus (VSV-G) harboring the widest host range. VSV-G binds to a low-density lipoprotein receptor (LDL-R) represented on all mammalian cell membranes including human- and some non-

mammalian cells [54,73,76]. Clinical grade RVVs are mainly spiked with the envelope proteins of the amphotropic MLV, the gibbon ape leukemia virus (GaLV), the simian endogenous retrovirus (RD114) or the VSV for *ex vivo* gene therapy, whereas the ecotropic envelope proteins are mainly employed for pre-clinical studies in mice and rats, respectively [77,78].

### 1.2.2 RETROVIRAL PACKAGING CELLS

To produce retroviral vectors, the third-generation plasmid-based vector system is either serially transfected (one plasmid after the other) or co-transfected (all three plasmids together) into packaging cell lines mainly using calcium phosphate, a polymer e.g., linear polyethylenimine (PEI) or electroporation. The packaging cells can synthesize all necessary proteins for viral vector assembly and are usually easy to transfect, e.g., the human embryonic kidney cell line (HEK293) or the HEK-T cell line, a 293-subline containing the simian virus 40 large tumor antigen [54]. Typically, adherent VPCs are transiently transfected with the respective retroviral plasmids. Two to three days post transfection, viral vectors are harvested from the cell supernatant and are subsequently used to stably deliver the transfer vector into the genomes of the respective target cells. The retroviral vector is not able to replicate further because the target cells do not contain the necessary packaging and envelope genes, respectively [77]. The development of adherent high producer VPCs is very labor-, time- and cost-intensive. For transient productions of large viral vector batches repetitive transient plasmid transfections in adherent VPCs growing in cell-stacks, roller bottles or cell-factories are needed [79–81]. For each harvest, repetitive plasmid transfections in freshly seeded adherent target cells are conducted, leading to large batch-to-batch variations of harvested vectors [82]. One example of such a production procedure is the production of clinical grade LVVs for the delivery of a chimeric antigen receptor (CAR) into human T cells for cancer immunotherapy. This manufacturing process contributes to exorbitant costs for one single dose ( $\geq$  US\$ 300.000) [83].

However, to efficiently manufacture stable clinical-grade VPCs instead, continuously producing viral vectors, cumbersome selection procedures over several months with different antibiotics are necessary to select single high expresser cell clones. In addition, the upscaling of such high producer VPCs is again strictly limited to the two-dimensional surface area. The definition of exact viable cell numbers (VCN) for each vector harvest is hampered resulting in large batch-to-batch variations of each viral vector harvest, limiting a continuous production procedure [59]. Unfortunately, another bottle neck resides in the relatively low quantity of produced clinical grade functional viral vectors. To successfully deliver viral vectors for gene therapy, titers of



$10^{11}$ - $10^{12}$  transduction competent particles per patient are necessary. The average titers of mainly adherently produced RVVs and LVVs remain between  $10^6$  and  $10^7$  transduction competent particles per mL (TU/mL) (reviewed in [77]). Thus, fully stable VPCs generated in a short time and growing in serum-free suspension continuously producing high quantities of functional viral vectors are indispensable.

To date only a small number of HEK293-based stable  $\gamma$ -RV-based VPCs containing two or all three retroviral components are available. For example, the pioneering VPCs Phoenix-Eco or Phoenix-Ampho both stably express an ecotropic or amphotropic Env and the MLV-derived packaging and catalytic proteins Gag and Pol. After the stable introduction of a transfer vector, a stable vector production over 30 days can be achieved [84]. The VPC CatPac stably expresses the feline endogenous virus (FeLV)-*gag*, *pol* genes as well as the FeLV *env* gene [85]. The suspension VPCs 293GP-A2, -GLV9 or -R30 stably express all MLV-based components, either with an amphotropic-, GaLV- or RD114-Env [86,87]. The generation of those VPCs, however still required cumbersome and cost-intensive steps for transfection, suspension adaptation and single clone selection.

### 1.3 TRANSPOSON-VIRAL VECTORS

To efficiently transfer a genetic expression cassette stably into a eukaryotic cell genome, many parameters concerning the genetic organization, transfection technique as well as copy numbers within specific gene *loci* must be considered. For gene therapeutic purposes LV-/RV-based vectors are frequently used, fulfilling most of these criteria. However, a non-viral transposon-based vector system harbors great potential for fast and efficient gene transfer accomplishing safety and efficiency requirements for clinical applications [39]. Transposable elements (TEs) are mobile genetic elements present in all prokaryotes and eukaryotes. They were discovered more than 60 years ago in maize by Barbara McClintock, who received the Nobel Prize in 1983 [88]. Transposable elements including retrotransposons (class I) and DNA transposons (class II) make up approximately ~45 % and ~3 % of the human genome [89]. The DNA transposons are characterized by a transposase gene flanked by inverted repeats (IRs) that complement each other. Moreover, the IRs are flanked by direct repeats (DR) being called IR/DR or Terminal Inverted Repeats (TIRs). The translated transposase binds to the TIRs and exercises the transposable element by a “cut and paste” mechanism leaving the DRs as a footprint behind. The mobilized genetic element is subsequently re-integrated at a new chromosomal locus in the host cell genome [90]. Most DNA transposons were inactivated millions of years ago due

to accumulations of mutations. Molecular reconstitution however led to the reactivation of a fossil Tc1/mariner-type TE of a salmonid fish subfamily and was called *Sleeping Beauty* (SB) [91]. The reactivated SB can efficiently transfer transgenes into mammalian cells and even hematopoietic stem cells (HSCs). SB shows higher activity in vertebrates compared to other identified active transposon systems. Molecular evolution even led to the generation of the hyperactive transposase called SB100X with a 100-fold improved activity. Using the hyperactive SB100X, transposition efficiencies of up to 90 % were reached in HSCs upon one transposition event [92]. The SB100X transposon system is currently used for stable gene therapeutic *in vitro* and preclinical *in vivo* applications [39].

For stable transposition of a transgene into respective target cells, a two-component transposition system is typically employed, illustrated in **figure 3**.

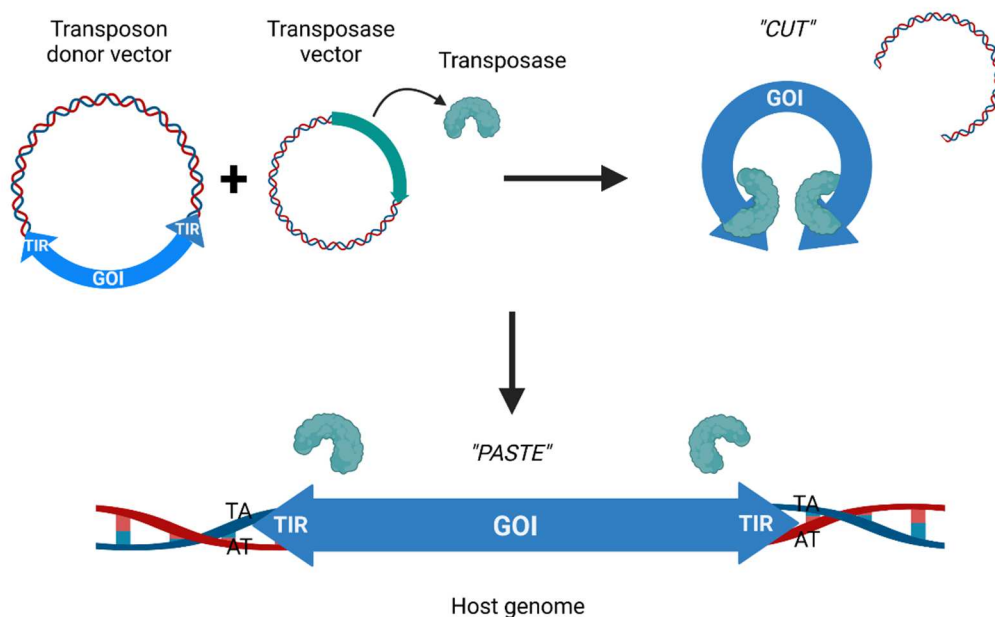


FIGURE 3: Illustration of the DNA transposition process. The illustrated *Sleeping Beauty* transposition process shows a two-component plasmid system. The transposon donor vector, containing the gene of interest is flanked by the terminal inverted repeats (TIRs) and the transposase vector harbors the transposase gene. The expressed transposase binds to the TIRs of the donor vector, forming a synaptic complex, where the two ends of the donor vector are attached by the transposase and form a loop structure. The GOI is cut from the donor backbone and the excised DNA is then re-inserted into another location of the genome, here as example TA sites. Illustration was created with Biorender.com.

Therefore, the transposase gene is separated from the TIR-flanked transposon donor vector. The two components thus are non-autonomous transposable elements and consist of one donor vector harboring the GOI and if necessary, a selectable marker

gene flanked by the TIRs of the transposase and one component carrying the *transposase* gene with a heterologous promoter. After transfection into the target cells, the expressed transposase stably transposes the donor vector into the genome, preferably at multiple copies per cell [91].

To circumvent the laborious and cost-intensive screening for single highly productive VPC clones and to rapidly adapt VPCs for different applications, a novel strategy combining the viral vector cassettes with the TIRs of the transposase was established. This strategy allows the rapid transposition of transposon-viral hybrid vectors for the generation of stable VPCs within only three to four weeks [93]. In addition, the transposition events within the VPC genomes lead to highly efficient and even multiple stable gene insertions resulting in stable and highly productive VPCs within weeks [93]. Here, the transposase is delivered *in trans* using a plasmid-or mRNA-based transposase delivery system, respectively. This technology generates polyclonal VPCs producing viral vectors continuously over months. However, it had been exclusively applied to adherent VPCs so far [93]. The combination of rapid transposition for the establishment of stable polyclonal suspension VPCs growing in serum free media harbors great potential for industrial productions of relevant clinical therapeutics.

## 2 AIM OF THE STUDY

The presented work aimed at a proof-of-concept (POC) study for the development of scalable packaging cells (VPCs) to produce ecotropic MLV-based vectors. Today's production of viral vectors at large-scale using adherent VPCs is very time-, labor- and cost extensive. Therefore, the utilization of a fully stable suspension VPC growing in serum-free medium continuously and efficiently producing viral vectors over a long period of time is indispensable. This thesis begins with the establishment of a stable retroviral VPC continuously producing ecotropic MLV-based vectors in serum-free suspension. Therefore, a hybrid *Sleeping Beauty* (SB)-based transposon-viral vector system was utilized to speed up the selection procedures to establish a fully stable and high-yield polyclonal VPC. Continuously harvested retroviral vectors were tested for functionality after further processing using ultrafiltration devices and freeze-thaw cycles. The functionality of those vectors was assessed using gene transduction experiments in murine fibroblasts, myeloblasts as well as murine bone marrow-derived hematopoietic stem and progenitor target cells. However, a limiting factor of this hybrid technology is the utilization of a plasmid-based transposase construct. During co-transfection, the plasmid-based transposase can possibly integrate into the VPC genome causing stable expressions of an active transposase. Thus, leading to remobilization events of transposon donor vectors within the host cell genome, resulting in instable and potentially decreased vector productivities. The plasmid-based transposase construct was thus exchanged with an *in vitro* synthesized transposase encoding mRNA for co-transfection. This strategy was tested in transient transfection experiments and subsequently used to generate another stable polyclonal ecotropic MLV-based VPC. For comparison two additional stable VPCs were generated using a simple plasmid-based transfer vector and a plasmid-based transposase construct being co-transfected with a transposon-based transfer vector. Functional and physical titers of all three VPCs were assessed to identify the VPC with the highest vector yields. To prepare for VPC cultivations in automated bioreactors, the most productive VPC was expanded in 100 mL shake flasks and cultivated at higher viable cell densities. Lastly and upon a first 500 mL stirred-tank bioreactor cultivation experiment, the VPC was validated during a ten days cultivation process for future large-scale productions.

### 3 PUBLICATION I

**Establishment of a novel stable human suspension packaging cell line producing ecotropic retroviral MLV(PVC-211) vectors efficiently transducing murine hematopoietic stem and progenitor cells.**

**Yasemin van Heuvel<sup>a,b</sup>, Karen Berg<sup>a,c</sup>, Tanja Hirsch<sup>d</sup>, Kristina Winn<sup>a</sup>, Ute Modlich<sup>d</sup>, Jörn Stitz<sup>a,\*</sup>**

<sup>a</sup> Research Group Pharmaceutical Biotechnology, Faculty of Applied Natural Sciences, TH Köln – University of Applied Sciences, Chempark Leverkusen E28, Kaiser-Wilhelm-Allee, 51368 Leverkusen, Germany

<sup>b</sup> Institute of Technical Chemistry, Leibniz University Hannover, Callinstraße 5, 30167 Hannover, Germany

<sup>c</sup> Research Group Translational Hepatology and Stem Cell Biology, Cluster of Excellence REBIRTH, Department of Gastroenterology, Hepatology, and Endocrinology, Hannover Medical School, Carl-Neuberg-Str. 1, 30625 Hannover, Germany

<sup>d</sup> Research Group for Gene Modification in Stem Cells, Paul-Ehrlich-Institute, Division of Veterinary Medicine, Paul-Ehrlich-Str. 51-59, 63225 Langen, Germany

\*Corresponding author. Email address: joern.stitz@th-koeln.de (J. Stitz)

**Type of authorship:** First author

**Type of article:** Research article

**Share of the work:** 80 %

**Journal:** Journal of Virological Methods

**DOI:** 10.1016/j.jviromet.2021.114243

**Date of publication:** 24 July 2021

## Abstract

---

Retroviral vectors derived from murine leukemia virus (MLV) are amongst the most frequently utilized vectors in gene therapy approaches such as the genetic modification of hematopoietic cells. Currently, vector particles are mostly produced employing adherent viral packaging cell lines (VPCs) rendering the scale up of production laborious, and thus cost intensive. Here, we describe the rapid establishment of a human suspension 293-F cell line-derived ecotropic MLV VPC. Using transposon vector technology, a packaging and envelope expression cassette as well as a transfer vector facilitated the establishment of a stable VPC yielding high titers of up to  $5.2 \times 10^6$  transducing units/mL (TU/mL). Vectors were concentrated using ultrafiltration devices and upon one freeze-thaw-cycle still routinely yielded titers of  $> 1 \times 10^6$  TU/mL. Formation of replication-competent retroviruses was not detected. However, and as a first-generation transfer vector was used in this proof-of-concept (POC) study, gag gene sequences were transduced into target cells within a range of 1–10 copies per 1000 genomes indicating the homologous recombination of packaging construct elements with the transfer vector. High yield VPC vector productivity was stable over a couple of months and unintended integration of the transposase gene was not observed. Ecotropic MLV vector particles were demonstrated to efficiently transduce primary murine hematopoietic stem and progenitor cells. This novel concept should foster the future establishment of suspension VPCs.

**Keywords:** Suspension packaging cell, Murine leukemia virus (MLV), Viral vector, Hematopoietic stem cell, Transposon vector

### 3.1 INTRODUCTION

Viral vectors derived from donors of the *retroviridae* family are frequently used to enable stable gene transduction in somatic gene therapy. The most prominently utilized vector systems are derived from the lentivirus human immunodeficiency virus type 1 (HIV-1) and the gamma-retrovirus ( $\gamma$ -RV) murine leukemia virus (MLV). For some applications, lentiviral vectors are favorably employed as they enable integration of transduced transgenes into the genome of non-dividing target cells (Cooray et al., 2012; Sinn et al., 2005). Despite their inability to transduce non-cycling cells, retroviral vectors derived from MLV mediate efficient stable gene transfer into a variety of cell types from different donor species reviewed in Maetzig et al., 2011. Most notably, these vectors are used in somatic gene therapy applications aiming at the genetic modification of hematopoietic stem cells (HSCs; Lundstrom, 2018). *In vivo* models, studying disease mechanisms, frequently employ murine HSCs (Javazon et al., 2012; Zeng et al., 2013). To modify the host cell range of retroviral vectors and to enhance gene transfer efficiencies into some target cell types, pseudotyping with heterologous envelope proteins is a common procedure (Li et al., 2018). Currently and to achieve superior gene transduction, the G-protein of pantropic vesicular stomatitis virus (VSV-G), and alternatively, the envelope proteins of polytropic feline endogenous retrovirus RD-114 are frequently used to modify human target HSCs (Bauler et al., 2020; Piovan et al., 2017; Radek et al., 2019). However, the expression of VSV-G is cytotoxic disabling the establishment of stable and continuously vector particle producing packaging cells (Yee et al., 1994). Thus, VSV-G pseudotyped vectors need to be produced either by transient transfection or by employing inducible gene expression systems (Ory et al., 1996). RD-114 Env is not cytotoxic but does not mediate vector particle entry into rodent cells excluding MLV(RD-114) pseudotype vector particles from the utilization in preclinical gene transfer studies targeting murine HSCs (Tailor et al., 1999). Retroviral vectors decorated with the Env proteins of ecotropic Moloney MLV (MoMLV), and thus showing a restricted tropism to rodent cells, were demonstrated to be valuable tools for this purpose (Modlich et al., 2009). Ecotropic vector particles can be produced upon transient triple co-transfection of HEK-293 T cells with the required envelope and packaging constructs as well as a transfer vector containing the respective packaging signal Psi ( $\psi$ ). However, this technique is time- and cost-intensive and can result in notable batch-to-batch variations concerning vector titer. The use of stable packaging cells continuously producing ecotropic MLV vectors is therefore favorable. To date, only adherent stable ecotropic viral packaging cells (VPCs) producing high vector titers of more than  $1 \times 10^6$  TU/mL are available (Rodrigues and Coroadinha, 2011). However, vector

production at larger-scale using adherent VPCs is challenging as it requires cultivation in numerous individual flasks or multiple connected culture dishes such as the so-called cell factory culture system (Przybylowski et al., 2006). In addition, the relatively low cell density per volume of cultivation media limits the productivity of adherent VPCs. To enable vector production at larger-scale using higher cell densities, an ecotropic VPC growing in suspension was developed using human lymphoblast WIL-2 cells. Unfortunately, this VPC revealed inferior productivity as compared to adherent VPCs using standard cultivation conditions. Expansion in the presence of sodium butyrate, known to elevate vector titers, was required to reach titers higher than  $1.0 \times 10^6$  TU/mL (Soneoka et al., 1995; Chan et al., 2001). The use of transposon vectors enables the rapid establishment of stable and highly productive transgenic cell pools omitting the time-intensive isolation and screening of cell clones (reviewed in Tschorn et al., 2020). We previously reported the generation of *Sleeping Beauty*-derived transposon vectors encompassing the required three retroviral vector components, namely, a transfer vector, a packaging and an envelope construct encoding the Env proteins of Friend MLV (FrMLV) molecular clone PVC-211 and their utility to rapidly establish stable adherent VPCs. We were able to show that the high-titer vector productivity of up to  $2.3 \times 10^6$  TU/mL of established VPC was mainly caused by the high abundance of transfer vector transcripts available for packaging. This resulted from a very high copy number of transposon vectors harboring the retroviral transfer vectors per cell genomes (Berg et al., 2019). In this POC study presented here, we applied this multiplex transfection and transposition-based methodology to the establishment of a stable suspension VPC using human 293-F host cells. MLV(PVC-211) pseudotype vectors were previously shown to efficiently transduce murine and hamster cell lines as well as cell lines from different donor species recombinantly expressing the murine cationic amino acid transporter (CAT; Stitz, 2011). We here examined the potential of MLV (PVC-211) vectors to mediate gene transfer into primary murine hematopoietic stem and progenitor cells (HSPCs).

## 3.2 MATERIALS AND METHODS

### 3.2.1 CELLS AND PLASMIDS

Embryonic human kidney suspension Freestyle™-293-F cells were grown in Freestyle™ 293 expression medium supplemented with GlutaMAX™ (Gibco, Germany). Cells were cultured at 37 °C, 8 % CO<sub>2</sub> and at 137 rpm in shake flasks (Thermo Fisher, Germany) using a Minitron shaker incubator (INFORS HT, Switzerland) with an orbit of 5 cm. The adherent cell lines, namely, murine fibroblast



NIH/3T3 (ATCC CRL- 1658) and SC-1 cells (ATCC CRL-1404), African green monkey kidney fibroblast-like COS-7 cells (ATCC CRL-1651) and recombinant COS-7mCAT cells (Berg et al., 2019) were all grown in high glucose (4.5 g/L) Dulbecco's modified Eagle's medium (DMEM) supplemented with 2 mM L-Glutamine and 10 % FBS (Gibco, Germany). Murine 32D myeloblast-like cells (ATCC CRL-11,346) were cultivated in RPMI 1640 medium (Gibco, Germany) supplemented with 2 mM L-Glutamine, 10 % FBS, 4.5 g/L glucose and 10 % mouse Interleukin-3 (Thermo Fisher, Germany). Cells were expanded at 37 °C in a humidified atmosphere at 5 % CO<sub>2</sub>. For passage, adherent cells were detached using 1 mM EDTA in PBS. Prior to seeding, target cell viability was assessed using 0.1 % (v/v) Erythrosine B (Carl Roth, Karlsruhe, Germany). The plasmid MSCVneo (MSCV retrovirus system, Takara, USA) was opened in the multiple cloning site (MCS) using EcoRI and BamHI. A DNA fragment entailing the EGFP encoding region, a neomycin resistance gene (*neoR*) followed by a synthetic intron (In; both amplified from pIRESneo, Clontech, USA; GenBank accession no. U89673) and the tripartite post-transcriptional regulatory element of woodchuck hepatitis virus (WPRE; nucleotides 1093–1684; GenBank accession no. J04514) was generated by PCR. Primers introducing the target motifs for abovementioned restriction enzymes were used for the amplification. The amplicon was digested accordingly and subsequently inserted into the linearized recipient first generation MSCVneo vector – encompassing full-length long terminal repeats (LTRs) and a part of the 5'-*gag* gene reaching into the packaging signal - to generate MSCV-EGFP-In-WPRE. This vector served as a template to amplify the entire retroviral transfer vector region using the LTR-specific primers 5'LTR-MSCV-FseI-for 5'-AAAAGGCCGGCCCTGAAGCCTATAGAG TACGAGCCATAG-3' and 3'LTR-MSCV-NotI-rev 5'-AAAAGCGGCCGCAT- GAAAGACCCCCGCTGAGGGTAG-3' introducing the restriction motifs of FseI and NotI. The recipient vector harbored the 5' and 3' terminal inverted repeats (TIRs, as previously described by Berg et al., 2020) of the transposon *Sleeping Beauty*. The TIRs flank two copies of the core chicken beta-globin insulator sequences (cHS4; GenBank accession no. U78775.2), each of an approximate size of 1.2 kb, reported by Sharma et al. (2012) to elevate expression levels by 2.2-fold in mammalian cells. A MCS separating both cHS4-derived regions contained single FseI and NotI sites. Upon according digestion using NotI and FseI, the aforementioned DNA-fragment was inserted into the transposon donor vector to result in the construct SB-cHS4-MSCV-EGFP. Further cloning strategy details, primer sequences as well as the novel vectors are available upon reasonable request.

### 3.2.2 ESTABLISHMENT OF STABLE VPCs AND RECOMBINANT TARGET CELLS

293-F cells were transfected using the linear 40 kDa polyethylenimine transfection reagent (PEI; Polysciences Inc., USA) at a mass ratio of 1:3 (DNA: PEI) according to the manufacturer's instructions. One day prior to transfection,  $1.5 \times 10^6$  cells/mL were seeded in total volumes of 20 mL in 125 mL Erlenmeyer flasks (plain bottom, Nalgene™, Thermo Fisher; Germany). On the following day,  $3 \times 10^7$  cells were seeded in 6 mL Freestyle expression medium for transfection. Co-transfections with the viral vector components harboring transposon donor vectors and a human codon optimized transposase gene encompassing constructs were performed as previously described (Berg et al., 2020). Briefly, cell line VPC-MSCV-EGFP was established upon co-transfection with SB-gpIpW (11.25 µg), SB-eIhW (11.25 µg), the transposase construct (5 µg) and the transfer vector entailing plasmid SB-cHS4-MSCV-EGFP (22.5 µg). One day post transfection, cells were expanded in fresh medium at a density of  $2 \times 10^6$  cells/mL. To establish a stable transgenic VPC and three days post transfection, initially concentrations of 0.5 µg/mL puromycin, 50 µg/mL hygromycin and 100 µg/mL G418 (all InvivoGen, Toulouse, France) were applied for selection. Over a period of three weeks, the selection pressure was iteratively elevated with each passage to reach the final concentrations of 10 µg/mL puromycin, 200 µg/mL hygromycin and 200 µg/mL G418. Except for preparations for vector particle harvest, VPC-MSCV-EGFP cells were constantly expanded and passaged in the presence of the aforementioned high concentrations of all three antibiotics to secure sustainable constant productivity.

### 3.2.3 VIRAL VECTOR TITRATION

To assess the viral vector titers produced by the established VPC,  $1.0 \times 10^5$  adherent target cells were seeded in 2 mL per well in six-well dishes one day prior to transduction (Nunc, Wiesbaden, Germany). Murine 32D myeloblast-like cells were seeded at a density of  $2 \times 10^5$  cells in 500 µL in 24-well dishes. In parallel, stable suspension VPC-MSCV-EGFP cells were seeded at a density of  $5 \times 10^6$  cells/mL in a total volume of 20 mL in 125 mL shaking flasks or, alternatively and for larger-scale production, in a total volume of 100 mL in 500 mL shaking flasks, respectively. Cells were expanded for 16 h in the absence of antibiotics followed by vector particle harvest. To obtain cell-free vector preparations, harvested supernatants were passaged through a 0.45 µm pore size PVDF filter (Carl Roth, Germany). To concentrate vectors, 20 mL of VPC supernatants were reduced to 1 mL using ultrafiltration devices Vivaspin 20 (50.000 MWCO; Sartorius, Germany). Different dilutions of vector samples in total volumes of 1 mL were subjected to transduction of target cells

overnight. The following day, 1 mL of cultivation medium was added to transduced cells. Three days post transduction, cells were detached and analyzed employing flow cytometry (S3e, Bio Rad, USA; CytoFLEX, Beckman Coulter Life Sciences, USA) to determine the percentage of EGFP-positive cells. Vector titers were calculated as described previously by Salmon and Trono (2007) employing supernatant dilutions resulting in gene transfer efficiencies between 1.0 % and 10.0 % EGFP-positive cells.

### **3.2.4 DETECTION OF REPLICATION-COMPETENT RETROVIRUSES (RCRs) AND RECOMBINATION OF THE TRANSFER VECTOR WITH THE GAG GENE OF THE PACKAGING CONSTRUCT**

To ensure that detected gene transfer efficiencies were purely a result of vector-mediated transduction and not caused by the unintended generation of RCRs originating from the recombination of vector components, GFP marker rescue assays were performed in triplicate in two independent experiments as previously described in detail (Cosset et al., 1995; Berg et al., 2019). Briefly,  $1.5 \times 10^6$  susceptible NIH/3T3 target cells harboring the transfer vector LEGFP-N1 (Clontech, USA) and selected using 1000  $\mu\text{g}/\text{mL}$  G418 were seeded on the day of transduction in T75 flasks without antibiotics. Cells were exposed to pre-titrated supernatants of VPC-MSCV-EGFP containing  $2 \times 10^7$  TU of MLV (PVC-211) viral vectors. Upon the expansion of cells for at least five days without passage or medium exchange, potentially RCR-containing supernatants were harvested, and contaminating cells were removed by passage through a 0.45  $\mu\text{m}$  filter. Naive NIH/3T3 cells were exposed to these supernatant preparations and expanded for three days. Subsequently, cells were examined using flow cytometry and fluorescence microscopy to detect EGFP-positive cells resulting from the mobilization of the transfer vector by potentially generated RCRs. In addition, a reverse transcriptase (RT) assay with a detection sensitivity of 10 pg RT per 40  $\mu\text{l}$  sample (Colorimetric reverse transcriptase assay, Roche, Switzerland) was conducted following the manufacturer's instructions using cell-free supernatants from VPC-MSCV-EGFP as positive control and transduced NIH/3T3/LEGFP-N1 and "RCR-transduced" naive NIH/3T3 cells as control samples. The same procedure was repeated after 14 days of cultivation. To assess the potential recombination with the gag/pol genes and the transfer vector components we first established highly susceptible African green monkey COS-7 cells recombinantly expressing the ecotropic receptor mCAT. Briefly, cells were co-transfected with the transposase construct CMV-SB100x and the construct SB-mCATIpW, which enables receptor expression coupled to a puromycin resistance gene as described previously (Berg et al., 2019). Resulting COS-7mCAT cells were subsequently selected upon expansion in the presence of

3 µg/mL puromycin. Highly susceptible  $1.5 \times 10^6$  COS-7mCAT cells were transduced using  $2 \times 10^7$  TU of MLV(PVC-211) vector particles and expanded. The experiment was conducted in triplicate. Four days post transduction, cell-free supernatants were employed to conduct the aforementioned RT-assay. Cells were also analyzed employing flow cytometry to detect successful transduction and expression of the *egfp* reporter gene. In parallel, genomic DNA was harvested using the Monarch® genomic DNA purification kit (NEB, USA). An equivalent of 10,000 genomes (60 ng) of genomic DNA originating from transduced COS-7mCAT cells and non-transduced cells serving as a negative control were used to perform genomic PCR using the Phusion® High-Fidelity DNA Polymerase following the manufacturer's instructions (NEB, USA). Genomic DNA of VPC-MSCV-EGFP cells served as a positive control. In parallel and to determine the sensitivity of *gag* detection, serial dilutions of the packaging construct SB-gpIpW were mixed with 60 ng of genomic DNA of COS-7mCAT cells. Using the oligonucleotides GAG-for (5'-GCTCTGCA GAATGGCCAACCTTTAAC-3') and GAG-rev (5'-CCTGCGATAGGCTTC CTTAAGTCTC-3') generating amplicons of a size of 1019 bp, genomic PCR was performed with an initial denaturation step of 30 s at 98 °C, followed by denaturation for 10 s at 98 °C, annealing for 30 s at 60 °C and elongation for 30 s at 72 °C. 35 cycles were conducted followed by a final extension step for 5 min at 72 °C.

### 3.2.5 DETECTION OF THE TRANSPOSASE GENE IN VPC-MSCV-EGFP PACKAGING CELLS

The unintended integration of the transposase coding region into genomes of the packaging cell VPC-MSCV-EGFP as a result of stable transfection could potentially lead to genetic instability, and thus loss of vector particle productivity. To examine this, we conducted genomic PCR analysis. Genomic DNAs were purified from naive 293-F and VPC-MSCV-EGFP cells as aforementioned. 60 ng of genomic DNA of naive 293-F cells served as a negative control. To determine the sensitivity of SB100x coding region detection, serial dilutions of the transposase construct CMV-SB100x were mixed with 60 ng of genomic DNA of 293-F cells. The oligonucleotides SB100x-for (5'-ACAGGACATTCTGGA- GAAACGTGCTGTGG-3') and SB100x-rev (5'-TTCTTCAGCTCGGCCCA- CAGATTCTCG-3') amplifying a DNA fragment of 436 bp were employed to performed genomic PCR using the Phusion® High-Fidelity DNA Polymerase (NEB, USA). The amplification conditions included an initial denaturation step of 30 s at 98 °C, followed by 35 cycles of denaturation for 10 s at 98 °C, annealing for 15 s at 63 °C and elongation for 30 s at 72 °C. A final extension step for 5 min at 72 °C was performed.

### 3.2.6 MURINE HSPC ISOLATION AND CULTURE

Bone marrow (BM) was collected from C57BI/6 mice by flushing femurs and tibias with IMDEM, 10 % fetal calf serum (Gibco, Germany), 1 % L-Glutamine 2 mM (Gibco, Germany) and 2 % penicillin/streptomycin (50 U/mL and 50 mg/mL, PAA, Pasching, Austria). Mononuclear cells were isolated by gradient centrifugation on Histopaque (Percoll; Sigma Aldrich, Germany) at 760 g for 20 min at RT, no brake. Subsequently, the interphase was collected and washed with 35 mL cold PBS. The cell pellet was resuspended in PBS pH 7.2 supplemented with 0.5 % BSA and 2 mM EDTA for further magnetic cell sorting (MACS) purification of lineage marker-negative (lin<sup>-</sup>) cells using the MACS Lineage Cell Depletion Kit (Miltenyi Biotec, Germany). All steps were performed as described within the manufacturer's protocol. Purified lin<sup>-</sup> cells were diluted in fetal calf serum supplemented with 10 % DMSO and frozen in cryogenic storage vials at a slow cooling rate of 1 °C/min. Cells were stored at -80 °C or transferred to liquid nitrogen.

### 3.2.7 TRANSDUCTION OF HSPCs

Murine HSPCs were transduced with the MLV(PVC-211) vectors harvested from VPC-MSCV-EGFP cells as described in Modlich et al. (2009). Practically,  $5 \times 10^5$  lin<sup>-</sup>BM cells were thawed and pre-stimulated for three days in serum-free medium (StemSpan, Stem-Cell Technology, Grenoble, France), 2 mM glutamine (Gibco, Germany), 1 % penicillin/streptomycin containing 50 ng/mL mSCF, 100 ng/mL hFlt3L and 100 ng/mL hIL-11. Cells were incubated at 37 °C and 5 % CO<sub>2</sub> in a humidified cell culture incubator. After three days of pre-stimulation, a 24-well plate was pre-loaded with 10 µg/cm<sup>2</sup> of recombinant human fibronectin fragments RetroNectin® (48 µg/mL, TaKaRa, France) for 30 min at RT, then blocked with 2 % BSA in PBS for 30 min at RT and finally washed once with HBSS/Hepes Buffer (2.5 %, v/v; Moritz et al., 1996). Retroviral vector particles diluted in ice-cold PBS were added at different multiplicities of infections (MOIs) multiplied by two. During coating, 40 % – 50 % of the vector particles remained unbound as previously described (Modlich et al., 2009). This observation was reconfirmed in this study conducting transduction experiments employing naive SC-1 target cells (data not shown). The plate was then centrifuged at 700 g for 30 min at 4 °C. Unbound particles within PBS were removed and  $2 \times 10^5$  HSPCs were seeded in 500 µL Stem-Span + Cytokines as described above onto each well. Cells were then incubated at 37 °C, 5 % CO<sub>2</sub> a humidified cell culture incubator for 48 h. Successful transduction was detected using flow cytometry for the expression of EGFP. Viability of cells was examined two days post transduction using

the 0.1 % (v/v) Erythrosin B (Carl Roth, Germany) and DAPI solution (Thermo Fischer; USA) in accordance with the manufacturer's instructions, respectively.

### **3.3 RESULTS**

#### **3.3.1 ESTABLISHMENT OF THE PACKAGING CELL LINE VPC-MSCV-EGFP AND VECTOR TITRATION**

To establish a stable retroviral suspension VPC human HEK 293-F cells were co-transfected with the transposon vectors SB-gpIpW (packaging construct), SB-eIhW (envelope construct), the transposase construct CMV-SB100x as described earlier (Berg et al., 2019) and the murine stem cell virus transfer vector SB-MSCV-EGFP shown in **Figure 4**.

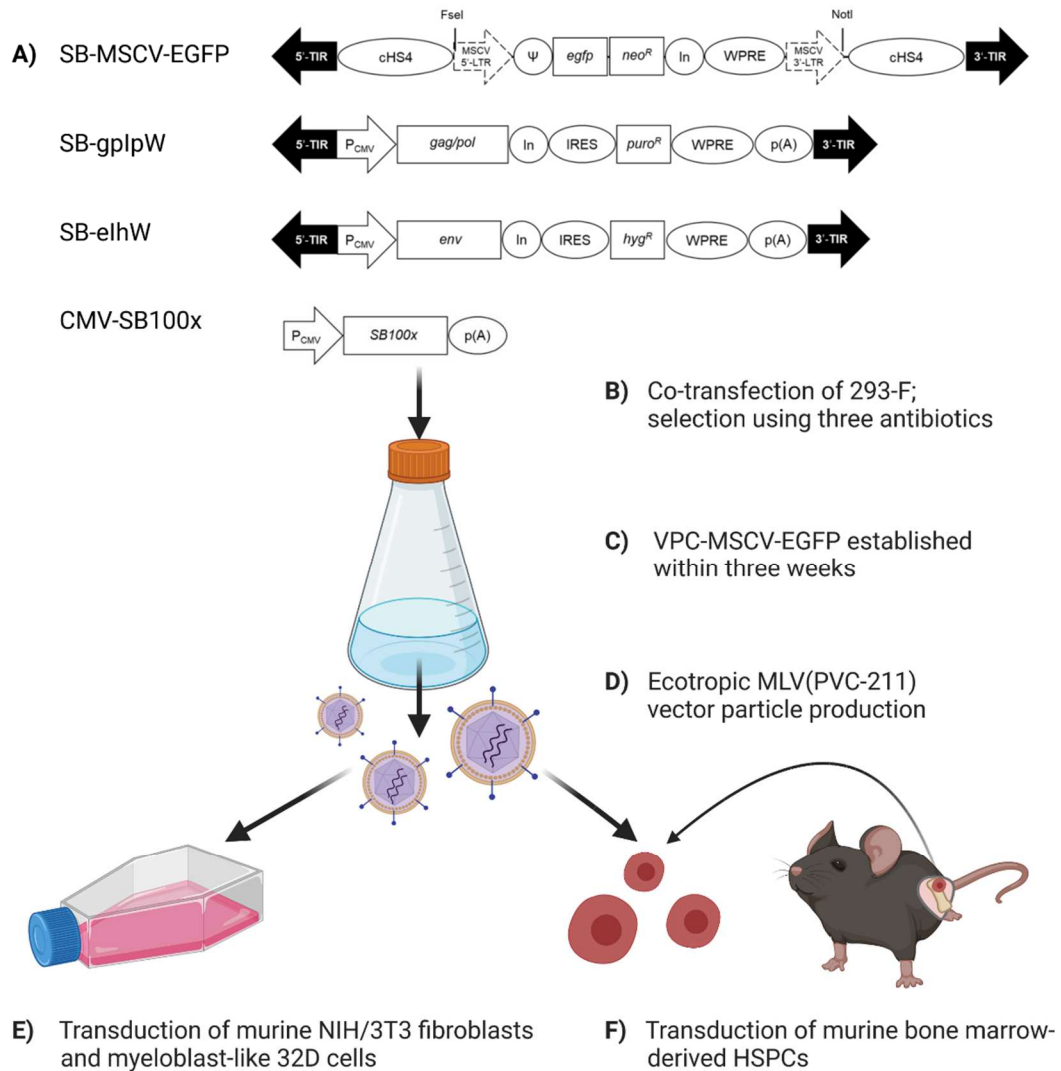


FIGURE 4: Schematic illustration of the constructs used in this study and experimental design of cell line establishment and retroviral vector-mediated gene transfer. (A) The transfer vector SB-MSCV-EGFP with the 5'- and 3'-terminal inverted repeats (TIRs; black arrows) of Sleeping Beauty flanking the 5'- and 3'-long terminal repeats (LTRs; dotted arrows) of murine embryonic stem cell virus (MSCV) and the packaging signal  $\Psi$  are indicated. Core chicken beta- GLOBIN insulator sequences (cHS4) shield the retroviral transfer vector on both sides. The transcription of the full-length transfer vector entailing the reporter gene *egfp* and the *neomycin-resistance* gene (*neoR*) is driven by the viral promoter located in the 5'-LTR. A synthetic intron (In) and the Woodchuck hepatitis virus post transcriptional regulatory element (WPRE) are shown. Restriction motifs for the insertion of the entire transfer vector sequence are indicated. In the packaging construct SB-gpI<sub>p</sub>W, a CMV promoter/enhancer element (pCMV) drives the expression of the MoMLV genes *gag/pol* followed by a synthetic intron, an internal ribosome entry site (IRES), a *puromycin-resistance* gene (*puroR*), the WPRE and the polyadenylation signal (p(A)) of the bovine growth hormone gene. The envelope construct SB-elhW encompasses the human codon-optimized *ecotropic envelope* gene (*env*) derived from the Friend MLV molecular clone PVC-211 and the *hygromycin-resistance* gene (*hygR*) again coupled by a In and an IRES. The transposase construct CMV-SB100x harbors the human codon-optimized gene of the hyper-active *Sleeping Beauty* transposase variant SB100x. (B) All constructs were co-transfected into human suspension 293-F cells. (C) Application of selection pressure using escalating concentrations of all three antibiotics, namely,

puromycin, neomycin (G418) and hygromycin resulted in the establishment of the polyclonal packaging cell line VPC-MSCV-EGFP. (D) Ecotropic MLV(PVC-211) pseudotype vector particles were harvested from cell-free expression medium in the absence of antibiotics. (E) Vector titration experiments were conducted using murine NIH/3T3 fibroblast and myeloblast-like 32D target cells. (F) Murine hematopoietic lineage-negative stem and progenitor cells (HSPCs) were transduced utilizing different multiplicities of infection (MOIs) to assess gene transfer efficiency.

Four days post transfection, cells were kept at a density of  $2 \times 10^6$  cells/mL and subjected to selection in the presence of antibiotics as described in the materials and methods section. As a last selection step, all three antibiotics were added for seven days at a final concentration of 10  $\mu\text{g/mL}$  puromycin, 200  $\mu\text{g/mL}$  hygromycin and 200  $\mu\text{g/mL}$  G418 giving rise to the new packaging cell VPC-MSCV-EGFP. Cell-free MLV(PVC-211) vector-containing supernatants were harvested from VPCs grown without selection pressure for at least 8 h. Vector preparations were titrated using murine NIH/3T3 fibroblast and 32D myeloblast-like target cells followed by flow cytometric analysis to detect successfully transduced EGFP-positive cells.

As shown in **Table 2A**, titrations conducted in triplicate revealed high mean vector titers of  $5.2 \times 10^6$  TU/mL in NIH/3T3 and  $4.0 \times 10^5$  TU/mL in 32D target cells underlining the high productivity of the packaging cell line VPC-MSCV-EGFP. Contaminations of vector preparations with RCRs were not detected in two independent experiments performed in triplicate using a GFP marker rescue-assay with an estimated sensitivity of one RCR in  $1 \times 10^7$  TU/mL containing VPC supernatant (Cosset et al., 1995). In addition, and four- and ten-days post transduction, cell-free supernatants of NIH-3T3/LEGFP indicator cells transduced with MLV(PVC-211) vector preparations did not reveal any detectable reverse transcriptase-activity (data not shown).



TABLE 2: Transduction-competent vector particles harvested from the packaging cell VPC- MSCV-EGFP. (A) Fresh vector preparations harvested from a total VPC culture volume of 20 mL were titrated in triplicate using NIH/3T3 and 32D murine target cells. Standard deviations (SD) are indicated. (B) In four independent experiments, cell-free supernatants were harvested from cultivation volumes of 20 mL from cultivations in 125 mL shake flask (experiments 1, 2 and 3) or from 100 mL after scale-up employing 500 mL shake flasks (experiment 4). MLV vector particles were subsequently concentrated using ultrafiltration, stored at  $-80^{\circ}\text{C}$  and thawed for titrations performed in triplicate in NIH/3T3 target cells.

A

Target cells	Mean Titer [TU/mL]	SE
NIH/3T3	$5.2 \times 10^6$	$\pm 0.36 \times 10^6$
32D	$4.0 \times 10^5$	$\pm 0.34 \times 10^5$

B

Experiment	Mean Titer [TU/mL]	SE
1	$3.7 \times 10^6$	$\pm 0.36 \times 10^6$
2	$6.8 \times 10^6$	$\pm 0.34 \times 10^5$
3	$1.4 \times 10^7$	$\pm 0.97 \times 10^6$
4	$8.1 \times 10^6$	$\pm 0.17 \times 10^6$

The MSCV-derived transfer vector employed here contained 5'-gag gene sequences in the packaging signal. This could potentially mediate recombination events with the packaging construct encoding Gag/Pol. We therefore examined if gag sequences were unintendedly transduced into susceptible target cells. COS-7mCAT cells were transduced in triplicate using a high MOI of 13.3. Four days post transduction, successful gene transfer was detected using flow cytometry analysis revealing the expression of EGFP in 85.0 %, 85.6 % and 85.5 % of the target cells, respectively (data not shown). Using a colorimetric RT-assay, no detectable RT-activities were observed in cell-free supernatants (data not shown). As shown in **Figure 5**, gag DNA fragments with the expected size of 1019 bp could be amplified with a sensitivity of 10 copies in 10,000 genomes using templates of genomic DNA isolated from naive COS-7mCAT cells mixed with different amounts of the plasmid SB-gpIpW. Amplicons were also readily detected using genomic DNA of VPC-MSCV-EGFP cells serving as a positive control while no amplicons were observed employing genomic DNA of non-transduced naive COS-7mCAT cells utilized as a negative control. Gene transduction

of *gag* was detected in all three samples of transduced COS-7mCAT cell populations with an estimated copy number in the range of 10–100 per 10,000 cell genomes.

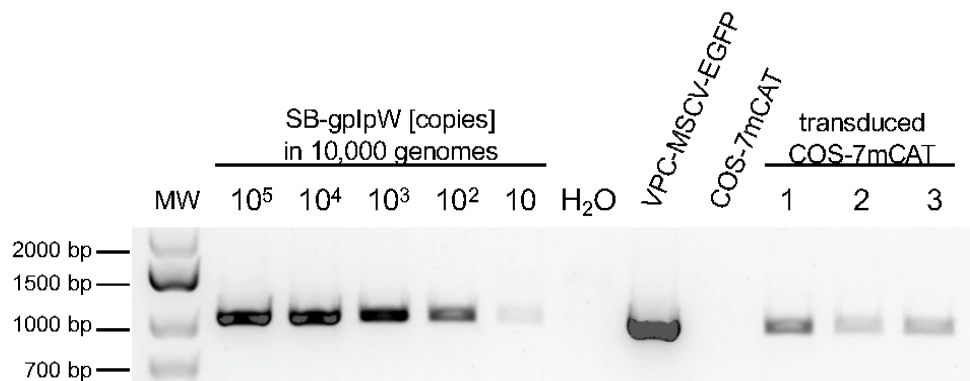


FIGURE 5: Detection of *gag* gene sequences in genomic DNA of transduced COS-7mCAT target cells. 60 ng of genomic DNA of untreated COS-7mCAT cells equivalent to 10,000 genomes was mixed with different amounts of the packaging construct SB-gpIpW to determine the sensitivity of *gag* detection. The same amount of genomic DNA isolated from COS-7mCAT cells transduced in three experiments as well as the genomic DNA of VPC-MSCV-EGFP and naive untreated COS-7mCAT cells serving as positive and negative controls, respectively were employed as templates for PCR yielding amplicons with a size of 1,019 bp. MW, DNA marker.

### 3.3.2 DETECTION OF THE TRANSPOSASE GENE IN VPC-MSCV-EGFP CELLS

The undesired integration of the transposase coding region into genomes of the polyclonal packaging cell VPC-MSCV-EGFP and the sustained expression of the SB100x protein could potentially facilitate excision and/or translocation of TIR-flanked transfer vectors, envelope and packaging construct expression cassettes causing genetic instability leading to a loss of productivity. To examine this, genomic DNA was isolated from packaging cells and naive 293-F serving as a negative control. Genomic PCR-analysis was performed using SB100x coding region- specific oligonucleotides. Detection of the transposon gene resulted in the amplification of DNA fragments with a size of 436 bp. To assess the sensitivity of the genomic PCR, serial dilutions of the CMV-SB100x transposase construct were mixed with the equivalent of 10,000 genomes (60 ng of genomic DNA). As visible in **Figure 6** and with a sensitivity of 10 copies in 1000 genomes, no integrated transposase gene could be detected in the packaging cells.

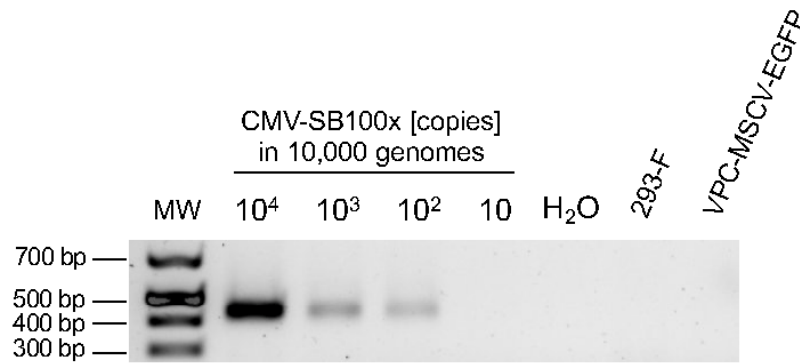


FIGURE 6: Detection of the transposase gene in genomic DNA of VPC-MSCV-EGFP cells. 60 ng of genomic DNA naive 293-F cells equivalent to 10,000 genomes was mixed with different amounts of the transposase construct CMV-SB100x to determine the sensitivity of detection. The same amount of genomic DNA isolated from VPC-MSCV-EGFP cells as well as the genomic DNA of naive 293-F serving as a negative control were used as templates for PCR yielding amplicons with a size of 436 bp. MW, DNA marker.

### 3.3.3 PREPARATION OF FROZEN HIGH-TITER MLV(PVC-211) VECTOR STOCKS

To prepare high-titer vector stocks, four independent vector particle harvests were performed. In three cases, VPCs were cultured in a total volume of 20 mL using 125 mL shake flasks. In order to demonstrate the easily performed scale up, one vector preparation was harvested from a total volume of 100 mL in 500 mL shake flasks. Cells were seeded in 100 mL media at a density of  $1 \times 10^6$  cells/mL and readily expanded. In all cases and regardless of the scale, cells were seeded at a density of  $5 \times 10^6$  cells/mL 16 h prior to vector particle harvest as described. In all four experiments conducted over a period of more than three months, and thus multiple passages, cell-free supernatants were concentrated 20-fold using the ultrafiltration device Vivaspin 20 and aliquots of 200  $\mu$ L were stored at  $-80$  °C. Upon thawing, vector samples were titrated in triplicate in NIH/3T3 target cells. As shown in **Table 2B**, vector titers ranging from  $3.7 \times 10^6$  to  $1.4 \times 10^7$  TU/mL were detected indicating that MLV(PVC-211) vector particle samples could be concentrated using ultrafiltration devices and even after one freeze-thaw-cycle reproducibly yielded high titers. Moreover, the production scale-up by a factor of five to a final volume of 100 mL resulted in vector preparations reaching  $8.1 \times 10^6$  TU/mL indicating no loss of productivity.

### 3.3.4 TRANSDUCTION OF MURINE BONE MARROW-DERIVED HEMATOPOIETIC STEM CELLS

Encouraged by the aforementioned results and for the first time, we examined MLV(PVC-211) pseudotype vector-mediated gene transfer efficiencies into HSPCs. Therefore, three vector preparations (A, B and C) harvested over a period of time of more than three months were thawed and titrated in murine SC-1 embryonal fibroblast revealing titers of  $5.6 \times 10^6$ ,  $2.6 \times 10^6$  and  $3.0 \times 10^6$  TU/mL, respectively. Using MOIs of two, four and six,  $2 \times 10^5$  bone marrow-derived  $\text{lin}^-$  HSPCs were transduced in the presence of RetroNectin<sup>®</sup> as described in detail in materials and methods. Untreated naive cells served as negative controls. As shown in **Table 3**, two days post transduction, gene transfer was readily detected using flow cytometry revealing 27.1 %, 19.4 % and 25.0 % EGFP-positive cells, respectively, upon transduction at a MOI of two.

TABLE 3: Transduction efficiencies in target murine lineage-negative hematopoietic stem and progenitor cells (HSPCs) using ecotropic MLV(PVC-211) pseudotype particles produced by VPC-MSCV-EGFP. Bone marrow-derived HSPCs were transduced employing multiplicities of infection (MOIs) of two, four and six in five different experiments using three individually harvested vector preparations (A, B and C). Two days post transduction, genetically modified EGFP-expressing cells were detected using flow cytometry. Cell viabilities were detected in parallel using DAPI stain respectively.

Experiment	Vector preparation	MOI	EGFP [%]	Viability [%]
1	A	2	25.0	89.6
2	B	2	19.4	89.8
3	C	2	27.1	90.0
4	C	4	34.6	86.0
5	C	6	37.2	88.0

This demonstrated the efficient gene transduction at a low MOI into primary murine HSPCs using MLV(PVC-211) pseudotype vector particles produced by the new suspension VPC. Employing MOIs of four and six higher gene transfer efficiencies of 34.6 % and 37.1 %, respectively, were achieved. Cell viability ranged from 86.0 %–90 %.

### 3.4 DISCUSSION

Efficient gene transfer into murine hematopoietic cells is a prerequisite for studies aiming at the examination of genetic disease mechanisms and the development of therapeutic approaches. Ecotropic MLV-derived vector particles mediate efficient gene transfer into HSPCs and differentiated lineages. To date, only adherent high vector titer producing ecotropic VPCs exist rendering the production of vectors at larger-scales cumbersome and time-consuming. As a POC study, we extended the previously reported concept of rapidly establishing MLV-derived VPCs using adherent HT1080 cells to human suspension 293-F host cells employing multiplex transfection and transposition (Berg et al., 2019). For the first time, we demonstrated the establishment of an ecotropic suspension VPC cultivated under serum-free conditions. The observed vector titers yielding more than  $1 \times 10^6$  TU/mL in NIH/3T3 target cells were superior to previously reported productivities of ecotropic suspensions VPCs derived from human lymphoblast WIL-2 cells reaching only up to  $7.5 \times 10^5$  TU/mL in the same target cells (Chan et al., 2001). Nonetheless, yielded titers using VPC-MSCV-EGFP were in the expected range according to previous reports using the human host cell lines CEM and Namalwa (Pizzato et al., 2001; Reuß et al., 2007). However, and in contrast to VPC-MSCV-EGFP, these packaging cells produced retroviral vector particles pseudotyped with the Env proteins of gibbon ape leukemia virus (GaLV), amphotropic MLV-4070Amc and dual-tropic MLV-10A1mc, respectively. The generated titers ranged from  $4 \times 10^5$  up to  $1 \times 10^7$  TU/mL in a variety of murine and human target cell lines. We also showed that high-titer vector stocks could be generated using ultra-filtration and storage at  $-80$  °C. Upon thawing, titers in the range of  $3.7 \times 10^6$  to  $1.4 \times 10^7$  TU/mL were readily detected. The vector particle harvests were conducted over a period of more than three months indicating a sustainable high productivity of the VPC under continuous selection pressure. Moreover, the scale-up of the serum-free production process to a five-fold higher volume did not impair VPC productivity. Consequently, we anticipate that VPC-MSCV-EGFP would also be of utility for the even larger-scale production processes using bioreactor systems. In addition to murine NIH/3T3 fibroblasts, murine myeloid-like 32D cells were shown to be efficiently transduced. This prompted us to assess the ability of MLV(PVC-211) pseudotype vectors to mediate efficient transduction of primary murine HSPCs. Reaching transduction rates of 27.1 %, 19.4 % and 25.0 % EGFP-positive cells, respectively, demonstrated the efficient gene transfer at a low MOI of two. Li and co-workers (2003) reported similar transduction efficiencies, namely, 21.4 %, 23.1 % and 29.7 % using ecotropic MLV vector particles produced by the stable adherent VPC Phoenix-ECO, and thus decorated with the Env proteins of

MoMLV (Li et al., 2003). The transduction protocol used, showed also similarity to the one applied in this study, using RetroNectin<sup>®</sup>-coated culture dishes, vector samples titrated in SC-1 cells and transduction of lin<sup>-</sup> HSPCs three days post isolation from mice. However, Li et al. employed a MOI of six to achieve the aforementioned gene transfer efficiencies, and thus three times more vectors per target cells as compared to our report here using a MOI of only two. In addition, when we employed MOIs of four and six, superior transduction efficiencies of 34.6 % and 37.1 %, respectively, were observed. This could indicate that the MLV(PVC-211) vectors are superior to MLV (MoMLV) particles in mediating transduction efficiencies into HSPCs. However, and to prove this assumption, a thoroughly conducted study comparing the two vector particle types would need to be performed. Therefore, both VPCs producing the two different ecotropic vector particles should be generated using identical transfer vectors and expression cassettes in the packaging and envelope constructs with the exception of the encompassed *env* genes. In addition, both VPCs would need to be cultivated in identical conditions as differences could presumably have a significant influence on transduction efficiency. An identical transduction protocol would be indispensable to obtain conclusive results. We observed constant vector particle productivity of VPC-MSCV-EGFP over a period of more than three months. This did not indicate genetic instability potentially caused by the undesired stable integration and expression of the transposase gene encoding SB100x mediating the ongoing excision and/or translocation of packaging components. However, we performed genomic PCR-analysis of the polyclonal packaging cells to examine this possibility. With a sensitivity of at least 10 copies in 1000 genomes we were unable to detect SB100x coding sequences. VPC-MSCV-EGFP cells were established using selection pressure applied by three antibiotics at escalating concentrations. We thus anticipate that the polyclonal VPC consists of only a small number of individual clones. In summary, our data make it feasible to assume that the VPC was free of any contamination with the transposase gene. In this POC study, we generated a second generation VPC expressing the structural genes *gag/pol* and *env* devoid of LTRs and other non-coding retroviral sequences from two separate constructs in *trans*. To minimize sequence homologies the packaging construct encompassed wild-type MoMLV coding sequences whereas the PVC-211mc *env* gene originated from FrMLV and, in addition, was human codon optimized (Berg et al., 2019) to minimize sequence homologies. Obviously, both constructs contained the same CMV-derived promoter/enhancer and IRES elements. To our knowledge, this was not reported in previous studies to result in the generation of RCRs in VPCs containing packaging and envelope constructs sharing such genetic elements (Morita et al., 2000). Although we used a first-generation transfer vector, we

did not detect any generation of RCRs in VPC-MSCV-EGFP cells employing RT- and transfer vector rescue-assays. However, the transfer vector employed here contained a 5'-*gag* coding sequence. This sequence homology of the packaging construct and the transfer vector most likely led to recombination events resulting in the transduction of the *gag* coding region within a range of 10–100 copies per 10,000 cell genomes. However, no detectable RT-activities were observed in supernatants of the transduced target cells indicating that no functional *pol* genes were transduced. In future approaches and to further improve the safety profile and minimizing the risk of undesired *gag* gene transfer by homologous recombination with the transfer vector, *gag* gene sequences could be eliminated from the transfer vector packaging signal sequence without significantly affecting vector titer or transgene expression (Kim et al., 1998). Furthermore, self-inactivating (SIN) transfer vectors could be used harboring a large deletion of the viral promoter in the U3-region of the 3'-LTR (Maetzig et al., 2011; Sinn et al., 2005). The 3'-LTR in the plasmid configuration is copied into the 5'-LTR in a target cell upon retroviral vector-mediated transduction, and thus does no longer enable full-length transcription of the transfer vector also excluding the risk associated with MLV promoter activity altering cellular gene expression profiles potentially leading to insertional mutagenesis. Troyanovsky and co-workers (2015) reported the production of SIN  $\gamma$ -RV vector particles employing a *piggyBac* based transposon vector system. We thus anticipate that also the utilization of SIN transfer vector cassettes could be successfully stably integrated in VPCs using *Sleeping Beauty*-derived transposon vector systems to address potential safety concerns. Although not attempted here, it seems feasible to assume that our transposon vector-based approach would also enable the establishment of 293-F based VPCs only expressing the structural *gag/pol* and *env* genes, including heterologous *env* genes of GaLV, MLV-4070Amc, RD114 and dual-tropic MLV-10A1mc to expand the tropism of pseudotyped vector particles to human cells. This would allow for subsequent flexible utilization using different transfer vectors encoding a variety of different transgenes of interest. The transfer vector constructs could be transiently or stably transfected, followed either by direct vector particle harvest two days post transfection or subsequent stringent selection for transgene-positive cells resulting in stable VPCs for continuous particle production, respectively. In another approach, transfer vector cassettes could also be stably integrated in such VPCs using *Sleeping Beauty* based transposon vectors co-transfected with a transposase construct as employed here. This may potentially lead to the undesired decrease of structural viral gene copy numbers per cell, and thus fading structural protein expression in some cell clones upon excision of the respective expression cassettes due to transient overexpression of the transposase. Yet, these cells

could be depleted using stringent selection employing high concentrations of the antibiotics (here puromycin and hygromycin) as the respective resistance genes are coupled to the expression of the *gag/pol* and *env* genes in our constructs. Alternatively, transposon vectors entailing the retroviral transfer vector cassette derived from other transposons could be used to circumvent this potential limitation. For example, a *piggyBac*-derived two-component vector system could be used to stably integrate the transfer vector (Trojanovsky et al., 2015). This way, the *piggyBac* transposase would not recognize the *Sleeping Beauty* TIRs and hence would not mediate the excision of packaging and envelope expression cassettes.

### 3.5 CONCLUSIONS

In summary, we demonstrated in this POC study the utility of transposon vectors and multiplex transfection for the rapid establishment of a suspension packaging cell line yielding high titers of ecotropic MLV(PVC-211) pseudotype vector particles. The yielded vectors mediated efficient gene transduction into murine cell lines and primary  $lin^{-}$  HSPCs. The formation of RCRs was not detected. However, and as a first-generation transfer vector was used, recombination with *gag* gene sequences were detectable. To improve biosafety profiles, future VPCs should be established employing second or third generation transfer vectors. Under constant selection pressure, the VPC described here consistently produced high-titer viral vector particles over a period of more than months. The stable integration of the transposase gene potentially causing genetic instability was not detected. The cultivation in shake flasks could easily be scaled-up to greater volumes without any notable loss of productivity. We thus anticipate that future 293-F cell-derived suspension VPCs established utilizing transposon vector technology should be applicable to bioreactor systems producing high titers of viral vectors at industrial scale.

#### AUTHOR STATEMENT

Yasemin van Heuvel: Conception, Methodology, Formula analysis, Data curation, Writing- Original draft preparation, Visualization. Karen Berg: Conception, Methodology. Tanja Hirsch: Methodology, Visualization, Formula analysis. Kristiana Winn: Methodology. Ute Modlich: Resources, Writing -Review & Editing, Supervision. Jörn Stitz: Conception, Resources, Writing -Review & Editing, Supervision, Project administration, Funding acquisition.



#### DECLARATION OF COMPETING INTEREST

The authors declare that they have no conflict of interest.

#### ACKNOWLEDGMENTS

This work was supported by grants EFRE-0500031 by the European Regional Development Fund (EFRE) of the European Union and the German Federal Ministry of Education and Research, funding program Forschung an Fachhochschulen, contract number 13FH242PX6 to JS. Fig. 1 was created with BioRender.com.

### 3.6 REFERENCES

1. Bauler, M., Roberts, J.K., Wu, C.C., Fan, B., Ferrara, F., Yip, B.H., Diao, S., Kim, Y.I., Moore, J., Zhou, S., Wielgosz, M.M., Ryu, B., Throm, R.E., 2020. Production of Lentiviral Vectors Using Suspension Cells Grown in Serum-free Media. *Mol. Ther. - Methods Clin. Dev.* 17, 58–68.  
<https://doi.org/10.1016/j.omtm.2019.11.011>
2. Berg, K., Schäfer, V.N., Bartnicki, N., Eggenschwiler, R., Cantz, T., Stitz, J., 2019. Rapid establishment of stable retroviral packaging cells and recombinant susceptible target cell lines employing novel transposon vectors derived from Sleeping Beauty. *Virology* 531, 40–47.  
<https://doi.org/10.1016/j.virol.2019.02.014>
3. Berg, K., Schäfer, V.N., Tschorn, N., Stitz, J., 2020. Advanced establishment of stable recombinant human suspension cell lines using genotype-phenotype coupling transposon vectors. In: *Genotype Phenotype Coupling, Methods in Molecular Biology*.  
<https://doi.org/10.1007/978-1-4939-9853-1>
4. Chan, L.M.C., Coutelle, C., Themis, M., 2001. A novel human suspension culture packaging cell line for production of high-titre retroviral vectors. *Gene Ther.* 8, 697–703.  
<https://doi.org/10.1038/sj.gt.3301456>
5. Cooray, S., Howe, S.J., Thrasher, A.J., 2012. Retrovirus and Lentivirus Vector Design and Methods of Cell Conditioning. pp. 29–57.  
<https://doi.org/10.1016/B978-0-12-386509-0.00003-X>
6. Cosset, F.L., Takeuchi, Y., Battini, J.L., Weiss, R.A., Collins, M.K., 1995. High-titer packaging cells producing recombinant retroviruses resistant to human serum. *J. Virol.* 69, 7430–7436.  
<https://doi.org/10.1128/jvi.69.12.7430-7436.1995>
7. Javazon, E.H., Radhi, M., Gangadharan, B., Perry, J., Archer, D.R., 2012. Hematopoietic stem cell function in a murine model of sickle cell disease. *Anemia* 2012.  
<https://doi.org/10.1155/2012/387385>
8. Kim, S.H., Yu, S.S., Park, J.S., Robbins, P.D., An, C.S., Kim, S., 1998. Construction of Retroviral Vectors with Improved Safety, Gene Expression, and Versatility. *J. Virol.* 72, 994–1004.  
<https://doi.org/10.1128/jvi.72.2.994-1004.1998>
9. Li, Q., Liu, Q., Huang, W., Li, X., Wang, Y., 2018. Current status on the development of pseudoviruses for enveloped viruses. *Rev. Med. Virol.* 28, 1–10.  
<https://doi.org/10.1002/rmv.1963>
10. Li, Z., Schwieger, M., Lange, C., Kraunus, J., Sun, H., Van Den Akker, E., Modlich, U., Serinsöz, E., Will, E., Von Laer, D., Stocking, C., Fehse, B., Schiedlmeier, B., Baum, C., 2003. Predictable and efficient retroviral gene transfer into murine bone marrow repopulating cells using a defined

- vector dose. *Exp. Hematol.* 31, 1206–1214.  
<https://doi.org/10.1016/j.exphem.2003.08.008>
11. Lundstrom, K., 2018. Viral vectors in gene therapy. *Diseases* 6(2):42. <https://doi.org/10.3390/diseases6020042>
  12. Maetzig, T., Galla, M., Baum, C., Schambach, A., 2011. Gammaretroviral vectors: Biology, technology and application. *Viruses* 3, 677–713. <https://doi.org/10.3390/v3060677>
  13. Modlich, U., Schambach, A., Zhixiong, L., Schiedlmeier, B., 2009. Murine Hematopoietic Stem Cell Transduction Using Retroviral Vectors, in: Baum C. (Eds) *Genetic Modification of Hematopoietic Stem Cells. Methods In Molecular Biology*TM. Humana Press, pp. 23–31. [https://doi.org/10.1007/978-1-59745-409-4\\_3](https://doi.org/10.1007/978-1-59745-409-4_3)
  14. Morita, S., Kojima, T., Kitamura, T., 2000. Plat-E: An efficient and stable system for transient packaging of retroviruses. *Gene Ther.* 7, 1063–1066. <https://doi.org/10.1038/sj.gt.3301206>
  15. Moritz, T., Dutt, P., Xiao, X., Carstanjen, D., Vik, T., Hanenberg, H., Williams, D.A., 1996. Fibronectin improves transduction of reconstituting hematopoietic stem cells by retroviral vectors: Evidence of direct viral binding to chymotryptic carboxy-terminal fragments. *Blood* 88, 855–862. <https://doi.org/10.1182/blood.v88.3.855.855>
  16. Ory, D.S., Neugeboren, B.A., Mulligan, R.C., 1996. A stable human-derived packaging cell line for production of high titer retrovirus/vesicular stomatitis virus G pseudotypes. *Proc. Natl. Acad. Sci. U. S. A.* 93, 11400–11406. <https://doi.org/10.1073/pnas.93.21.11400>
  17. Piovan, C., Marin, V., Scavullo, C., Corna, S., Giuliani, E., Bossi, S., Galy, A., Fenard, D., Bordignon, C., Rizzardi, G.P., Bovolenta, C., 2017. Vectofusin-1 Promotes RD114-TR-Pseudotyped Lentiviral Vector Transduction of Human HSPCs and T Lymphocytes. *Mol. Ther. - Methods Clin. Dev.* 5, 22–30. <https://doi.org/10.1016/j.omtm.2017.02.003>
  18. Pizzato, M., Merten, O.W., Blair, E.D., Takeuchi, Y., 2001. Development of a suspension packaging cell line for production of high titre, serum-resistant murine leukemia virus vectors. *Gene Ther.* 8, 737–745. <https://doi.org/10.1038/sj.gt.3301457>
  19. Przybylowski, M., Hakakha, A., Stefanski, J., Hodges, J., Sadelain, M., Rivière, I., 2006. Production scale-up and validation of packaging cell clearance of clinical-grade retroviral vector stocks produced in Cell Factories. *Gene Ther.* 13, 95–100. <https://doi.org/10.1038/sj.gt.3302648>
  20. Radek, C., Bernadin, O., Drechsel, K., Cordes, N., Pfeifer, R., Sträßer, P., Mormin, M., Gutierrez-Guerrero, A., Cosset, F.L., Kaiser, A.D., Schaser, T., Galy, A., Verhoeyen, E., Johnston, I.C.D., 2019. Vectofusin-1 Improves

- Transduction of Primary Human Cells with Diverse Retroviral and Lentiviral Pseudotypes, Enabling Robust, Automated Closed-System Manufacturing. *Hum. Gene Ther.* 30, 1477–1493. <https://doi.org/10.1089/hum.2019.157>
21. Reuß, S., Biese, P., Cosset, F.L., Takeuchi, Y., Uckert, W., 2007. Suspension packaging cell lines for the simplified generation of T-cell receptor encoding retrovirus vector particles. *Gene Ther.* 14, 595–603. <https://doi.org/10.1038/sj.gt.3302906>
  22. Rodrigues, A., M., P., Coroadinh, A., 2011. Production of Retroviral and Lentiviral Gene Therapy Vectors: Challenges in the Manufacturing of Lipid Enveloped Virus. *Viral Gene Ther.* <https://doi.org/10.5772/18615>
  23. Salmon, P., Trono, D., 2007. Production and Titration of Lentiviral Vectors. *Curr. Protoc. Hum. Genet.* 1–24. <https://doi.org/10.1002/0471142905.hg1210s54>
  24. Sharma, N., Hollensen, A.K., Bak, R.O., Staunstrup, N.H., Schröder, L.D., Mikkelsen, J.G., 2012. The Impact of cHS4 Insulators on DNA Transposon Vector Mobilization and Silencing in Retinal Pigment Epithelium Cells. *PLoS One* 7. <https://doi.org/10.1371/journal.pone.0048421>
  25. Sinn, P.L., Sauter, S.L., McCray, P.B., 2005. Gene Therapy Progress and Prospects: Development of improved lentiviral and retroviral vectors – design, biosafety, and production. *Gene Ther.* 12, 1089–1098. <https://doi.org/10.1038/sj.gt.3302570>
  26. Soneoka, Y., Cannon, P.M., Ramsdale, E.E., Griffiths, J.C., Kingsman, S.M., Kingsman, A.J., 1995. A transient three plasmid expression. *Nucleic Acids Res.* 23, 628–633.
  27. Stitz, J, 2011. Retroviral vector particles and methods for their generation and use. WO/2011/061336 May 26
  28. Tailor, C.S., Nouri, A., Lee, C.G., Kozak, C., Kabat, D., 1999. Cloning and characterization of a cell surface receptor for xenotropic and polytropic murine leukemia viruses. *Proc. Natl. Acad. Sci. U. S. A.* 96, 927–932. <https://doi.org/10.1007/s10973-016-5240-1>
  29. Troyanovsky, B., Bitko, V., Fouty, B., & Solodushko, V. (2015). Simple viral/minimal piggyBac hybrid vectors for stable production of self-inactivating gamma-retroviruses. *BMC Research Notes*, 8(1), 379. <https://doi.org/10.1186/s13104-015-1354-y>
  30. Tschorn, N., Berg, K., Stitz, J., 2020. Transposon vector-mediated stable gene transfer for the accelerated establishment of recombinant mammalian cell pools allowing for high-yield production of biologics. *Biotechnol Lett.* 42, 1103–1112. <https://doi.org/10.1007/s10529-020-02889-y>
  31. Yee, J.K., Friedmann, T., Burns, J.C., 1994. Generation of High-Titer Pseudotyped Retroviral Vectors With Very Broad Host

- Range. *Methods Cell Biol.* 43, 99–112. [https://doi.org/10.1016/s0091-679x\(08\)60600-7](https://doi.org/10.1016/s0091-679x(08)60600-7)
32. Zeng, L., An, L., Fang, T., Pan, B., Sun, H., Chen, C., Cao, J., Li, Z., Xu, K., 2013. A Murine Model of Hepatic Venous-occlusive Disease Induced by Allogeneic Hematopoietic Stem Cell Transplantation. *Cell Biochem. Biophys.* 67, 939–948. <https://doi.org/10.1007/s12013-013-9587-7>

## 4 PUBLICATION II

**Novel suspension retroviral packaging cells generated by transposition using transposase encoding mRNA advance vector yields and enable production in bioreactors.**

**Yasemin van Heuvel<sup>1,2</sup>, Stefanie Schatz<sup>1,2</sup>, Marc Hein<sup>3,4</sup>, Tanya Dogra<sup>4</sup>, Daniel Kazenmaier<sup>4,5</sup>, Natalie Tschorn<sup>1,2</sup>, Yvonne Genzel<sup>4</sup>, Jörn Stitz<sup>1,\*</sup>**

<sup>1</sup> Research Group Medical Biotechnology and Bioengineering, Faculty of Applied Natural Sciences, University of Applied Sciences Cologne, Campus Leverkusen, Germany

<sup>2</sup> Institute of Technical Chemistry, Gottfried Wilhelm Leibniz University Hannover, Hannover, Germany

<sup>3</sup> Otto-von-Guericke-University Magdeburg, Chair of Bioprocess Engineering, Magdeburg, Germany

<sup>4</sup> Max Planck Institute for Dynamics of Complex Technical Systems, Bioprocess Engineering, Magdeburg, Germany

<sup>5</sup> Faculty of Biotechnology, University of Applied Sciences Mannheim, Mannheim, Germany

\* **Correspondence:** Corresponding Author, joern.stitz@th-koeln.de

**Type of authorship:** First author

**Type of article:** Research article

**Share of the work:** 75 %

**Journal:** Frontiers in Bioengineering and Biotechnology, Section Preclinical Cell and Gene Therapy

**DOI:** 10.3389/fbioe.2023.1076524

**Date of publication:** 04 April 2023

## Abstract:

---

To date, the establishment of high-titer stable viral packaging cells (VPCs) at large-scale for gene therapeutic applications is very time- and cost-intensive. Here we report the establishment of three human suspension cell-derived ecotropic murine leukemia virus (MLV)-based VPCs. The classic stable transfection of an EGFP-expressing transfer vector resulted in a polyclonal VPC pool that facilitated cultivation in shake flasks of 100 mL volumes and yielded high functional titers of more than  $1 \times 10^6$  transducing units/mL (TU/mL). When the transfer vector was flanked by transposon terminal inverted repeats (TIRs) and upon co-transfection of a plasmid encoding for the transposase, productivities could be slightly elevated to more than  $3 \times 10^6$  TU/mL. In contrast, using mRNA encoding for the transposase, as a proof of concept, productivities were drastically improved by more than ten-fold exceeding  $5 \times 10^7$  TU/mL. In addition, these VPC pools were generated within only three weeks. The production volume was successfully scaled up to 500 mL employing a stirred-tank bioreactor (STR). We anticipate that the stable transposition of transfer vectors employing transposase transcripts will be of utility for the future establishment of high-yield VPCs producing pseudotype vector particles with a broader host tropism at large scale.

**Keywords:** sleeping beauty transposon, mRNA transfection, suspension cell, retroviral vector, murine leukemia virus (MLV), stirred-tank bioreactor, gene therapy

## 4.1 INTRODUCTION

Retroviral and lentiviral vectors represent more than 25 % of all viral vectors used in somatic gene therapy today (Ginn et al., 2018). Retroviral vectors mediate efficient stable gene transfer into a variety of cell types including early progenitor and hematopoietic stem cells. This qualifies these vectors to be the favorite choice for the treatment of inherited monogenic diseases. The majority of clinical trials aim at the treatment of adenosine deaminase-deficient severe combined immunodeficiency (ADA-SCID; (Blaese et al., 1995; Aiuti et al., 2002; Gaspar and Thrasher, 2005); X-linked severe immunodeficiency (SCID-X1; (Cavazzana-Calvo et al., 2000; Howe et al., 2008; Hacein-Bey-Abina et al., 2014; Cavazzana et al., 2016) or Wiskott-Aldrich syndrome (WAS; (Boztug et al., 2010; Braun et al., 2014; Hacein-Bey Abina et al., 2015; Ferrua et al., 2019)).

Gamma-retroviral vectors based on murine leukemia virus (MLV) can be produced continuously employing stable viral packaging cells (VPCs) expressing the viral structural genes gag/pol (packaging construct), env (envelope construct) and a transfer vector harboring the gene of interest in *trans* (Maetzig et al., 2011). Most commonly, a transfer vector-free clonal VPC is first generated by screening numerous cell clones for particle production efficiencies (Miller, 1990; Cosset et al., 1995; Morita et al., 2000; Wang et al., 2015). In a second step, the transfer vector of choice is stably transfected followed again by a time-intensive screening of cell clones yielding high-titer vector preparations. To date, mostly adherent VPCs derived from human cell lines are used for clinical grade vector productions hampering the scale-up for preclinical and clinical trials (Coroadinha et al., 2010; Park et al., 2018). In contrast, VPCs that grow in suspension at higher densities as well as in serum-free media allow for viral vector productions in large bioreactors. In pioneering studies, Ghani and colleagues (Ghani et al., 2006, 2007) established a retroviral packaging cell line derived from a human suspension 293SF cell producing retroviral titers of up to  $4 \times 10^7$  transducing units per mL (TU/mL) comparable to yields obtained with adherent VPCs. However, a time-intensive screening needed to be conducted to identify a high-yield transfer vector-positive VPC clone.

We previously reported on the generation of a stable polyclonal VPC using *Sleeping Beauty* (SB)- derived transposon vectors encompassing MLV-derived retroviral vector components, namely, an enhanced green fluorescent protein (EGFP) encoding transfer vector (pSB-LEGFP-N1), a packaging (pSB-Gag/Pol) and an ecotropic envelope construct (pSB-Env) were co-transfected with a transposase expression vector (pSB100X). Within three weeks, stable human adherent, as well as suspension VPCs



were generated. These VPCs produced MLV-based vectors at high titers efficiently transducing murine- and hamster cell lines, murine hematopoietic stem, and early progenitor cells (HSPCs) as well as cell lines from different donor species recombinant expressing the murine cationic amino acid transporter (mCAT; (Berg et al., 2019; van Heuvel et al., 2021). Here, we describe the establishment of a polyclonal 293-F-derived human suspension cell called MuPACK.e in only three weeks employing SB- and MLV-based packaging components.

Moreover, we examined whether the time-intensive screening for high-titer cell clones upon introduction of a transfer vector can be omitted. Therefore, we compared three different approaches: MuPACK.e cells were i) stably transfected with the transfer vector plasmid pLEGFP-N1 harboring the reporter gene *egfp* and a *neomycin resistance* gene (*neoR*) - the most commonly used approach. ii) The transfer vector plasmid now encompassing the TIRs of SB flanking the transfer vector cassette (pSB-LEGFP-N1) was co-transfected with the transposase-expression plasmid pSB100X construct. iii) To increase biosafety and to exclude the genomic integration of pSB100X, and thus the potential sustained expression of the transposase possibly resulting in the re-mobilization of vector components, we co-transfected pSB-LEGFP-N1 together with *in vitro* transcribed mRNA encoding the highly active SB100X transposase (Bire et al., 2013; Kebriaei et al., 2017; Tschorn et al., 2022). Subsequently, all three cell pools were selected for high transfer vector expression using escalating concentrations of neomycin (G418). Functional and physical vector titers were assessed conducting transduction experiments and vector particle quantification using capsid-specific ELISA and a quantitative reverse transcription PCR (RT qPCR). The most productive VPC established, using transposase transcripts, was further characterized employing enhanced cell densities and larger-scale production in an automated STR.

## 4.2 MATERIALS AND METHODS

### 4.2.1 CELLS

Embryonic human kidney suspension FreeStyle™ 293-F cells (Thermo Fisher Scientific, USA) were grown in FreeStyle™ 293 expression medium (Gibco, USA) or Dynamis™ supplemented with 8 mM L-glutamine (for STR, Gibco, USA) or GlutaMAX™ (for shake flasks, Gibco, USA). Cells were cultured at 37 °C, 8 % CO<sub>2</sub>, and at 137 rpm in shake flasks (Thermo Fisher Scientific, USA) using a Minitron shaker incubator (INFORS HT, Switzerland) with an orbit of 5 cm. The adherent NIH/3T3 murine fibroblast target cells (ATCC CRL-1658) were maintained in Dulbecco's modified Eagle medium high glucose, pyruvate (DMEM; Gibco, Germany),

supplemented with 10 % fetal bovine serum (FBS; Gibco, USA) at 37 °C in a humidified atmosphere at 5 % CO<sub>2</sub>. Cell number and viability was accessed using a cell counter (anvajo GmbH, Germany).

#### 4.2.2 PLASMIDS

The MLV-based retroviral transfer vector pLEGFP-N1 (Clontech, USA) harbors the *enhanced green fluorescent protein (EGFP)* and the *neomycin resistance (neoR)* genes. The generation of the transfer vector, the packaging construct, the envelope construct in transposon vector backbones and the transposase construct was described previously (Berg et al., 2019).

The *SB100X* gene was amplified from pCMV-SB100X (Berg et al., 2019) and inserted into pIVTRup (a gift from Ángel Raya (Addgene plasmid #101362; <http://n2t.net/addgene:101362>; RRID: Addgene\_101362). This plasmid served as a template for PCR amplification using primers containing the T7 promoter and polyT tail sequences respectively. The resulting amplicons were subjected to in vitro transcription (IVT) of SB100X-mRNA using HiScribe™ T7 ARCA mRNA Kit (NEB, USA) following the manufacturer's instructions, respectively. After DNase treatment, the mRNA was purified using the Monarch® RNA Cleanup Kit (NEB, USA). RNA purity was confirmed using a Tecan Infinite® and stored in aliquots at -80 °C. The final mRNA encompassed the 5'-Cap, the 5'-UTR, the coding sequence of the transposase, the 3'-UTR and the polyA tail (Tschorn et al., 2022).

#### 4.2.3 ESTABLISHMENT OF STABLE ECOTROPIC MLV-BASED VECTOR PACKAGING CELLS MuPACK.E

Packaging cells were generated by co-transfection of  $3 \times 10^7$  293-F cells in 20 mL shake flask cultures with 35.6 µg of pSB-Gag/Pol, 11.9 µg of pSB-Env and 2.5 µg of the transposase construct using polyethylenimine transfection reagent (PEI: DNA mass ratio of 3:1; linear PEI, 1 mg/mL, MW 40,000; Polysciences Inc., USA). 9 mL fresh medium was added three hours later and a complete medium exchange was performed on the following day. Two days post-transfection, cells were subjected to 4 µg/mL puromycin and 50 µg/mL hygromycin (both InvivoGen, France). Every passage, the concentration of both antibiotics was escalated to a final concentration of 10 µg/mL puromycin and 200 µg/mL hygromycin resulting in a stable VPC bulk population called MuPACK.e within 21 days.

The subsequent transfections with the respective transfer vectors were performed as described in detail (Bauler et al., 2020). For 30 million cells a total amount of 16.5 µg of

pDNA/mRNA was co-transfected. A mass ratio of 1:10 (transposase to transfer vector) for the plasmid-based transposase construct and a mass ratio of 1:1 for the mRNA encoding the transposase was used (PEI: DNA mass ratio of 2:1 and PEI:mRNA mass ratio of 4:1; linear PEI, 1 mg/mL, MW 40,000; Polysciences Inc., USA). The mRNA-PEI mixes in this case were always prepared in a separate tube and PEI was diluted directly into the mRNA-medium mixture. VPCs stably expressing a transfer vector were subjected to neomycin mediated selection pressure four days post-transfection at increasing concentrations ranging from 50 µg/mL to a final concentration of 200 µg/mL. Two weeks post antibiotic selection with neomycin, all three antibiotics were added at final concentrations of 10 µg/mL puromycin and 200 µg/mL hygromycin and neomycin. After three weeks, for transposition-based transfection and 2 months for classical plasmid-based transfection, and rigorous selection, cells were expanded, and cryo-stocks were prepared.

#### 4.2.4 MLV VECTOR PRODUCTIONS IN SHAKE FLASKS AND STR

Stable VPCs were seeded at a viable cell density of  $2 \times 10^6$  cells/mL in 500 mL shake flasks in 100 mL antibiotic-free FreeStyle™ medium or Dynamis™ supplemented with 8 mM L-glutamine. After 24 hours of production, retroviral vectors were harvested by centrifugation at 100 g for 3 min at RT and made cell-free using a PVDF syringe filter with a 0.45 µm pore size (Carl Roth, Germany). Retroviral vector preparations were frozen at -80 °C in 1.8 mL aliquots. For high-density VPC cultivations, the stable VPC was seeded at  $4 \times 10^6$  cells/mL in 250 mL shake flasks in 50 mL Dynamis™ medium supplemented with 8 mM GlutaMAX™ and MLV-based vectors were harvested after 48, 72 and 96 hours.

For larger-scale vector production, cultivation in an STR with a 500 mL working volume (DASGIP® Parallel Bioreactor System, Eppendorf AG, Cat. 76DG04CCBB) was performed. The STR was equipped with one inclined blade impeller (three blades, 30° angle, 50 mm diameter) and a macro-sparger. Production parameters are shown in **table 4**. Prior to inoculation, the stable VPC MuPACK.e.SB-LEGFP-N1<sub>mRNA</sub> was thawed and expanded in Dynamis™ medium supplemented with highest concentrations of antibiotics in shake flasks for two weeks. When cultures showed viabilities > 90 % and a density of  $2 \times 10^6$  cells/mL, cells were centrifuged (300 g, 5 min, RT) and the complete medium was replaced with fresh antibiotic-free Dynamis™ medium. The STR was inoculated with  $0.8 \times 10^6$  cells/mL and ran at 37 °C, pO<sub>2</sub> ≥ 40 %, pH 7.0 (deadband ± 0.3), and 150 rpm for 10 days. During cultivation thirteen independent viral vector harvests (5 mL) were taken from the cultivation vessel, made cell-free by

centrifugation (3000 g, 10 min at 4 °C) and stored at -80 °C. The STR was operated in batch mode.

TABLE 4: Operating bioreactor production parameters.

Parameter	Bioreactor DASGIP® Eppendorf
Basal medium	Dynamis™ + 8 mM L-glutamine
Initial working volume	500 mL
Agitation	150 rpm
Agitation direction	Downflow
Air flowrate	3 L/h
Initial dissolved oxygen (DO)	89.7 %
Temperature	37 °C
pH	7.09 no active control post inoculation
Initial VCD	$0.84 \times 10^6$ cells/mL

#### 4.2.5 VIRAL VECTOR TITRATION AND FLOW CYTOMETRY

To assess the viral vector titers produced by the established VPCs,  $1.0 \times 10^5$  adherent target NIH/3T3 murine fibroblasts were seeded in 2 mL per well in six-well dishes one day prior to transduction (Nunc, Wiesbaden, Germany). Dilutions of 1:1,000 and 1:10,000 and of retroviral vector samples produced in shake flasks in total volumes of 1 mL were added to target cells. The following day, 1 mL of fresh cultivation medium was added to transduced cells. Three days post-transduction, the percentage of EGFP-positive cells was analyzed using flow cytometry (S3e, Bio Rad, USA; FlowJo BD Biosciences, USA) and used to detect gene transduction efficiencies. Vector titers described as transducing units per mL (TU/mL) were calculated as follows:  $\text{titer} = (F\% / (100 \times V_{\text{mL}})) \times S \times D$  wherein F% is the percentage of GFP-positive transduced cells, S represents the number of seeded target cells on the day of transduction, D the dilution factor and  $V_{\text{mL}}$  the volume of viral vector in mL (Fehse et al., 2004).

For the viral vector titration using vectors produced in STR, adherent target cells were seeded in 48-well dishes at  $1 \times 10^4$  cells/well in 0.5 mL one day prior to transduction. The medium was removed and vector containing supernatant samples in different dilutions of 1:10, 1:100 and 1:1,000, respectively, in a total volume of 0.25 mL were added to the target cells. Three days post-transduction, cells were analyzed employing flow cytometry to determine the percentage of EGFP-positive cells. Vector titers were calculated as described previously employing supernatant dilutions resulting in gene transfer efficiencies between 1.0 % and 10.0 % EGFP-positive cells (Salmon and Trono, 2007).

To detect the fluorescence intensities of the three VPCs or transduced target cells expressing the EGFP expressing transfer vector,  $1 \times 10^6$  cells were centrifuged at 100 g for 5 min and the cell pellet was diluted in 1 mL flow cytometry buffer (phosphate-buffered saline (PBS), pH 7.2, 0.5 % bovine serum albumin (BSA) and 2 mM EDTA). Prior to flow cytometry, viability was determined using an anvajo cell counter (anvajo GmbH, Germany). A total of 10,000 gated single cells were subsequently analyzed for EGFP expression.

#### **4.2.6 QUANTIFICATION OF RETROVIRAL VECTORS USING AN ANTI MLV P30 IMMUNOASSAY**

To assess the efficiency of viral vector production, total particle concentration (i.e., physical titer) were quantified using a colorimetric MuLV core p30 antigen ELISA kit (Cell Biolabs, Inc (Cat. VPK-156, USA)). From each cell-free retroviral particle harvest, one sample was used to detect the total p30 concentration. Samples were thawed from  $-80\text{ }^{\circ}\text{C}$  and diluted 1:10,000 in expression medium and assayed in 96-well plates in duplicate.

#### **4.2.7 QUANTIFICATION OF TRANSFER VECTOR TRANSCRIPTS IN VECTOR PARTICLES USING RT-qPCR**

To quantify the viral vector transfer vector RNA (i.e., physical titer), a real-time reverse transcription quantitative PCR (RT-qPCR) was performed. Cell-free and viral vector-containing cell culture supernatant was used for the extraction and purification of vector RNA according to the manufacturer's instructions (NucleoSpin<sup>®</sup> RNA virus kit; Macherey-Nagel, Germany).

A two-step hot start RT-qPCR with sequence-unrelated tagged primers was used to specifically quantify viral vector EGFP mRNA copies (Kawakami et al., 2011). Briefly, an external calibration curve was generated for the EGFP-encoding sequence by amplifying from the pLEGFP-N1 transfer vector template plasmid using the primers: T7-gag/EGFP for 5'- TAATACGACTCACTATAGGGATGGTGAGCAAGGGC -3' and T7-gag/EGFP rev 5'- GCTAGCTTCAGCTAGGCATCTTACTTGTACAGCTCGTCC - 3'. 300 ng of the amplicons were *in vitro* transcribed to RNA for 2 hours at  $37\text{ }^{\circ}\text{C}$  using TranscriptAid T7 High Yield Transcription Kit (ThermoFisher Scientific, USA). Transcribed RNA standards were treated with 10 vol% DNase (30 min,  $37\text{ }^{\circ}\text{C}$ ) followed by 10 vol% EDTA treatment (15 min,  $65\text{ }^{\circ}\text{C}$ ) and purified using an RNA isolation kit (Macherey Nagel, Germany).

Subsequently, a hot start reverse transcription PCR was performed. Here, 1  $\mu$ l of each EGFP mRNA sample and of each generated RNA standard (ranging from 5.0E-07 ng to 5.0E+00 ng), 0.5  $\mu$ l of dNTPs, 6.5  $\mu$ l of nuclease-free water and 0.5  $\mu$ l MLV EGFP tagged RT primer (rev 5'-GCTAGCTTCAGCTAGGCATCTTACTTGTACAGCTCGT CCA -3') was first incubated at 65 °C for 5 min and then at 55 °C for 5 min. For cDNA synthesis, 2  $\mu$ l of 5X RT buffer (Thermo Fisher Scientific, USA), 1.25  $\mu$ l of nuclease-free water, and 0.25  $\mu$ l of Maxima H minus reverse transcriptase (Thermo Fisher Scientific, USA) were added and incubated (30 min, 60 °C), before the reaction was terminated (5 min, 85 °C). The generated cDNA was diluted to 100  $\mu$ l.

To perform the qPCR, 4  $\mu$ l diluted cDNA, 5  $\mu$ l of 2X QuantiNova SYBR green PCR mix (QIAGEN, Germany), and 0.5  $\mu$ l each of 1  $\mu$ M primers EGFP qPCR for 5'-CTCGCCGACCACTACC -3' and EGFP tagged qPCR rev 5'-GCTAGCTTCAGCTAGGCATC-3' were mixed. For the real-time quantification, samples were subjected to initial denaturation (5 min, 95 °C), before 40 amplification cycles (10 s, 95 °C; 20 s, 62 °C) were carried out. The melt curve analysis was between 65 °C and 90 °C. For absolute quantification, a regression curve analysis was formulated by plotting the CT values of ten-fold diluted RNA standards against the log<sub>10</sub> number of the RNA molecules (Frensing et al., 2014).

#### **4.2.8 DETECTION OF REPLICATION-COMPETENT RETROVIRUSES (RCRs): GFP MARKER RESCUE ASSAY AND REVERSE TRANSCRIPTASE (RT) ASSAY**

To ensure that detected gene transfer efficiencies were purely a result of vector-mediated transduction and not caused by the unintended generation of RCRs originating from the recombination of complementary vector components, GFP marker rescue assays were performed in triplicate as previously described in detail (Cosset et al., 1995; Berg et al., 2019; van Heuvel et al., 2021). In addition, NIH/3T3 target cells were exposed to vector preparations, expanded and supernatant of transduced cells was collected after five and twelve days. Subsequently, samples were examined using a reverse transcriptase (RT) assay with a detection sensitivity of 10 pg RT per 40  $\mu$ L sample (Colorimetric reverse transcriptase assay, Roche, Switzerland) following the manufacturer's instructions. Supernatants of stable VPCs and NIH/3T3 cells exposed to the supernatant of naïve 293-F cells served as positive controls and negative controls, respectively (data not shown).

#### 4.2.9 STATISTICS

An unpaired student's t test was used to calculate p values. P values of less than 0.05 were considered statistically significant (\*( $p \leq 0.05$ ), \*\*( $p \leq 0.01$ ), \*\*\*( $p \leq 0.001$ ), \*\*\*\*( $p \leq 0.0001$ )). Graphs and statistics were calculated using GraphPad Prism 7 for Windows 10 software (GraphPad Software, Inc USA).

### 4.3 RESULTS

#### 4.3.1 GENERATION OF STABLE MuPACK.e BASED VPCs

The stable polyclonal suspension VPC MuPACK.e based on ecotropic MLV was established as described using the expression cassettes illustrated in **figure 7**, namely the packaging and envelope construct pSB-Gag/Pol and pSB-Env together with the transposase encoding plasmid pSB100X followed by selection using puromycin and hygromycin. Upon transfection with the constructs illustrated in **table 5**, namely, i) only with pLEGFP-N1, ii) with pSB-LEGFP-N1 and the transposase construct and iii) with pSB-LEGFP-N1 and the mRNA of SB100X, stable cell pools were established in the presence of escalating concentrations of neomycin. Cell-free supernatants of the resultant VPCs MuPACK.e.LEGFP-N1, MuPACK.e.SB-LEGFP-N1 and MuPACK.e.SB-LEGFP-N1<sub>mRNA</sub> were harvested and frozen at -80 °C. Thawed harvests were subjected to three independent titration experiments conducted in triplicate using murine NIH/3T3 target cells. Transduced cells were analyzed three days later for EGFP expression.

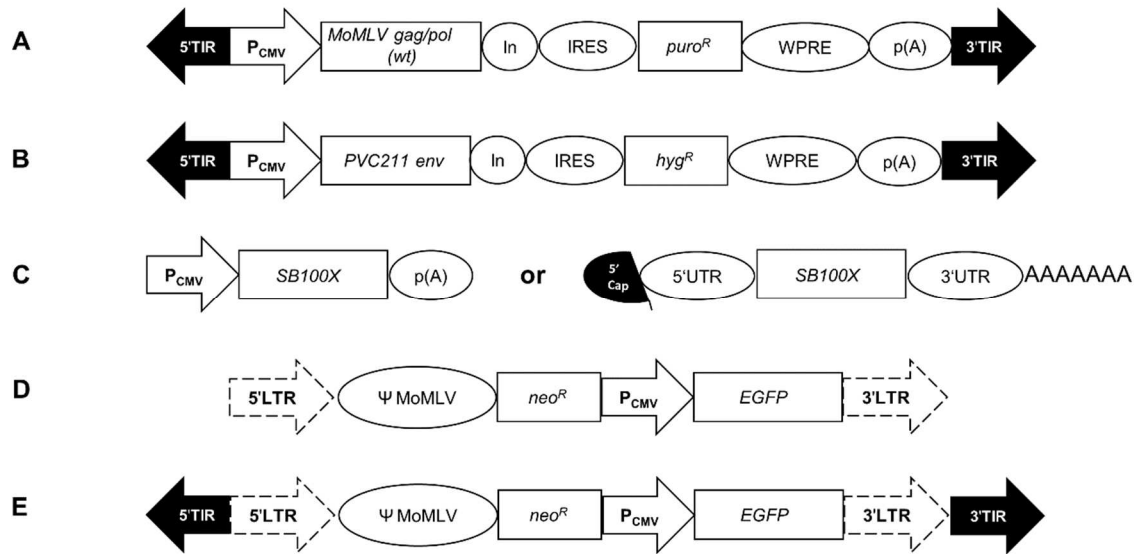


FIGURE 7: Genetic organization of expression cassettes. (A) In the packaging construct pSB-Gag/Pol, a CMV promoter/enhancer element ( $P_{CMV}$ ) drives the expression of the wildtype (wt) Moloney MLV (MoMLV) genes *gag/pol* followed by a synthetic intron (In), an internal ribosome entry site (IRES), a puromycin-resistance gene (*puroR*), the Woodchuck hepatitis virus tripartite posttranscriptional regulatory element (WPRE) and the polyadenylation signal (p(A)) of the bovine growth hormone gene. (B) The envelope construct SB-Env encompasses the human codon-optimized ecotropic envelope gene *env* derived from the Friend MLV molecular clone PVC-211 and the hygromycin-resistance gene (*hygR*). (C, left) The transposase construct pSB100X harbors the human codon-optimized gene of the hyper-active *Sleeping Beauty* transposase *SB100X*. (C, right) The transcript mRNA-SB100X encompasses the 5'Cap, the 5'UTR, the coding sequence of the transposase *SB100X*, the 3'UTR and a polyA tail (AAAAAAA). (D) The transfer vector pLEGFP.N1 encompasses the 5'- and 3'-long terminal repeats (LTRs; dotted arrows) of murine leukemia virus (MLV) flanking the packaging signal  $\Psi$  of MoMLV, a neomycin-resistance gene (*neoR*) and a  $P_{CMV}$  driven EGFP expression. (E) The transfer vector pSB-LEGFP.N1 contains the same genetic elements as pLEGFP.N1 but with the flanking 5'- and 3'-terminal inverted repeats (TIRs; black arrows) of *Sleeping Beauty*.

TABLE 5: Overview of plasmids and mRNA employed to generate polyclonal viral packaging cell lines.

VPC/ Plasmids/mRNA	MuPACK.e	MuPACK.e. LEGFP-N1	MuPACK.e. SB-LEGFP-N1	MuPACK.e. SB-LEGFP-N1 <sub>mRNA</sub>
pSB-Gag/Pol	X	X	X	X
pSB-Env	X	X	X	X
pSB100X	X	X	X	X
mRNA-SB100X				X
pLEGFP.N1		X		
pSB-LEGFP.N1			X	X



### 4.3.2 FUNCTIONAL TITERS OF GENERATED MLV-BASED VECTORS

As depicted in **table 6**, MuPACK.e.LEGFP-N1 generated mean vector titers ranging from  $9.63 \times 10^5$  to  $2.16 \times 10^6$  TU/mL. Viabilities of the VPC at the time of vector harvests varied between 76 and 85 %. With viabilities of always  $> 90$  %, MuPACK.e.SB-LEGFP-N1 revealed slightly higher titers of  $2.17 \times 10^6$  to  $3.21 \times 10^6$  TU/mL. MuPACK.e.SB-LEGFP-N1 showed stable productivity over a period of two months in the presence as well as absence of selection pressure (data not shown).

TABLE 6: Functional titers in TU/mL and physical titers in ng/mL (ELISA) of vector particles harvested from the stable VPCs. Frozen-thawed vector preparations harvested from volumes of 100 mL VPC cultures at viable cell densities (VCD) of  $4 \times 10^6$  cells/mL in FreeStyle™ medium in 500 mL shake flasks were titrated in triplicate in NIH/3T3 target cells or measured in a 1:10,000 dilution in an ELISA. In harvests 2 and 3 of VPC MuPACK.e.SB-LEGFP-N1mRNA cells were cultivated in Dynamis™ expression medium supplemented with 8 mM GlutaMAX™. Standard deviations (SD) of mean are indicated.

VPC	Harvest	Viability [%]	Mean Titer [TU/mL]	SD	Mean p30 [ng/mL]	SD
MuPACK.e. LEGFP-N1	1.	76	$9.63 \times 10^5$	$\pm 0.35 \times 10^5$	$6.38 \times 10^4$	$\pm 0.96 \times 10^4$
	2.	85	$1.26 \times 10^6$	$\pm 0.05 \times 10^6$	$8.02 \times 10^4$	$\pm 1.71 \times 10^4$
	3.	85	$2.16 \times 10^6$	$\pm 0.15 \times 10^6$	$1.16 \times 10^5$	$\pm 0.22 \times 10^5$
MuPACK.e. SB-LEGFP-N1	1.	92	$2.17 \times 10^6$	$\pm 0.11 \times 10^6$	$3.75 \times 10^4$	$\pm 1.89 \times 10^4$
	2.	90	$2.66 \times 10^6$	$\pm 0.21 \times 10^6$	$5.04 \times 10^4$	$\pm 0.17 \times 10^4$
	3.	94	$3.21 \times 10^6$	$\pm 0.32 \times 10^6$	$4.24 \times 10^4$	$\pm 1.54 \times 10^4$
MuPACK.e. SB-LEGFP-N1 <sub>mRNA</sub>	1.	80	$5.12 \times 10^7$	$\pm 0.51 \times 10^7$	$7.20 \times 10^4$	$\pm 0.78 \times 10^4$
	2.	73	$2.00 \times 10^7$	$\pm 0.05 \times 10^6$	$1.86 \times 10^5$	$\pm 0.24 \times 10^5$
	3.	90	$3.10 \times 10^6$	$\pm 0.55 \times 10^6$	$1.12 \times 10^5$	$\pm 0.01 \times 10^5$

The VPC MuPACK.e.SB-LEGFP-N1<sub>mRNA</sub> showed by far the highest productivity when cells were cultured in FreeStyle™ medium (harvests 1). Titers of  $5.12 \times 10^7$  TU/mL were detected at VPC viabilities of 80 %, respectively. When the VPC was expanded in Dynamis™ (harvests 2 and 3), known as one of the mediums of choice for batch- and fed-batch cultivation of highly efficient mammalian producer cells, to prepare for cultivation at high densities in an STR or in perfusion cultivation, cell viabilities varied between 73 % and 90 % and vector titer productivities of  $2.00 \times 10^7$  TU/mL and  $3.10 \times 10^6$  TU/mL were achieved. For high viable cell density cultivations (VCD), represented in **figure 8**, VPCs were cultivated at 50 mL scale and vector particle harvests at VCDs of 9, 10 and  $15 \times 10^6$  cells/mL were titrated in NIH/3T3 cells. VCDs correlated with functional vector titers ranging from  $3.58 \times 10^6$  TU/mL at  $9 \times 10^6$  cells/mL to  $3.43 \times 10^7$  TU/mL at  $15 \times 10^6$  cells/mL in NIH/3T3 cells.

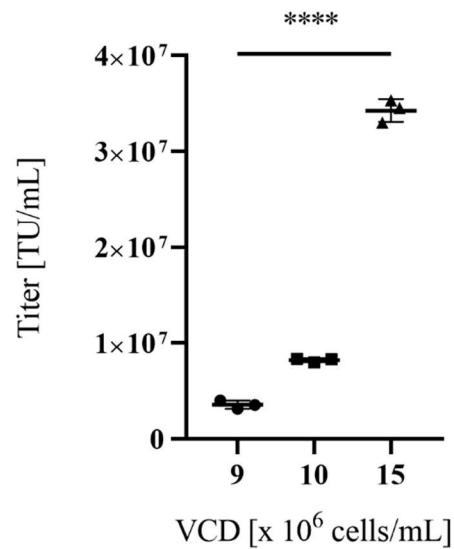


FIGURE 8: Titers of MLV-based vectors in NIH/3T3 target cells of VPC MuPACK.e.SB-LEGFP-N1mRNA. Viral vectors were harvested at three different viable packaging cell densities (VCDs) of 9-, 10- and 15  $\times 10^6$  cells/mL. Data shown represent values of technical triplicate experiments  $\pm$  standard deviation. Statistical significance for all three VPCs with  $n=3$  was determined to  $p \leq 0.0001$  (\*\*\*\*) using the tailed unpaired student's t-test.

These results were supported by the median fluorescence intensities (MFIs) of the three VPCs detected by flow cytometry and represented in **figure 9**. The highest expression of EGFP was detected in MuPACK.e.SB-LEGFP-N1mRNA showing a significantly higher MFI of more than 7,000 compared to the two other VPCs with MFIs between 4,000 and 5,000 ( $p \leq 0.0001$ ).

#### 4.3.3 PHYSICAL TITER ASSESSMENT USING P30 CAPSID-SPECIFIC ELISA

To evaluate the total amount of MLV capsid protein p30 within the three cell-free VPC harvests, a colorimetric ELISA assay was performed, depicted in **table 6**. Average p30 concentrations of all three harvests (not shown in **table 6**) were for MuPACK.e.LEGFP-N1  $8.65 \times 10^4$  ng/mL ( $\pm 2.65 \times 10^4$ ), for MuPACK.e.SB-LEGFP-N1  $4.34 \times 10^4$  ng/mL ( $\pm 0.65 \times 10^4$ ) and for MuPACK.e.SB-LEGFP-N1mRNA  $1.23 \times 10^5$  ng/mL ( $\pm 0.58 \times 10^5$ ).

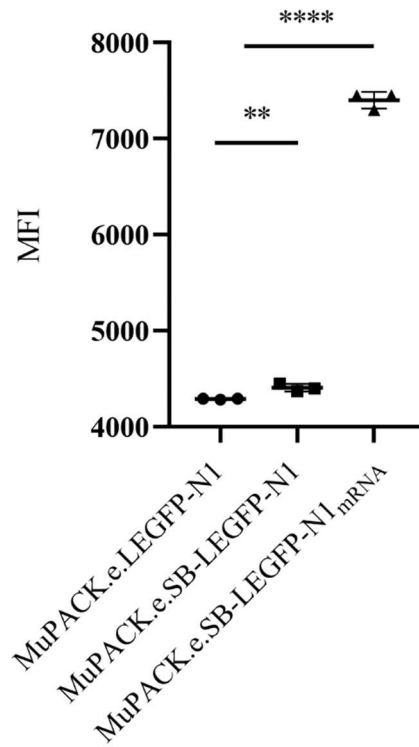


FIGURE 9: Median fluorescent intensities (MFI) of the three VPCs. Data shown represent measurements in technical triplicates  $\pm$  standard deviation. Statistical significance between MuPACK.e.SB-LEGFP-N1 and MuPACK.e.SB-LEGFP-N1<sub>mRNA</sub> based data with  $n=3$  was determined to  $p \leq 0.0001$  (\*\*\*\*); between MuPACK.e.LEGFP-N1 and MuPACK.e.SB-LEGFP-N1 was  $p \leq 0.01$  (\*\*) using a tailed unpaired student's t-test.

#### 4.3.4 DETECTION OF TRANSFER VECTOR TRANSCRIPTS IN VECTOR PARTICLES USING RT-QPCR

The different functional vector titers were likely to result from different transfer vector transcript amounts available for packaging into the vector particles. Thus, RT-qPCR was performed in duplicate using frozen cell-free samples from all VPC vector harvests and EGFP-specific primers. As illustrated in **figure 10**, the mean amount of mRNA detected confirmed the trend observed in functional vector titers obtained from all three VPCs. MuPACK.e.SB-LEGFP-N1<sub>mRNA</sub> ( $1.16 \times 10^{10}$  to  $2.78 \times 10^{10}$  copies/mL) revealed the highest amount of packaged transcripts as compared to MuPACK.e.SB-LEGFP-N1 ( $6.60 \times 10^9$  to  $8.96 \times 10^9$  copies/mL), while MuPACK.e.LEGFP-N1 yielded the lowest amounts of encapsidated mRNA ( $1.42 \times 10^9$  to  $4.16 \times 10^9$  copies/mL).

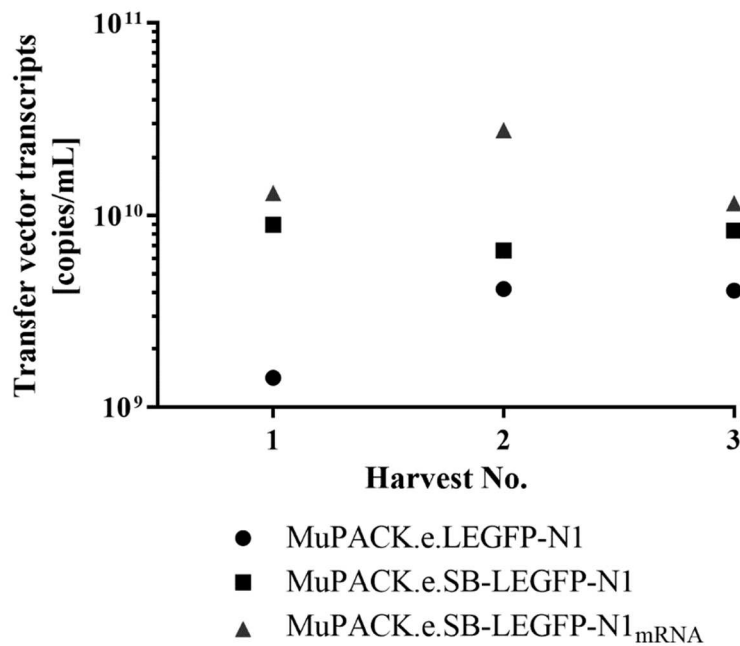


FIGURE 10: Physical titers of transfer vector transcripts in vector particles measured by real-time RT-qPCR. EGFP-specific primers WERE used to generate amplicons using LEGFP-N1 mRNA packaged in vector particles in each three harvests of the three VPCs (depicted in **table 5**). Mean values from assays performed in analytical duplicates are indicated.

#### 4.3.5 PRODUCTION AND FUNCTIONAL TITER OF MLV VECTORS IN STR

To enable vector production at a larger-scale, a cultivation in STR was examined with the most productive stable VPC MuPACK.SB-LEGFP.N1<sub>mRNA</sub>. Cells were cultivated for 10 days in 500 mL Dynamis™ medium supplemented with 8 mM L-glutamine in the absence of antibiotics and medium change as described in detail in materials and methods. All production parameters are represented in **table 4**. **Figure 11** shows the retroviral vector titers detected in NIH/3T3 cells during a 10-day STR procedure. The VPC culture revealed increasing productivity up to day 6. As illustrated in **figure 11A** and at the onset of the culture process, the titers were rather low with about  $1 \times 10^5$  TU/mL correlating with the low VCD of less than  $2 \times 10^6$  cells/mL. With increasing VCDs up to  $6 \times 10^6$  cells/mL (**figure 11B**) the transduction-competent particle numbers also increased, generating titers of up to  $2.81 \times 10^6$  TU/mL in NIH/3T3 cells on day 6. From day 6 to day 7, productivity stayed on a small plateau and from day 7 on, the VCDs continuously decreased to  $3.72 \times 10^6$  cells/mL resulting in declining titers of  $2.04 \times 10^6$  TU/mL down to  $1.4 \times 10^5$  TU/mL at the end of the STR process on day 10. A linear scalability was observed until day 6 of production remaining then on a plateau. From day 8 on and as no medium exchange was performed, the vector production rate, as well as vector titer, dropped in correlation with the decline in VCDs and

viability, respectively. While osmolality slightly decreased over time from 249 to 212 mOsm, pH values remained considerably stable around 7.0 (+ deadband) throughout the process (**figure 11C**).

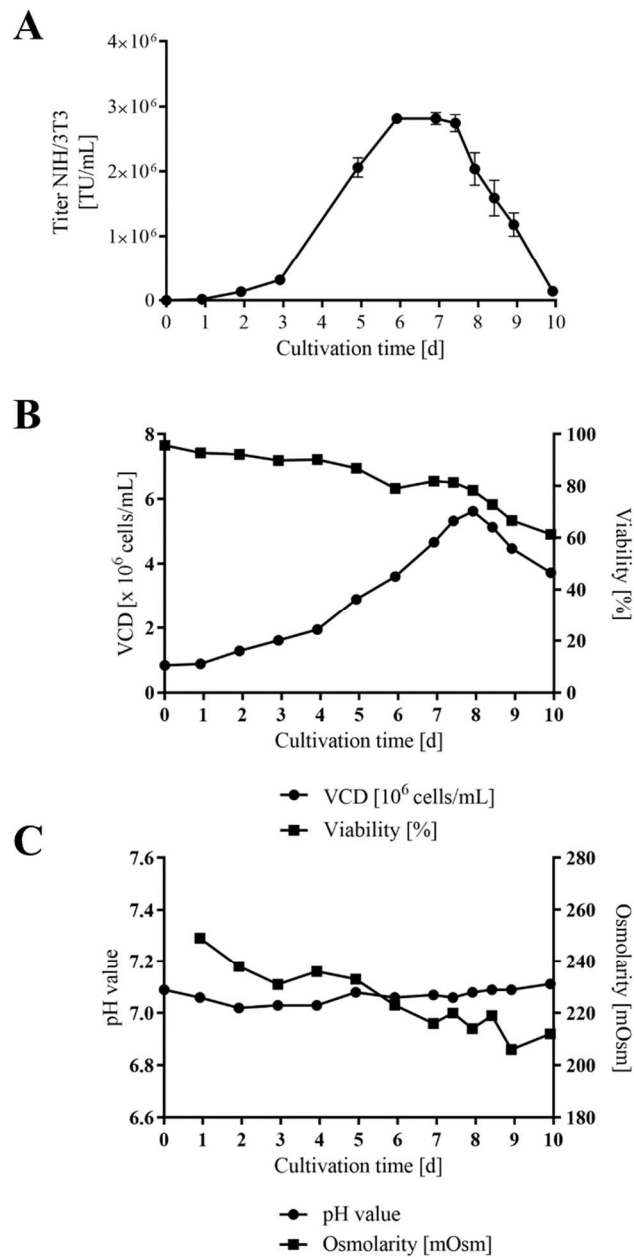


FIGURE 11: Stirred-tank bioreactor vector particle production over 10 days with VPC MuPACK.e.SB-LEGFP-N1mRNA. (A) NIH/3T3 cells were transduced with cell-free MLV vector containing supernatants harvested at twelve time points. Data points represent average values of technical triplicates, standard deviations are shown as vertical error bars. (B) Viable VPC density (VCD) in  $1 \times 10^6$  cells/mL (dots) and cell viability in % (rectangles) during a ten-day STR cultivation. (C) PH values (dots) and Osmolarity in mOsm (rectangles) during a ten-day STR cultivation.

#### 4.3.6 DISCUSSION

To facilitate high vector yield production in larger-scale, stable suspension VPCs are indispensable. In the first step and within only three weeks, we established the polyclonal ecotropic MLV-derived suspension VPC MuPACK.e using transposon vector components as previously described and shown in efficient transduction experiments in murine myeloblast-like cells as well as in hematopoietic stem and progenitor cells (Berg et al., 2019; van Heuvel et al., 2021). The establishment of stable high-titer producing VPCs co-expressing the transfer vector of choice is a tedious and time-consuming process. To reduce development times, we compared in a proof-of-concept study three stable gene transfer techniques. In one approach i) the transfer vector plasmid pLEGFP-N1 was simply stably transfected. ii) The transfer vector cassette was flanked by SB-derived TIRs and co-transfected with a transposase plasmid construct pSB100X aiming at the stable transposition of the viral vector component into the VPCs genomes. iii) To exclude the undesired stable transfection of pSB100X and the expression of the transposase over a period of one week, pSB-LEGFP-N1 was co-transfected with mRNA-SB100X.

MuPACK.e.LEGFP-N1 produced vectors at high titers of  $9.63 \times 10^5$  to  $2.16 \times 10^6$  TU/mL in NIH/3T3 target cells. These results exceed previously reported ecotropic MLV vector titers. Chan et al. established a human lymphoblast WIL-2 cells-derived suspension VPC using conventional plasmid transfection obtaining  $7.5 \times 10^5$  TU/mL in NIH/3T3 cells (Chan et al., 2001). MuPACK.e.SB-LEGFP-N1 generated only moderately improved titers between  $2.17 \times 10^6$  to  $3.21 \times 10^6$  TU/mL.

MuPACK.e.SB-LEGFP-N1<sub>mRNA</sub> showed drastically increased productivities reaching vector titers of up to  $5.12 \times 10^7$  TU/mL when cultivated in 100 mL shake flask volumes at a cell density of  $4 \times 10^6$  cells/mL in FreeStyle™ or in Dynamis™ medium, respectively. In addition, these results were supported by the physical titers detected using an anti-p30 ELISA. MuPACK.e.SB-LEGFP-N1<sub>mRNA</sub> showed p30 amounts a power of ten higher than the other two VPCs. Contaminations with RCRs resulting from recombination events of the retroviral vector components were not detected in any of the vector particle preparations conducting a GFP-marker rescue assay and a sensitive RT-detection assay (data not shown).

The high abundance of the transfer vector RNA available for packaging in concert with high level expression of Gag/Pol is a crucial prerequisite for the efficient formation of transduction-competent vector particles (Berg et al., 2019; Sweeney and Vink, 2021). Flow cytometric analysis of the three VPCs revealed different expression levels of

EGFP, and thus indicating differences in transfer vector transcript amounts. MuPACK.e.SB-LEGFP-N1<sub>mRNA</sub> showed a significantly higher MFI compared to the two other VPCs.

Consequently, and to assess whether these differences also mirrored the copy number of encapsidated transfer vector mRNA, vector particle harvests from all three VPCs were examined using RT-qPCR. MuPACK.e.SB-LEGFP-N1<sub>mRNA</sub> showed the highest amount of packaged transfer vector RNA followed by MuPACK.e.SB-LEGFP-N1 and MuPACK.e.LEGFP-N1 confirming the trend observed in functional vector titers. However, the RNA levels were two to three orders of magnitude higher than the functional titers in respective target cells. This gap using two different measurements was previously reported by Geraerts and colleagues 2006 (Geraerts et al., 2006). Transfer vector RNAs detected in the supernatant of the VPCs using qPCR are not necessarily encapsulated (Onafuwa-Nuga et al., 2005; Rulli et al., 2007; Eckwahl et al., 2016).

FreeStyle™ medium limits the VCDs to  $4 \times 10^6$  cells/mL. We thus conducted a high VPC density experiment in Dynamis™ medium in a 50 mL shake flask scale. VCDs could be elevated to  $15 \times 10^6$  cells/mL reaching titers of up to  $3.43 \times 10^7$  TU/mL in NIH/3T3 cells. This encouraged us to conduct a first STR pilot cultivation. VPC MuPACK.e.SB-LEGFP-N1<sub>mRNA</sub> was expanded to a larger-scale using 500 mL volume STR employing Dynamis™. When the VPC was seeded at a VCD of  $0.84 \times 10^6$  cells/mL, the maximal cell density peaked at  $5.62 \times 10^6$  cells/mL along with increasing viability. The highest vector titers of up to  $2.81 \times 10^6$  TU/mL were obtained on day 6. Osmolality and pH values were moderately decreasing and remained stable, respectively, over the entire cultivation period of 10 days. Viral vector titer and viability decline from day 7 on correlated with the decreasing availability of essential nutrients within the expression medium and with an increase of metabolic degradation products. In addition, and observed previously, the amount of cellular proteases may have increased, and thus degraded MLV vector particles (Genzel et al., 2010; Petiot et al., 2011; Hein et al., 2021). Therefore, and to reach productivities of  $> 1 \times 10^7$  TU/mL in fed-batch approaches, the seed VCD of VPCs should be increased to 2 or  $4 \times 10^6$  cells/mL allowing the cells to linearly grow to densities of  $15 \times 10^6$  cells/mL or even higher values within the first two or three days. Alternatively, fully automated high-density perfusion reactors could be employed, and process parameters would need to be optimized.

Serving as a proof-of-concept, only one VPC pool per transfection technique of the transfer vector was examined here. However, our findings still strongly indicate that

the use of transposon-encoding mRNA is superior to the employment of a plasmid-based transposase. Using a ratio of 1:1 (transposase transcript to transfer vector plasmid) instead of a ratio of 1:10 (plasmid-based transposase to transfer vector plasmid) for stable transposition presumably led to a higher availability of active transposases, elevating transposition efficiency. The high amount of transposon-encoding mRNA probably resulted in enhanced copy numbers of SB-LEGFP-N1 per cell genome. Transposase transcripts limit transposase expression to about 18 hours (Bire et al., 2013). Within this time, a high abundance of transiently co-transfected transposon donor plasmids are available and are likely to facilitate superior transposition. Using mRNA-based transposase appears to avoid overexpression inhibition (OPI) or cytotoxicity observed when plasmid-based transposase constructs are used (Grabundzija et al., 2010; Galla et al., 2011; Bouuaert et al., 2013). OPI is most likely a result from high transposase activity over a period of up to 14 days. A prolonged expression of the transposase could lead to re-mobilization and possibly depletion of packaging and envelope donor expression cassettes resulting in less efficient production of viral vector particles.

To date, larger-scale retroviral vector productions are mainly done in cell-factories, packed-bed bioreactors or fixed-bed-bioreactors using adherent VPCs. The cells thus grow on a limited area of the stacked cultivation devices or scaffolds such as beads and microfibers (Merten et al., 2001; Wang et al., 2015; Powers et al., 2020). MLV vectors pseudotyped with the Env proteins of Gibbon ape Leukemia virus (GaLV) with titers ranging from  $7.88 \times 10^5$  up to  $3 \times 10^7$  TU/mL could be generated using fixed-bed bioreactors in volumes of 200 mL to 1.4 L, respectively (Merten et al., 2001). Using STRs and perfusion reactors instead, generated MLV vectors pseudotyped with GaLV Env and vesicular stomatitis virus G protein (VSV-G) with titers between  $5 \times 10^5$  and  $3.1 \times 10^7$  TU/mL, respectively (Merten et al., 2001; Ghani et al., 2006). The packaging cell line PG13 stably transfected with a transfer vector reached titers of  $2 \times 10^6$  TU/mL and a *piggy-bac* transposon SIN packaging cell line produced titers of up to  $3 \times 10^6$  TU/mL. A non-transposon-based amphotropic suspension packaging cell line called 293GP-A2 produced titers of  $4 \times 10^7$  TU/mL at a VCD of  $12 \times 10^6$  cells/mL. However, the mean time to develop this stable VPC took months (reviewed in Park et al., 2018).

Ecotropic MLV vectors, as shown here in our proof-of-concept study, were not yet produced at such titers. We thus anticipate that the VPC MuPACK.e and our approach to rapidly establish VPCs within only three weeks using mRNA transposase transcripts will foster future viral vector productions at larger-scale to facilitate



preclinical *ex vivo* gene transfer studies into murine primary cells, respectively. The methodology reported here should also be applicable to SIN-transfer vectors harboring a much lower risk for proto-oncogene insertion sites (Hacein-Bey-Abina et al., 2014; Morgan et al., 2021). Transposon vector utilizing strategies should also prove useful to establish VPCs producing vectors with a broadened host cell range utilizing heterologous envelope proteins stemming from the amphotropic molecular clone MLV 4070Amc or dual tropic 10A1mc (Ghani et al., 2007), GaLV, feline endogenous retrovirus RD114 or VSV-G (Ghani et al., 2006; 2009).

#### DATA AVAILABILITY STATEMENT

The raw data supporting the conclusion of this article will be made available by the authors, without undue reservation.

#### AUTHOR CONTRIBUTIONS

Yasemin van Heuvel: Writing -Review & Editing, Original draft preparation, Conceptional, Methodology, Formular analysis, Data curation, Visualization. Stefanie Schatz: Methodology, Formular analysis, Data curation. Marc Hein: Methodology, Visualization, Formular analysis. Tanya Dogra: Methodology, Formular analysis. Daniel Kazenmaier: Methodology. Natalie Tschorn: Methodology. Yvonne Genzel: Resources, Writing -Review & Editing, Supervision. Jörn Stitz: Conceptional, Resources, Writing -Review & Editing, Supervision, Project administration, Funding acquisition.

#### FUNDING

This work was supported by the German Federal Ministry of Education and Research, funding program Forschung an Fachhochschulen, contract number 13FH242PX6 to JS.

#### ACKNOWLEDGMENTS

We would like to thank Nancy Wynserski for her great help to develop the RT-qPCR protocol.

#### CONFLICT OF INTEREST

The authors declare that the research was conducted in the absence of any commercial or financial relationships that could be construed as a potential conflict of interest.

## PUBLISHER'S NOTE

All claims expressed in this article are solely those of the authors and do not necessarily represent those of their affiliated organizations, or those of the publisher, the editors and the reviewers. Any product that may be evaluated in this article, or claim that may be made by its manufacturer, is not guaranteed or endorsed by the publisher.

#### 4.3.7 REFERENCES

- Aiuti, A., Slavin, S., Aker, M., Ficara, F., Deola, S., Mortellaro, A., et al. (2002). Correction of ADA-SCID by stem cell gene therapy combined with nonmyeloablative conditioning. *Science* (1979) 296, 2410–2413. doi: 10.1126/science.1070104.
- Bauler, M., Roberts, J. K., Wu, C. C., Fan, B., Ferrara, F., Yip, B. H., et al. (2020). Production of Lentiviral Vectors Using Suspension Cells Grown in Serum-free Media. *Mol Ther Methods Clin Dev* 17, 58–68. doi: 10.1016/j.omtm.2019.11.011.
- Berg, K., Schäfer, V. N., Bartnicki, N., Eggenschwiler, R., Cantz, T., and Stitz, J. (2019). Rapid establishment of stable retroviral packaging cells and recombinant susceptible target cell lines employing novel transposon vectors derived from Sleeping Beauty. *Virology* 531, 40–47. doi: 10.1016/j.virol.2019.02.014.
- Bire, S., Gosset, D., Jégot, G., Midoux, P., Pichon, C., and Rouleux-Bonnin, F. (2013). Exogenous mRNA delivery and bioavailability in gene transfer mediated by piggyBac transposition. *BMC Biotechnol* 13. doi: 10.1186/1472-6750-13-75.
- Blaese, R. M., Culver, K. W., Miller, A. D., Carter, C. S., Fleisher, T., Clerici, M., et al. (1995). T lymphocyte-directed gene therapy for ADA-SCID: Initial trial results after 4 years. *Science* (1979) 270, 475–480. doi: 10.1126/science.270.5235.475.
- Bouuaert, C. C., Lipkow, K., Andrews, S. S., Liu, D., and Chalmers, R. (2013). The autoregulation of a eukaryotic DNA transposon. *Elife* 2013, 1–23. doi: 10.7554/eLife.00668.
- Boztug, K., Schmidt, M., Schwarzer, A., Banerjee, P. P., Díez, I. A., Dewey, R. A., et al. (2010). Stem-Cell Gene Therapy for the Wiskott–Aldrich Syndrome. *New England Journal of Medicine* 363, 1918–1927. doi: 10.1056/NEJMoa1003548.
- Braun, C. J., Boztug, K., Paruzynski, A., Witzel, M., Schwarzer, A., Rothe, M., et al. (2014). Gene Therapy for Wiskott–Aldrich Syndrome—Long-Term Efficacy and Genotoxicity. *Sci Transl Med* 6. doi: 10.1126/scitranslmed.3007280.
- Cavazzana-Calvo, M., Hacein-Bey, S., De Saint Basile, G., Gross, F., Yvon, E., Nusbaum, P., et al. (2000). Gene therapy of human severe combined immunodeficiency (SCID)-X1 disease. *Science* (1979) 288, 669–672. doi: 10.1126/science.288.5466.669.
- Cavazzana, M., Six, E., Lagresle-Peyrou, C., André-Schmutz, I., and Hacein-Bey-Abina, S. (2016). Gene Therapy for X-Linked Severe Combined Immunodeficiency: Where Do We Stand? *Hum Gene Ther* 27, 108–116. doi: 10.1089/hum.2015.137.
- Chan, L. M. C., Coutelle, C., and Themis, M. (2001). A novel human suspension culture packaging cell line for production of high-titre retroviral vectors. *Gene Ther* 8, 697–703. doi: 10.1038/sj.gt.3301456.
- Coroadinha, A. S., Gama-Norton, L., Amaral, A. I., Hauser, H.,

- Alves, P. M., and Cruz, P. E. (2010). Production of Retroviral Vectors: Review. *Curr Gene Ther* 10, 456–473. doi: 10.2174/156652310793797739.
- Cosset, F. L., Takeuchi, Y., Battini, J. L., Weiss, R. A., and Collins, M. K. (1995). High-titer packaging cells producing recombinant retroviruses resistant to human serum. *J Virol* 69, 7430–7436. doi: 10.1128/jvi.69.12.7430-7436.1995.
  - Eckwahl, M. J., Telesnitsky, A., and Wolin, S. L. (2016). Host RNA packaging by retroviruses: A newly synthesized story. *mBio* 7. doi: 10.1128/mBio.02025-15.
  - Fehse, B., Kustikova, O. S., Bubenheim, M., and Baum, C. (2004). Pois(s)on - It's a question of dose.. *Gene Ther* 11, 879–881. doi: 10.1038/sj.gt.3302270.
  - Ferrua, F., Cicalese, M. P., Galimberti, S., Giannelli, S., Dionisio, F., Barzaghi, F., et al. (2019). Lentiviral haemopoietic stem/progenitor cell gene therapy for treatment of Wiskott-Aldrich syndrome: interim results of a non-randomised, open-label, phase 1/2 clinical study. *Lancet Haematol* 6, e239–e253. doi: 10.1016/S2352-3026(19)30021-3.
  - Frensing, T., Pflugmacher, A., Bachmann, M., Peschel, B., and Reichl, U. (2014). Impact of defective interfering particles on virus replication and antiviral host response in cell culture-based influenza vaccine production. *Appl Microbiol Biotechnol* 98, 8999–9008. doi: 10.1007/s00253-014-5933-y.
  - Galla, M., Schambach, A., Falk, C. S., Maetzig, T., Kuehle, J., Lange, K., et al. (2011). Avoiding cytotoxicity of transposases by dose-controlled mRNA delivery. *Nucleic Acids Res* 39, 7147–7160. doi: 10.1093/nar/gkr384.
  - Gaspar, H. B., and Thrasher, A. J. (2005). Gene therapy for severe combined immunodeficiencies. *Expert Opin Biol Ther* 5, 1175–1182. doi: 10.1517/14712598.5.9.1175.
  - Genzel, Y., Dietzsch, C., Rapp, E., Schwarzer, J., and Reichl, U. (2010). MDCK and Vero cells for influenza virus vaccine production: a one-to-one comparison up to lab-scale bioreactor cultivation. *Appl Microbiol Biotechnol* 88, 461–475. doi: 10.1007/s00253-010-2742-9.
  - Geraerts, M., Willems, S., Baekelandt, V., Debyser, Z., and Gijssbers, R. (2006). Comparison of lentiviral vector titration methods. *BMC Biotechnol* 6. doi: 10.1186/1472-6750-6-34.
  - Ghani, K., Cottin, S., Kamen, A., and Caruso, M. (2007). Generation of a high-titer packaging cell line for the production of retroviral vectors in suspension and serum-free media. *Gene Ther* 14, 1705–1711. doi: 10.1038/sj.gt.3303039.
  - Ghani, K., Garnier, A., Coelho, H., Transfiguracion, J., Trudel, P., and Kamen, A. (2006). Retroviral vector production using suspension-adapted 293GPG cells in a 3L acoustic filter-based perfusion bioreactor. *Biotechnol Bioeng* 95, 653–660. doi: 10.1002/bit.20947.
  - Ghani, K., Wang, X., de Campos-Lima, P. O., Olszewska, M., Kamen, A., Rivière, I., et al. (2009).

- Efficient Human Hematopoietic Cell Transduction Using RD114- and GALV-Pseudotyped Retroviral Vectors Produced in Suspension and Serum-Free Media. *Hum Gene Ther* 20, 966–974. doi: 10.1089/hum.2009.001.
- Ginn, S. L., Amaya, A. K., Alexander, I. E., Edelstein, M., and Abedi, M. R. (2018). Gene therapy clinical trials worldwide to 2017: An update. *Journal of Gene Medicine* 20, 1–51. doi: 10.1002/jgm.3015.
  - Grabundzija, I., Irgang, M., Mátés, L., Belay, E., Matrai, J., Gogol-Döring, A., et al. (2010). Comparative analysis of transposable element vector systems in human cells. *Molecular Therapy* 18, 1200–1209. doi: 10.1038/mt.2010.47.
  - Hacein-Bey Abina, S., Gaspar, H. B., Blondeau, J., Caccavelli, L., Charrier, S., Buckland, K., et al. (2015). Outcome following Gene Therapy in Patients with Severe Wiskott-Aldrich Syndrome HHS Public Access Author manuscript. *JAMA* 313, 1550–1563. doi: 10.1001/jama.2015.3253.Outcome.
  - Hacein-Bey-Abina, S., Pai, S.-Y., Gaspar, H. B., Armant, M., Berry, C. C., Blanche, S., et al. (2014). A Modified  $\gamma$ -Retrovirus Vector for X-Linked Severe Combined Immunodeficiency. *New England Journal of Medicine* 371, 1407–1417. doi: 10.1056/NEJMoa1404588.
  - Hein, M. D., Chawla, A., Cattaneo, M., Kupke, S. Y., Genzel, Y., and Reichl, U. (2021). Cell culture-based production of defective interfering influenza A virus particles in perfusion mode using an alternating tangential flow filtration system. *Appl Microbiol Biotechnol* 105, 7251–7264. doi: 10.1007/s00253-021-11561-y.
  - Howe, S. J., Mansour, M. R., Schwarzwaelder, K., Bartholomae, C., Hubank, M., Kempinski, H., et al. (2008). Insertional mutagenesis combined with acquired somatic mutations causes leukemogenesis following gene therapy of SCID-X1 patients. *Journal of Clinical Investigation* 118, 3143–3150. doi: 10.1172/JCI35798.
  - Kawakami, E., Watanabe, T., Fujii, K., Goto, H., Watanabe, S., Noda, T., et al. (2011). Strand-specific real-time RT-PCR for distinguishing influenza vRNA, cRNA, and mRNA. *J Virol Methods* 173, 1–6. doi: 10.1016/j.jviromet.2010.12.014.
  - Kebriaei, P., Izsvák, Z., Narayanavari, S. A., Singh, H., and Ivics, Z. (2017). Gene Therapy with the Sleeping Beauty Transposon System. *Trends in Genetics* 33, 852–870. doi: 10.1016/j.tig.2017.08.008.
  - Maetzig, T., Galla, M., Baum, C., and Schambach, A. (2011). Gammaretroviral vectors: Biology, technology and application. *Viruses* 3, 677–713. doi: 10.3390/v3060677.
  - Merten, O. W., Cruz, P. E., Rochette, C., Geny-Fiamma, C., Bouquet, C., Gonçalves, D., et al. (2001). Comparison of different bioreactor systems for the production of high titer retroviral vectors. *Biotechnol Prog* 17, 326–335. doi: 10.1021/bp000162z.

- Miller, A. D. (1990). Retrovirus Packaging Cells. *Cell* 14, 5–14.
- Morgan, M. A., Galla, M., Grez, M., Fehse, B., and Schambach, A. (2021). Retroviral gene therapy in Germany with a view on previous experience and future perspectives. *Gene Ther* 28, 494–512. doi: 10.1038/s41434-021-00237-x.
- Morita, S., Kojima, T., and Kitamura, T. (2000). Plat-E: An efficient and stable system for transient packaging of retroviruses. *Gene Ther* 7, 1063–1066. doi: 10.1038/sj.gt.3301206.
- Onafuwa-Nuga, A. A., King, S. R., and Telesnitsky, A. (2005). Nonrandom Packaging of Host RNAs in Moloney Murine Leukemia Virus. *J Virol* 79, 13528–13537. doi: 10.1128/jvi.79.21.13528-13537.2005.
- Park, J., Inwood, S., Kruthiventi, S., Jenkins, J., Shiloach, J., and Betenbaugh, M. (2018). Progressing from transient to stable packaging cell lines for continuous production of lentiviral and gammaretroviral vectors. *Curr Opin Chem Eng* 22, 128–137. doi: 10.1016/j.coche.2018.09.007.
- Petiot, E., Jacob, D., Lanthier, S., Lohr, V., Ansorge, S., and Kamen, A. A. (2011). Metabolic and Kinetic analyses of influenza production in perfusion HEK293 cell culture. *BMC Biotechnol* 11, 84. doi: 10.1186/1472-6750-11-84.
- Powers, A. D., Drury, J. E., Hoehamer, C. F., Lockey, T. D., and Meagher, M. M. (2020). Lentiviral Vector Production from a Stable Packaging Cell Line Using a Packed Bed Bioreactor. *Mol Ther Methods Clin Dev* 19, 1–13. doi: 10.1016/j.omtm.2020.08.010.
- Rulli, S. J., Hibbert, C. S., Mirro, J., Pederson, T., Biswal, S., and Rein, A. (2007). Selective and Nonselective Packaging of Cellular RNAs in Retrovirus Particles. *J Virol* 81, 6623–6631. doi: 10.1128/jvi.02833-06.
- Salmon, P., and Trono, D. (2007). Production and Titration of Lentiviral Vectors. *Curr Protoc Hum Genet*, 1–24. doi: 10.1002/0471142905.hg1210s54.
- Sweeney, N. P., and Vink, C. A. (2021). The impact of lentiviral vector genome size and producer cell genomic to gag-pol mRNA ratios on packaging efficiency and titre. *Mol Ther Methods Clin Dev* 21, 574–584. doi: 10.1016/j.omtm.2021.04.007.
- Tschorn, N., van Heuvel, Y., and Stitz, J. (2022). Transgene Expression and Transposition Efficiency of Two-Component Sleeping Beauty Transposon Vector Systems Utilizing Plasmid or mRNA Encoding the Transposase. *Mol Biotechnol*. doi: 10.1007/s12033-022-00642-6.
- van Heuvel, Y., Berg, K., Hirsch, T., Winn, K., Modlich, U., and Stitz, J. (2021). Establishment of a novel stable human suspension packaging cell line producing ecotropic retroviral MLV(PVC-211) vectors efficiently transducing murine hematopoietic stem and progenitor cells. *J Virol Methods* 297, 114243. doi: 10.1016/j.jviromet.2021.114243.
- Wang, X., Olszewska, M., Qu, J., Wasielewska, T., Bartido, S.,

Hermetet, G., et al. (2015). Large-scale clinical-grade retroviral vector production in a fixed-bed bioreactor. *Journal of*

*Immunotherapy* 38, 127–135. doi:  
10.1097/CJI.000000000000072.

## 5 PUBLICATION III

### **Infectious RNA: Human Immunodeficiency Virus (HIV) Biology, Therapeutic Intervention, and the Quest for a Vaccine.**

**Yasemin van Heuvel<sup>1,2</sup>, Stefanie Schatz<sup>1,2</sup>, Jamila Franca Rosengarten<sup>1,2</sup> and Jörn Stitz<sup>1\*</sup>**

<sup>1</sup>Research Group Pharmaceutical Biotechnology, Faculty of Applied Natural Sciences, TH Köln—University of Applied Sciences, Chempark Leverkusen, Kaiser-Wilhelm-Allee, 51368 Leverkusen, Germany

<sup>2</sup>Institute of Technical Chemistry, Leibniz University Hannover, Callinstraße 3-9, 30167 Hannover, Germany

\*Correspondence: joern.stitz@th-koeln.de

**Type of authorship:** First author

**Type of article:** Review

**Share of the work:** 75 %

**Journal:** Toxins MDPI

**DOI:** 10.3390/toxins14020138

**Date of publication:** 14<sup>th</sup> of February 2022



## Abstract:

---

Different mechanisms mediate the toxicity of RNA. Genomic retroviral mRNA hijacks infected host cell factors to enable virus replication. The viral genomic RNA of the human immunodeficiency virus (HIV) encompasses nine genes encoding in less than 10 kb all proteins needed for replication in susceptible host cells. To do so, the genomic RNA undergoes complex alternative splicing to facilitate the synthesis of the structural, accessory, and regulatory proteins. However, HIV strongly relies on the host cell machinery recruiting cellular factors to complete its replication cycle. Antiretroviral therapy (ART) targets different steps in the cycle, preventing disease progression to the acquired immunodeficiency syndrome (AIDS). The comprehension of the host immune system interaction with the virus has fostered the development of a variety of vaccine platforms. Despite encouraging provisional results in vaccine trials, no effective vaccine has been developed, yet. However, novel promising vaccine platforms are currently under investigation.

**Keywords:** retroviruses; HIV; virus replication; mRNA splicing; antiretroviral therapy (ART); HIV vaccines

**Key Contribution:** The genomic RNA of HIV-1 enables employing complex splicing patterns the encryption of multiple proteins within a limited coding capacity. The viral RNA and related proteins mediate toxicity via multiple different pathways. The circumvention of the host cell immune system and the progressing elimination of T helper cells leads to AIDS and opportunistic infections. The aberrant interaction of viral RNA-binding proteins can result in cellular transcriptional deregulations, tumor formation and apoptosis. Besides the further improvement of treatment using ART, vaccination strategies are required to prevent the progression to AIDS upon infection.

## 5.1 INTRODUCTION

RNA viruses are recognized as the leading causes of human infectious diseases. Since the first discovery of infectious RNA viruses in humans in 1900, namely, the yellow fever virus (YFV) from the family *Flaviviridae*, a total of 214 human RNA viruses have been identified, to date [1,2]. Many of these viruses, such as rabies virus (RABV), poliovirus (PV), dengue virus (DENV), and measles virus (MeV), have been transmitted in humans since several hundreds of years [3–6]. In the last couple of decades, numerous human pathogenic RNA viruses have emerged by crossing the species barrier from their natural animal host to humans. These zoonotic transmissions include the Ebola virus (EBOV), Zika virus (ZIKV), severe acute respiratory syndrome coronavirus types 1 and 2 (SARS-CoV-1, SARS-CoV-2), middle east respiratory syndrome coronavirus (MERS-CoV), and of course the human immunodeficiency virus types 1 and 2 (HIV-1, HIV-2) [7]. HIV belongs to the virus family *Retroviridae* and is grouped into the genus *Lentivirus*, first isolated, and identified in 1983 [8,9]. The first transmission to humans most likely occurred during the past century, assumingly between 1920 and 1940. HIV originated from several zoonotic transmission events from non-human primate simian immunodeficiency viruses in Central African chimpanzees (SIVcpz; HIV-1) and West African sooty mangabey monkeys (SIVsmm; HIV-2) [10]. Since 1983, the HIV epidemic has caused an estimated 36.3 million deaths and 37.7 million people living with the infection worldwide in 2020 [11].

The infection with HIV mostly occurs during sexual contact across mucosal surfaces. Maternal-infant exposure and shared use of needles during drug abuse can also facilitate transmission of the virus [12]. The viral tropism mainly targets T helper cells—key regulators of humoral and cellular immune responses—where most of the viral replication takes place. HIV induces the most extreme form of immune subversion caused by pathogens in humans and leads to a continuous loss of CD4+ T helper cells. The diminishment of the T helper cell population increasingly weakens the immune system. During the progression to the acquired immunodeficiency syndrome (AIDS), the ability to prevent infections with other pathogens collapses and causes death by opportunistic infections [10]. HIV also infects other cell types such as macrophages, dendritic cells, and resting T cell subsets. These host cells also play a pivotal role in innate and adaptive immunity. All three cell types often function as viral reservoirs harboring transcriptionally inactive proviruses. This allows HIV to establish a persisting infection and to escape from detection and eradication by immune cells and therapeutic interventions, respectively [10]. To date, antiretroviral therapy (ART) is the only available treatment of infected humans, saving several

thousands of lives each year. ART relies on the combination of three or four virus replication inhibitors. However, ART does not cure infection but limits virus replication, viral load, and thus the progression to AIDS. This transforms the formerly fatal HIV infection to a chronic disease. The required long-term treatment, however, leads to the development of multi-drug resistant viruses and is burdened with undesired adverse effects such as anorexia, nausea, vomiting, and diarrhea associated with the discontinuation of the therapy. ART is also cost-intensive. Considering increasing numbers of infected people, the costs for ART treatment will become unaffordable. Thus, a vaccine is urgently needed to fight the epidemic. However, no sufficiently potent vaccine against HIV has yet been developed [13]. This review will first focus on the genomic organization of HIV, the virion structure, and the replication cycle from virus cell entry to the egress of new infectious particles as well as the cytotoxicity of infection. An overview is provided on antiviral compounds used in ART and phase III clinical trials of vaccine candidates.

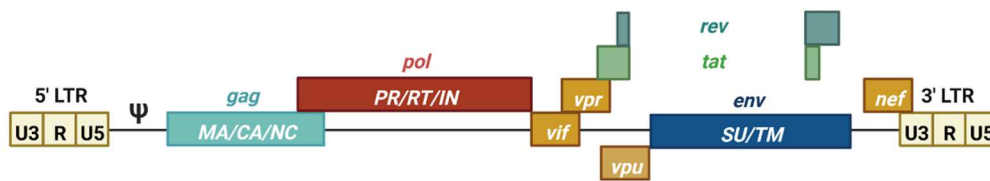
## 5.2 HIV-1 STRUCTURE AND REPLICATION CYCLE

### 5.2.1 GENOME AND VIRION STRUCTURE

The RNA genome (gRNA) of HIV-1, with approximately 9 kb, is considerably small. However, it contains all necessary information to synthesize all 15 proteins needed for replication and assembly of new virions in the infected host cells [14,15]. The viral genome encapsulated in virions consists of a dimer of single stranded positively sensed gRNAs. The different open reading frames (ORFs) are illustrated in **Figure 12**, except for the ORF encoding the antisense protein, yet uncharacterized for its role in the replication cycle [14,16]. The genome encompasses nine different ORFs and some of the viral genes overlap, thus enabling the encryption of many proteins within a limited coding capacity. The genome is flanked by the long terminal repeats (LTRs). They contain the essential information— including the viral promoter—for gene expression, integration, and reverse transcription and are divided into the U3, R, and U5 elements [10]. The cis-acting regulatory element U3 is divided into a modulatory, an enhancer, and a basal region and contains three binding sites for splice factors as well as two binding sites for host cell transcription factors, e.g., Nuclear Factor- $\kappa$ B (NF- $\kappa$ B). The R element contains the trans-acting responsive region (TAR), forming a RNA stem-loop structure that plays an important role in viral replication, i.e., the activation of transcription [17,18]. The U5 element contains the polyadenylation signal (poly A) and regulatory regions for reverse transcription. The U5 element is followed by the primer binding site (PBS), the dimerization initiation signal (DIS), and the major splice-

donor site (D1), all not shown in **Figure 12**. The packaging signal Psi ( $\psi$ ) mediates the packaging of the viral gRNA [19]. The consecutive gag gene encodes the structural viral core proteins. The precursor protein p55-Gag is processed by the viral protease during virion maturation into the subunits matrix (MA), capsid (CA) and nucleocapsid (NC) proteins. The pol gene encodes the subunit viral enzymes protease (PR), reverse transcriptase (RT), and integrase (IN), also originating from a precursor protein upon viral protease-mediated cleavage. The third structural gene env encodes the two envelope glycoproteins gp120-SU (surface unit) and the gp41-TM (transmembrane unit). The pol gene is followed by the two regulatory genes rev and tat as well as four accessory genes vif, vpr, and vpu. Tat and Rev are indispensable for viral replication, accumulate within the host cell nucleus and bind to their cognate mRNA structures, namely, the Rev-responsive element (RRE) and TAR. Rev is an important nuclear export factor that mediates the transport of partially spliced and unspliced viral mRNAs into the cytoplasm. Tat is a strong transcriptional activator [20–22]. Vif, Vpr, and Vpu influence the rate of virus particle production. The accessory nef gene at the end of the gRNA elevates HIV infectivity and downregulates several host cell proteins including CD4 and the major histocompatibility complex I (MHC I) [23]. Moreover, Vif, Vpu, and Nef counteract several cellular restriction factors to secure efficient replication. **Table 7** provides an overview of the best characterized restriction factors.

## HIV-1 genome



## HIV-1 mature virion

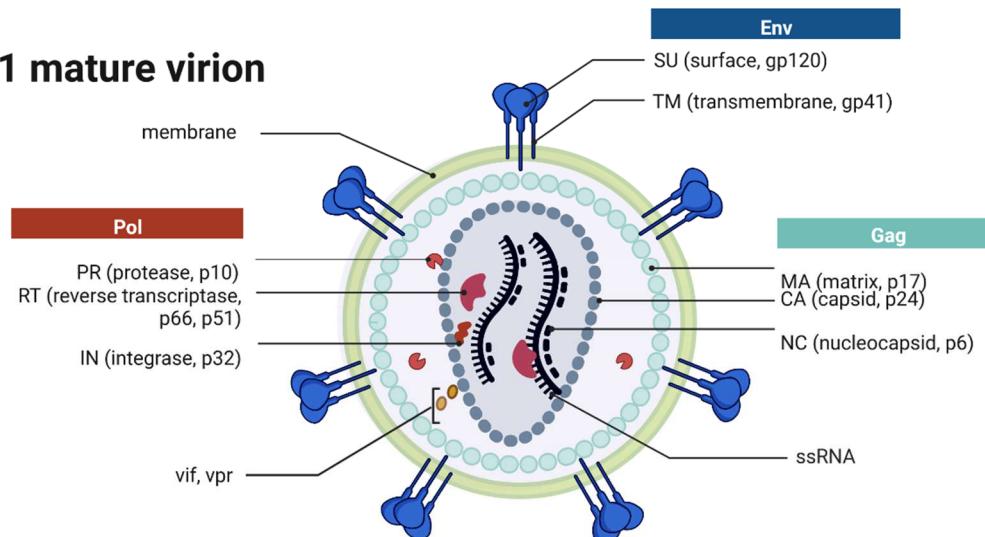


FIGURE 12: HIV-1 genome and virion structure. (Top) Schematic overview of the genomic organization of the HIV-1 genome encompassing the open reading frames coding for the different structural, regulatory, and accessory proteins. The dimeric, linear gRNA is ~9 kb long and flanked by the 5'- and 3'-long terminal repeats (LTRs) that contain the viral promoter and sequences required for reverse transcription, integration, and gene expression. The LTRs are distinguished into cis-acting regulatory elements, namely, U3, R, and U5 regions followed by the packaging signal Psi ( $\psi$ ). Gag encodes the structural proteins matrix (MA), capsid (CA), and nucleocapsid (NC) forming the viral core. Pol codes for the viral enzymes protease (PR), reverse transcriptase (RT), and the integrase (IN). The Pol gene is followed by the two regulatory genes *rev* and *tat* and three accessory genes *vif*, *vpr*, and *vpu*. Env encodes the viral envelope glycoproteins—the surface unit (SU) gp120 and the transmembrane unit (TU) gp41. Env is followed by another accessory gene *nef*. (Bottom) The mature enveloped virion has a spherical shape and is enveloped by a lipid bilayer membrane derived from the host cell containing 7–35 envelope glycoproteins trimers. The inner layer of the membrane anchors the Gag-derived MA proteins and also harbors Vpr and PR. The capsid is found within the center of the virion and contains the two copies of gRNA, RT, and IN. The gRNA is stabilized by the NC proteins.

TABLE 7: Selected examples of cellular HIV restriction factors, mechanism of action, and viral counter measures.

Restriction Factor (RF)	RF Mechanism of Action	HIV Counter Reaction	References
APOBEC3G	Encapsidated into virion, induces G-to-A hyper mutation during reverse transcription	Vif	[24,25]
IFITMs/IFI16	Excludes viral mRNA from polysome processing, inhibits the protein synthesis	Nef	[26]
SAMHD1	Deoxynucleoside triphosphate triphosphohydrolase 1 activity, prevents reverse transcription	Vpx (only HIV-2)	[25]
SerinC3/5	Incorporated into the virion, inhibits membrane fusion	Nef	[27]
Tetherin/BST-2	Anchors virions on the cell surface of infected cells, inhibits virion release	Vpu	[28,29]
TRIM5 $\alpha$ /TRIMCyp /TRIM22	Binds directly to HIV-1 capsids, accelerates uncoating and inhibits reverse transcription	p24-CA variation	[30]

The mature membrane-enveloped HIV-1 virion is spherical in shape with a diameter of approximately 120 nm. The virion's lipid bilayer membrane contains, besides several host cell proteins, ~7–35 envelope trimers consisting of gp120-SU and the gp41-TM [23,31–33]. Both proteins are encoded in the env gene and originate from the Env polyprotein gp160 upon cleavage by the cellular furin-like protease [27]. The membrane envelopes the matrix protein (p17-MA) formed core. The viral capsid is formed by 1000 to 1500 cone-shaped hexameric capsid proteins (p24-CA) [34]. The capsid encapsulates two copies of positive-sense and single-stranded gRNAs stabilized by the nucleocapsid proteins (p7-NC). The mature virion harbors the viral enzymes reverse transcriptase (p66-/p51-RT), protease (p10-PR), integrase (p32-IN), and the accessory protein Vpr that are needed in the maturation process [23,35].

### 5.2.2 RECEPTORS AND CELL ENTRY

**Figure 13** provides an overview of the HIV-1 replication cycle. The HIV-1 infection of a host cell is receptor-dependent and begins with the binding of the envelope protein gp120-SU to the primary host cell receptor CD4 and the co-receptors, chemokine receptor type 5 (CCR5), or C-X-C motif chemokine receptor type 4 (CXCR4). The

binding induces conformational changes of the envelope protein trimers, which leads to the fusion of the virion with the host cell membrane [36]. In more detail, when Env binds to the co-receptor, the virus exposes the fusion peptide at the N-terminus of gp41-TM, which inserts into the cell membrane. Again, dramatic conformational rearrangements, forming a very stable six-helix bundle, pull both membranes into close proximity, reaching a hemifusion state initiating in a last step the fusion of both membranes [36–38]. Although cryo-electron microscopic images of this process exist, many structural aspects of the proteins involved are still not fully understood. Once the fusion pore opens, the virion releases its interior into the cytoplasm of the host cell [39].

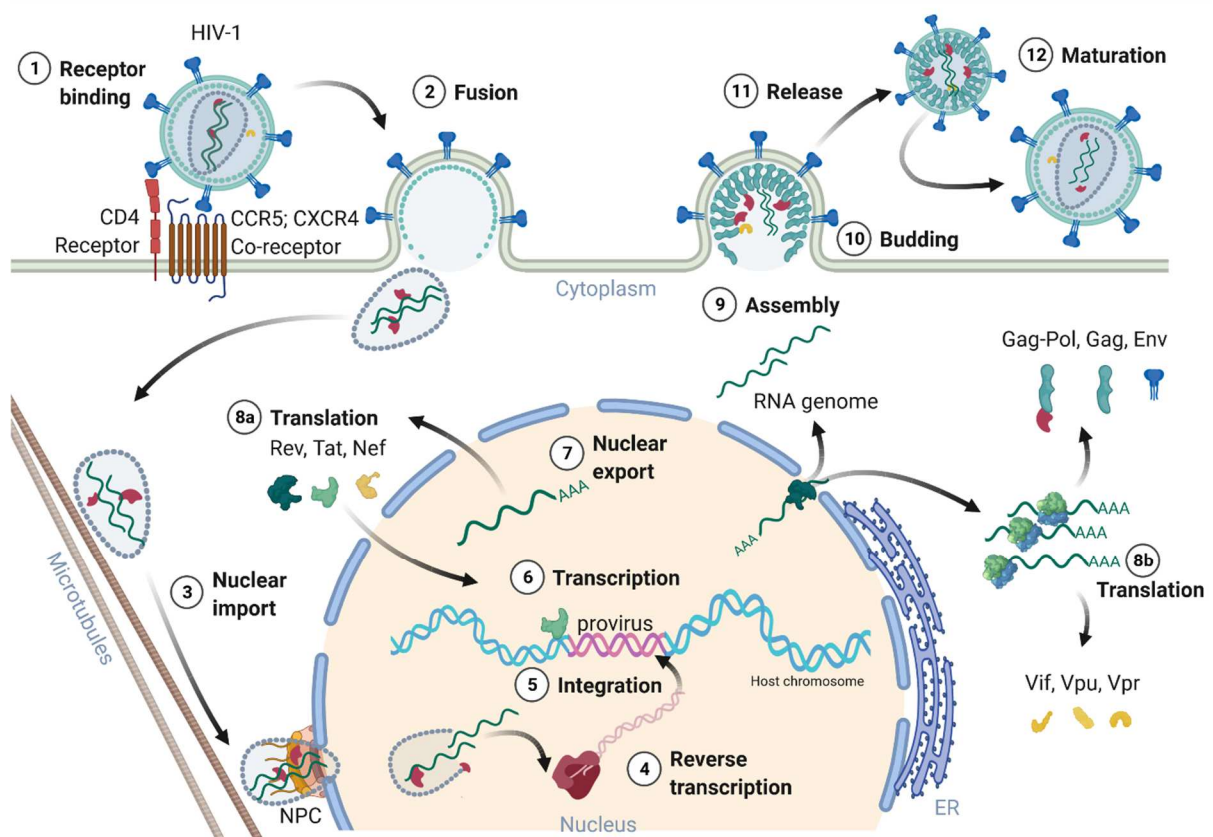


FIGURE 13: Schematic overview of the HIV-1 replication cycle. (1) The HIV-1 infection begins with the binding of the envelope glycoproteins gp120-SU to the primary CD4 receptor and chemokine co-receptors (CCR5 or CXCR4) on the host cell surface. (2) The virion's membrane envelope then fuses with the cellular membrane, releasing the viral capsid into the cytoplasm. (3) The capsid travels along the microtubules to the nucleus. The capsid docks to the nuclear pore complex (NPC) and passes through the pore into the nucleus. (4) The capsid partially uncoats during nuclear cell entry and the reverse transcription of the viral gRNA into the provirus is completed inside the nucleus. (5) The integrase together with cellular co-factors promote the integration of the provirus into highly active chromosomal regions of the host genome. (6) Tat activates gene transcription of the provirus. (7) Rev recruits several host proteins to export the intron-containing viral mRNAs. (8a/8b) Viral mRNA translation occurs within the cytoplasm, first Rev, Tat, and Nef are expressed. Signal peptide containing proteins such as Vpu and Env enter the endoplasmic reticulum (ER) for further posttranscriptional modifications. Glycosylated Env passes through the Golgi apparatus and is cleaved by the cellular furin-like proteases

into gp120-SU and gp41-TM. (9) Two viral gRNAs, Gag, Pol, Env, and Vpr assemble to nascent HIV-1 particles at the cell membrane. (10) Immature HIV-1 particles bud from the cell membrane. (11) Immature HIV-1 particles are released from the host cell. (12) During maturation, Gag and Pol precursor proteins are cleaved by the viral protease into their subunits MA, CA, and NC as well as the viral enzymes PR, RT, and IN. Upon finalization of the maturation, the newly formed HIV-1 virions are prepared for the next host cell infection, reinitiating a new replication cycle.

### 5.2.3 NUCLEAR ENTRY, REVERSE TRANSCRIPTION AND UNCOATING

The cone shaped ~60 nm in diameter capsid, consisting of 250 hexamers and 12 pentamers, was believed to partially uncoat or disassemble already within the cytoplasm [20,23,36,40]. However, most recent studies of Zila and colleagues in 2021 provided astonishing insights into the viral capsid and its trafficking along the microtubules of the cell towards the nuclear pore complex (NPC), revealing that the entire capsid enters the nucleus [40]. As the capsid enters the cytoplasm, it travels along the microtubules towards the nucleus aided by dynein and kinesin-1. Next, the capsid docks with its narrow end to the NPC interacting with the NPC-proteins Nup358 and Nup62. Upon nucleoplasm entry, the capsid partially disassembles, releasing the CA interior [40,41]. Dharan and colleagues discovered that the uncoating as well as reverse transcription are completed within the host cell nucleus [41], which was confirmed by two other studies of Burdick and colleagues [42] as well as Müller and co-workers [43] showing that proviral DNA could only be detected inside the nucleus. Therefore, the reverse transcription already starts within the intact capsid and is finalized upon capsid nucleus entry [42,43]. Burdick et al. also discovered that the complete uncoating takes place 1.5 h before provirus integration into the host cell genome and within a range of 1.5  $\mu\text{m}$  proximate to the gene-rich loci in the euchromatin regions. The reverse transcription of the viral gRNA to proviral dsDNA in infected cells is an important step of the replication cycle. The RNA/DNA-dependent DNA polymerase and RNase H are part of p66-RT, whereas p51-RT provides conformational stability. The reverse transcription starts with the so-called first strand transfer and the synthesis of the single stranded DNA (ssDNA). The ssDNA is hybridized to the 3'-end of the viral genome and the negative strand DNA synthesis continues. The second strand transfer leads then to the transcription of the positive strand DNA and dsDNA synthesis is finalized [44]. Template switching events and error-prone RT activity contribute to the high genetic variability of HIV [45].



#### 5.2.4 GENOME INTEGRATION

Retroviruses permanently integrate their reverse transcribed proviruses into the host cell genome, making the virus an everlasting part of the infected host cell. The integrated provirus can remain dormant within the host, and thus escape from the immune system's detection and response. These properties render HIV to a latent and life-long infection [46]. The proviral integration is mediated by the viral IN in concert with RT [10]. The integrase forms together with the provirus a strong nucleoprotein complex targeting active transcription units for integration into the genome [47]. These units are found in clusters within the less condensed euchromatin characterized by high transcriptional activity. The integration process is divided into two steps. First, the 3'-ends of the provirus is processed and the two terminal nucleotides are removed, exposing a 3'-hydroxyl group and a 5'-overhang. Next, the targeted host DNA is cleaved, and the processed provirus is integrated, ligating the 3'-ends with the 5'-ends of the target DNA [48,49].

#### 5.2.5 TRANSCRIPTION, SPLICING AND PROTEIN EXPRESSION

After integration of the provirus, it either remains transcriptionally silent and enters latency or initiates the production of new virions. The protein expression of HIV-1 is regulated at the epigenetic, transcriptional, and posttranscriptional level [50–52]. Latently infected cells serve as viral reservoirs, resisting eradication during ART and by the immune system due to the absence of target viral protein expression. Latency is induced by infection of resting cells not supporting efficient viral transcription, by inactive proviral integration sites, epigenetic silencing, and by the differentiation of infected effector immune cells to resting memory cells, respectively [52,53]. However, transcription of the provirus and replication can be reactivated. The HIV-1 provirus utilizes the host transcription machinery. Host transcription factors such as NF- $\kappa$ B, specificity protein 1 (Sp1) and activator protein 1 (AP-1) are known activators of HIV transcription [50,51,54]. General transcription factors, mediator, and RNA polymerase II (RNA Pol II) assemble into the preinitiation complex at the 5'-LTR promoter. The HIV-1 5'-LTR contains three possible transcription start sites (TSS) consisting of three consecutive guanosins (G) at the junction between the R and U3 region. Depending on the TSS used for transcription, the untranslated 5'-region (5'-UTR) of the proviral RNA transcript begins with a single, two, or three G residues [55]. Promoter clearing is mediated by the phosphorylation of the C-terminal domain of RNA pol II mediated by the transcription factor TFIIF [56,57]. A short RNA segment of about 60 nucleotides is transcribed before promoter-proximal pausing occurs. The pausing is triggered by the formation of the TAR RNA stem-loop and the binding of negative transcription

elongation factors (N-TEFs) to the preinitiation complex [18,58,59]. The pause is released by Tat binding to TAR, acting as a transcription factor activating positive transcription elongation factor b kinase (P-TEFb) [18,60,61]. In cells, the majority of P-TEFb is part of the 7SK small nuclear ribonucleoprotein (7SK snRNP), in which the catalytic activity of P-TEFb is inhibited by the Hexim-1 protein [62]. McNamara and colleagues suggested a model of Tat-mediated recruitment of the protein phosphatase 1G (PPM1G) to 7SK snRNP to the HIV promoter [61]. PPM1G then dephosphorylates P-TEFb, thus releasing it from the 7SK snRNP complex. When Tat binds to the released P-TEFb it induces re-phosphorylation. Tat and the activated P-TEFb kinase bind to TAR, bringing the kinase in proximity to the stalled RNA Pol II transcription complex. P-TEFb phosphorylates the C-terminal domain of RNA Pol II and N-TEFs, facilitating the elongation of the viral transcript [18,61,63]. The HIV provirus undergoes three transcription phases [53]: During latency no virions are produced, although stochastic transcriptional bursts at the LTR promoter occur [64]. Upon cell activation, e.g., by immune stimuli, host transcription factors such as NF- $\kappa$ B can reactivate viral transcription and induce the expression of Tat protein, enabling a positive feedback loop. The Tat-mediated transcriptional boost results in the production of full-length gRNA ready to be encapsidated or serving as templates for alternative splicing. The full-length gRNA consists of nine partially overlapping ORFs. Therefore, it is alternatively spliced to generate mRNAs, encoding all viral proteins [14,15,65]. The mRNAs are categorized into three classes: (I) full-length, unspliced ~9 kb gRNA, (II) intron-containing, partially spliced ~4 kb mRNAs, and (III) intronless, fully spliced ~2 kb mRNAs [15,66]. The gag and pol gene products are translated from the unspliced full-length gRNA, whereas the other viral proteins Nef, Rev, Tat, Env precursor protein, Vpr, Vif, and Vpu are produced from either partially or fully spliced mRNAs. **Figure 14** provides an overview of the mRNA classes as well as splice donor and acceptor sites present in the HIV-1 mRNA transcript. All HIV mRNAs that undergo splicing utilize the major splice donor site (D1), which defines the first exon between the 5'-Cap and D1 included in all viral mRNAs [65,66]. The exon defined by D4 and either the splice acceptors A3, A4, or A5 and the final exon between A7 and the poly A tail are additional constitutive exons present in all HIV mRNAs [66]. The full-length gRNA transcript is sequentially spliced, starting at D1 to a downstream splice acceptor site and a prerequisite for further downstream splicing [67]. The packaging signal  $\Psi$  is removed, and thus ensures selective full-length gRNAs encapsidation into new virions [68]. Splicing of the viral mRNAs is tightly regulated by the cellular spliceosome. As the splicing of D1 to a downstream splice acceptor is mandatory for all subsequent splice events, suppression of splicing at D1 results in unspliced

transcripts [66,67]. Noteworthy, the 5'-UTR of the full-length transcript can adopt different secondary conformations depending on the number of guanosines at the 5'-Cap [69]. RNAs that start with a 1GCap fold into a structure that masks D1 and favors the formation of RNA dimers, whereas RNAs with 2GCap or 3GCap fold differently and expose the D1 site for splicing [55,70]. To generate partially spliced mRNAs, splicing events are regulated by a complex interplay of several splicing regulatory elements that modulate the usage of splice sites [15]. Unspliced and partially spliced mRNAs harbor the intron, spanning from D4 to A7. This is pivotal as this intron contains the RRE indispensable for the Rev-mediated nuclear export of intron-containing mRNAs.

### HIV-1 mRNA transcripts

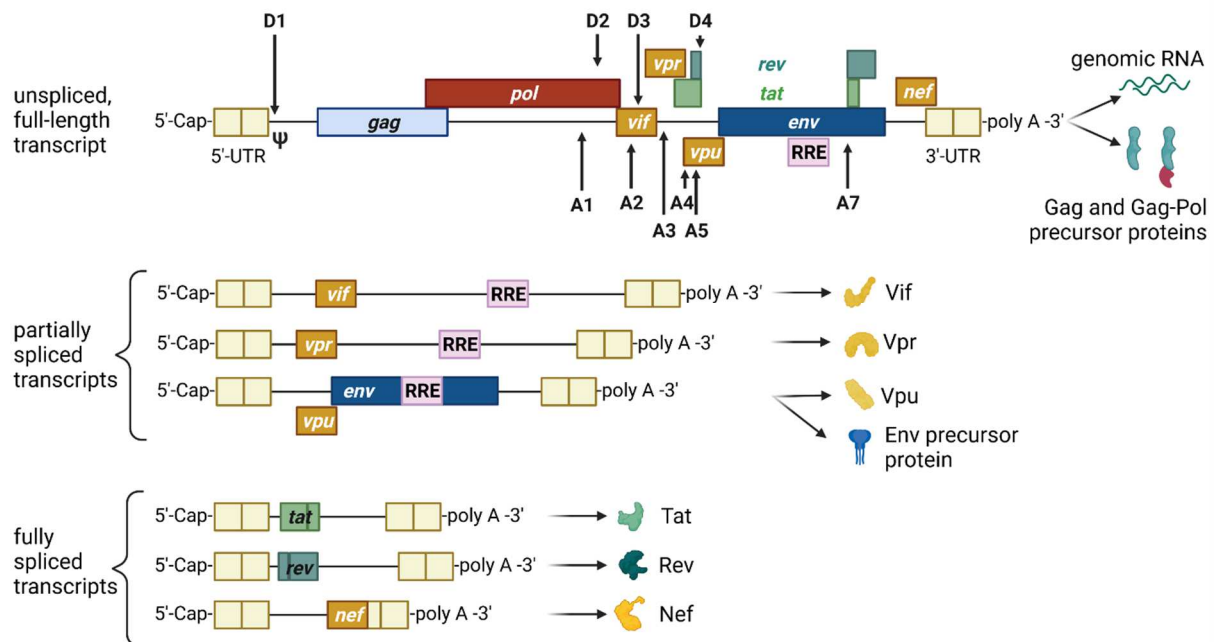


FIGURE 14: HIV-1 mRNA transcripts and splice sites. HIV-1 transcripts are categorized into three classes: unspliced, full-length genomic gRNA (~9 kb), partially spliced, intron-containing mRNAs (~4 kb) and fully spliced, intronless mRNAs (~2 kb). The class of unspliced mRNAs serves either as gRNA later encapsidated into a virion or as a template for the synthesis of Gag and Gag-Pol precursor proteins. Splicing at splice donor sites (D) to splice acceptor sites (A) generates either partially or fully spliced transcripts depending on the splice sites utilized. All processed HIV mRNAs are spliced at the major splice donor site D1 to a downstream splice acceptor, removing the packaging signal  $\Psi$ . In fully spliced mRNAs, the Rev-responsive element (RRE)-containing intron flanked by D4 and A7 is spliced out. The viral proteins Tat, Rev, and Nef are translated from fully spliced mRNAs, whereas Vif, Vpr, Vpu, and the Env precursor protein gp160 are translated from partially spliced transcripts harboring the RRE structure. All transcripts are flanked by untranslated regions (UTR) at the 5'- and 3'-end.

Only intronless mRNAs are exported across the NPC by cellular mRNA export pathways. Consequently, only the fully spliced viral mRNA transcripts are exported to the cytoplasm and translated early in the viral replication cycle, first enabling the expression of Tat, Rev, and Nef proteins. In contrast, incompletely spliced, intron-

containing mRNAs are excluded from the nuclear export pathway and degraded [71,72]. Once expressed, Rev is transported into the nucleus, where it accumulates and co-transcriptionally binds RRE present in incompletely spliced viral transcripts mediating nuclear export [71,73]. This way, HIV circumvents the nuclear mRNA degradation of RRE-containing transcripts. Rev recruits the cellular export factor chromosomal maintenance 1 (CRM1), which mediates the RanGTP-dependent export of the Rev:RNA:CRM-1 complex to the cytoplasm [50,71,73]. In summary, viral gene expression is regulated via transcription, splicing patterns, and RNA structures. Early in the viral gene expression only fully processed mRNAs are translated into the accessory protein Nef and the regulatory proteins Tat and Rev. Nef increases viral infectivity by remodeling signal pathways, downregulating the expression of cell surface proteins such as CD4, major histocompatibility complex-I, and activation of viral transcription through NF- $\kappa$ B [74,75]. Tat activates and stimulates transcription of the provirus by interaction with cellular co-factors at the TAR RNA structure. Rev enables the export of RRE-containing incompletely processed RNAs, shifting the viral protein expression to proteins necessary for the production of new virions. The mRNAs encoding the p55-Gag precursor, p160-Gag-Pol precursor, and Vif and Vpr proteins are translated by polysomes in the cytosol [76]. The Gag-Pol precursor proteins are translated from the full-length gRNA by a ribosomal frameshift during translation [77]. The bicistronic vpu/env mRNA is translated into Vpu and Env precursor gp160 in the rough endoplasmic reticulum (ER). Inside the ER, the Env precursor gp160 assembles into trimers and travels to the Golgi apparatus, in which gp160 gets glycosylated and cleaved by furin-like proteases into the mature Env glycoprotein complex consisting of the subunits gp120-SU and gp41-TM [78]. Env and Vpu are transported to the plasma membrane via the secretory pathway for incorporation into assembling viral particles [78]. In conclusion, all components needed to initiate virus assembly are now available.

### 5.2.6 ASSEMBLY, BUDDING AND VIRION MATURATION

The viral structural Gag precursor protein is sufficient for the formation of new particles. Gag consists of four structural domains separated by protease cleavage sites: the N-terminal MA domain, the CA domain, the NC domain flanked by two spacer peptides (SP1 and SP2), and the C-terminal p6 domain. Each domain performs specific functions during assembly and budding of the viral particle via interactions with viral and cellular proteins and RNAs. The gRNA molecules form a dimer selectively recruited for packaging. Intramolecular and intermolecular interactions of gRNA and Gag polyprotein mediate the selective packaging of the viral genome into assembling

particles. The 5'-UTR of the gRNA folds into complex structures consisting of several stem-loops, including the packaging signal  $\Psi$  and the dimerization initiation signal (DIS). Recent studies by the Summers group revealed that gRNAs exhibiting a sequestered 1GCap at the 5'-UTR are preferentially packaged and adopt a dimer competent conformation [55,79,80]. In this conformation, the DIS is exposed and two gRNA molecules dimerize through intermolecular DIS base pairing. The gRNA dimers expose several binding sites located in the DIS and  $\Psi$  stem-loops for the interaction with the NC domain of the Gag precursor proteins [81]. Binding of gRNA also promotes the dimerization of Gag by protein-protein interactions [82,83]. The Gag:gRNA complex travels to and is anchored in the plasma membrane through the N-terminal myristoylation signal present in the MA domain. HIV-1 assembles at the cell membrane in specific cholesterol- and phosphatidylinositol-(4,5)-bisphosphate (PI(4,5)P<sub>2</sub>)-rich microdomains called lipid rafts. The targeting of Gag to the membrane is regulated by the electrostatic interaction of the highly basic regions located in the MA domain with PI(4,5)P<sub>2</sub> and the binding of tRNA<sup>Lys</sup>, which prevents binding of MA to intracellular membranes [84–86]. In addition, and upon simultaneous binding of PI(4,5)P<sub>2</sub> and gRNA, Gag folds from a compact to an extended conformation enabling the anchoring of the myristoylation signal to the plasma membrane and initiating the multimerization of Gag proteins [87,88]. Gag and Gag-Pol protein multimerization at the plasma membrane is stabilized by CA-CA and CA-SP1 protein-protein interactions [89]. The assembly of Gag at the plasma membrane also induces the retention of Env trimers at assembly sites mediated by an interaction between the Gag MA domain and the C-tail of the Env protein gp41-TM [78]. In addition to Env, the p6 domain of Gag captures Vpr [90]. The growing Gag multimer bends the membrane and forms a spherical nascent particle still connected to the membrane. However, and for the release of the particle, HIV-1 relies on the cellular endosomal sorting complexes required for transport (ESCRT) machinery [91]. Gag recruits the ESCRT complexes via adaptor proteins, which recognize amongst others the amino acid motifs PTAP and LYPX(n)L present in the p6 domain. Tumor susceptibility gene 101 protein (Tsg101) is part of the ESCRT-I complex, binds to the PTAP motif, and forms a supercomplex with ESCRT-II, whereas the adaptor protein apoptosis-linked gene 2-interacting protein X (Alix) recognizes LYPX(n)L and interacts with ESCRT-III. The ESCRT-III complex constricts the membrane and catalyzes the release of the immature particle [91].

The viral particle matures and reorganizes its structural proteins, gRNAs, and enzymes, resulting in the formation of an infectious virion. The maturation is initiated by the auto-activation of the PR sequentially cleaving the Gag and Gag-Pol precursor

proteins releasing the viral enzymes PR, RT, and IN and the structural proteins p17-MA, p24-CA, and p7-NC [92,93]. The structural changes are mandatory for viral infectivity. The NC protein binds tightly to the gRNA dimer and stabilizes linkage between the two gRNA molecules [81,94]. The CA proteins assemble around the NC:gRNA complex encapsidating the viral genome as well as RT and IN [92]. The processing of Gag into its subunits renders the incorporated Env trimers' fusogenicity. The HIV-1 virion concludes the productive cell infection and is now armed for a new replication cycle [95].

### 5.2.7 CYTOTOXICITY OF HIV INFECTION

RNAs are able to cause diseases in many different ways controlling and also disrupting multiple genetic and metabolic pathways in the cell [96]. For example, the transcription of non-coding repeat expansions can lead to toxic RNAs—e.g., the dominantly inherited and multisystemic disease myotonic dystrophy type 1 (DM1), where CTG repeat expansions in the 3'UTR of the DM1 protein kinase (DMPK) gene generate DMPK mRNAs that are trapped in ribonuclear foci, compromising the availability of RNA-binding protein (RBP) levels. RNA foci are believed to sequester bound RBPs and result in toxicity [97,98]. Many disease-related genes encode RBPs, where mutated gene products accumulate as aggregates disrupting cellular functions involved in RNA metabolism [99,100]. Mutations in the RBPs, TAR DNA (TARDBP), FUS RNA-binding protein (FUS), Ataxin 2 (ATXN2) as well as EWS RNA-binding proteins (EWSR1) and many more have been shown to greatly influence disease risks, e.g., amyotrophic lateral sclerosis (ALS) and frontotemporal dementia (FTD) [100]. RNAs also play a pivotal role in the HIV infection cycle and pathogenesis. Viral gene expression is regulated via transcription splicing patterns and RNA structures interacting with viral and host cell RBPs. Cellular RBPs are strongly recruited away from their cellular functions and cellular cognate target RNAs in response to viral infection, which skews the availability of target RNAs towards HIV transcripts [101]. Maybe most importantly, the two viral regulatory trans-acting nuclear RBPs of HIV, Tat and Rev bind cis-acting RNA motifs, the TAR and RRE of the newly transcribed HIV genomic RNA, and thus mediate the deregulation of the host cell RNA and protein synthesis machinery to enable efficient virus replication [102,103]. As illustrated in **Figure 15**, TAR (located in the HIV leader RNA element) and RRE (located in the HIV env gene) motifs fold into complex secondary RNA structures folding into highly conserved stem loops and bulges. Rev and RRE are known to assemble to a homo-oligomeric ribonucleoprotein complex needed for the nuclear export of intron containing messenger RNAs from the nucleus into the cytoplasm.

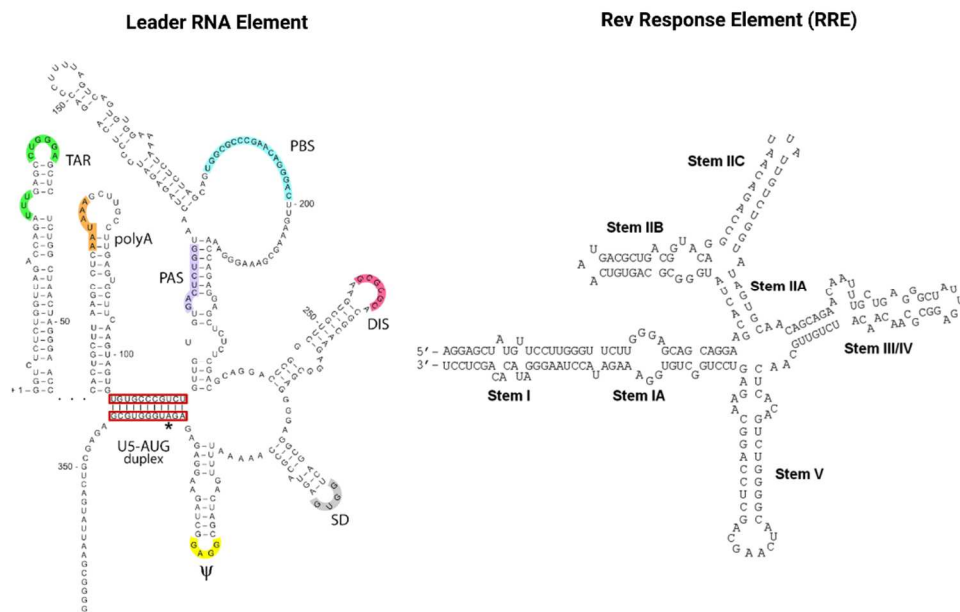


FIGURE 15: The cis-acting RNA regulatory elements of HIV-1. The untranslated highly conserved leader RNA including TAR (left) and the RRE (right). The leader RNA is located in the R and U5 regions of the LTRs of the HIV genome and consists of several regulatory domains: trans-activation response element (TAR); polyadenylation hairpin (polyA); primer activation signal (PAS); primer-binding site (PBS); dimerization initiation sequence (DIS); splice donor (SD); RNA packaging signal ( $\Psi$ ); translation start codon of gag (AUG). The highly conserved RRE is located in the env gene sequence of the viral genome and contains ~350 nucleotides generating seven stem loops and bulges. Stem IIB and Stem IA are defined as primary and secondary Rev-binding sites (left). Left image adapted from: copyright © 2012, Das et al.; CC BY 2.0 license BioMed Central Ltd. [102]. Right image adapted from: copyright © 2012, Fernandes et al.; CC BY-NC 3.0 license Landes Bioscience [103].

RRE as well as TAR are also known as target RNA structures for small molecules intervening the HIV replication cycle. However, until today, little is known about the cytotoxic and disease-causing effects of Rev-RRE in contrast to Tat-TAR [103,104]. Tat recruits the histone acetyltransferases to the viral promoter to activate the transcription of the viral genome. In addition, the RNA helicase A (RHA) acts as a strong TAR-binding cellular co-factor and enhances HIV-1 LTR-driven gene expression and virus production. The RBP Tat enters the nucleus and binds to the host cell RBP P-TEFb. This complex then interacts with TAR on the RNA enhancing the activity of RNA-Pol II, and thus transcription levels [96,105]. Tat's role as the trans-activator of HIV transcription is fully characterized. Other replication-independent effects mediated by the viral soluble protein Tat cause diseases. Cells constantly release Tat into the extracellular space where it exerts cytotoxicity harming cells in proximity, also known as bystander toxicity, as illustrated in **Figure 16** [104].

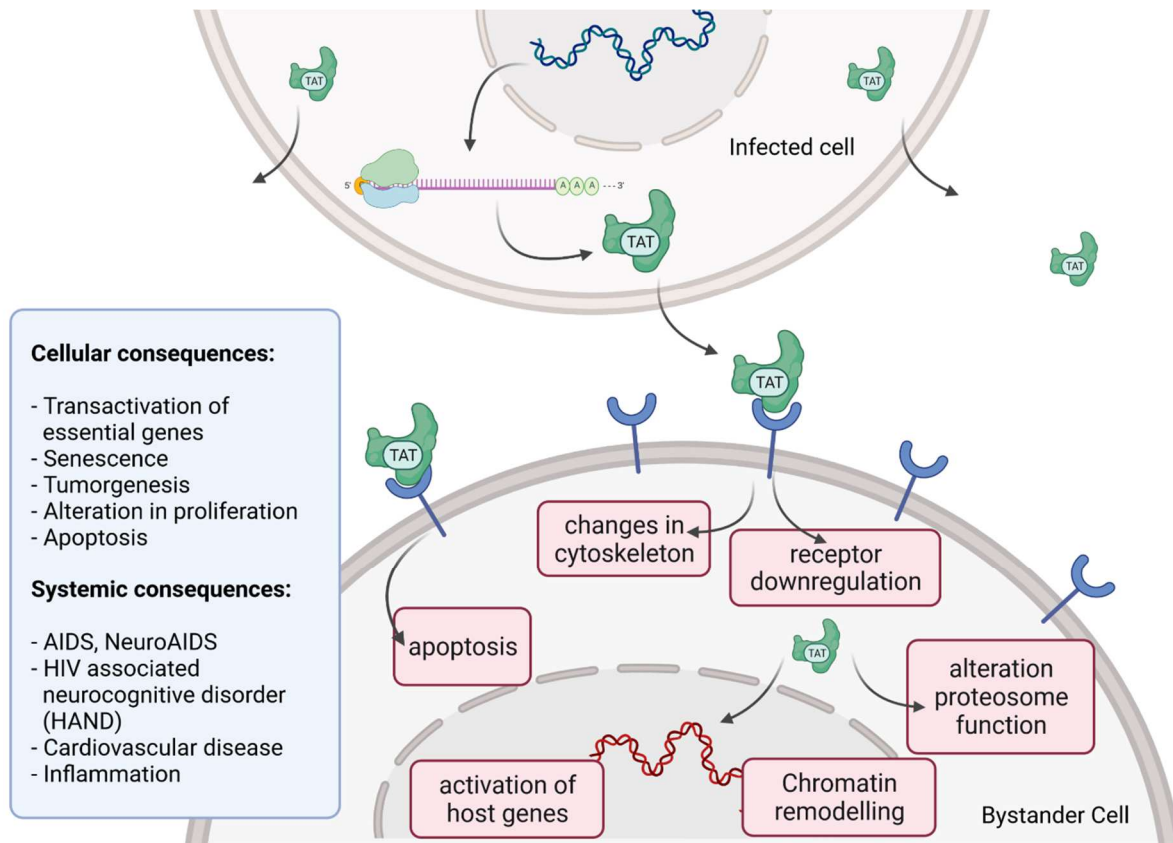


FIGURE 16: HIV Tat bystander toxicity. Upon infection, Tat accumulates inside the cell but is also released into the extracellular compartment. Tat binds to a range of different surface receptors facilitating the cellular uptake by endocytoses. Chromatin remodeling and transcriptional regulation of gene expression in the nucleus as well as receptor downregulation, changes in the organization of the cytoskeleton and induction of apoptosis can be caused by Tat. Different cellular and systemic alterations are listed (left).

Upon infection, Tat accumulates at the inside of the plasma membrane of infected cells and is released into the extracellular compartment. Tat actively recruits monocytes and macrophages into the areas of infection. By binding to a variety of cell surface receptors, e.g., heparan sulfate proteoglycans (HSPGs), chemokine receptors, integrins and lipoprotein receptor-related protein-1 (LRP-1), Tat is able to penetrate into a range of different cell types, amongst others, monocytes, macrophages, lymphocytes, astrocytes, neurons, and cardiomyocytes. Here, Tat induces the release of mainly pro-inflammatory chemokines and cytokines (e.g., CCL2, TNF- $\alpha$ , IL-2, IL-6, IL-8) that activate transmigration and can be toxic to uninfected bystander cells as cardiomyocytes and the heart. Tat alters the activity of the proteasome complex (e.g., down regulation of cellular proteins and up regulation of viral proteins). As one example, Tat induces the upregulation of Connexin 43 mRNA and proteins in cardiomyocytes and increases lipofuscin levels, a known aging heart biomarker. Tat also leads to the alteration of actin filaments, tight junctions and adhesion molecules, altering the organization of the cytoskeleton. Inside the nucleus Tat recruits RBPs and



binds TAR inducing transcriptional regulation of gene expression and chromatin remodeling resulting in many different cellular and systemic alterations [96,104]. In the case of HIV-associated neurocognitive disorder (HAND), Tat can induce neurotoxicity directly as well as indirectly by triggering inflammation through the activation and recruitment of macrophages, microglia and astrocytes into the affected areas of the brain [104]. Latest findings suggest that Tat causes the emergence of neurocognitive and cardiovascular impairments in about 50 to 60% of HIV-infected individuals as a result of Tat's bystander toxicity [104,106].

### 5.3 ANTIRETROVIRAL THERAPY (ART)

HIV transmission occurs most frequently during sexual contact through exposure to infectious virions penetrating mucosal surfaces [12]. Alternative transmission routes include percutaneous inoculation among drug abusers and intrauterine infection from mother to child during pregnancy. HIV detection is earliest possible approximately 10 days post infection, employing sensitive polymerase chain reaction (PCR) tests [107,108]. The primary infection phase, two to four weeks post infection, can be nearly asymptomatic or is characterized by flu-like symptoms while viral plasma levels typically peak at this phase. In the second phase a decline of plasma viremia results in a chronic establishment of a viral set point, i.e., the individual stable viral load (HIV RNA) of an infected person. The typical CD4<sup>+</sup> T cell count in a healthy adult amounts to 500 to 1200 cells per  $\mu\text{L}$ . During the progression of HIV infection to the occurrence of AIDS, a decline of the CD4<sup>+</sup> T cell count to  $<100$  cells per  $\mu\text{L}$  is observed [107,108]. This progressive loss of CD4<sup>+</sup> T cells is accompanied by diseases and malignancies in the infected individuals such as opportunistic infections with *Candida albicans* and *Pneumocystis jirovecii*, resulting in pneumonia or human herpesvirus, causing Kaposi's sarcoma [109,110]. The majority of untreated infected individuals die after a 10-year latency period. In 2020, 73% of the 37.6 million HIV-infected individuals had access to antiretroviral therapy (ART) [111]. ART is a combination of three or four antiviral compounds administered in a lifelong treatment regimen [112–114]. The therapy does not cure HIV-infected patients but enables the management of HIV infection as a chronic disease. To date, more than 40 antiretroviral drugs categorized in 7 classes are approved by the U.S. Food and Drug Administration (FDA) and recommended for HIV treatment [115]. **Table 8** gives an overview of these classes and some exemplary compounds. These antiviral compounds interfere with key steps of the viral replication cycle and comprise the (I) nucleoside reverse transcriptase inhibitors (NRTIs) including the first approved antiretroviral drug zidovudine (Retrovir), (II) non-nucleoside reverse transcriptase inhibitors (NNRTIs), (III) protease inhibitors (PIs), (IV) integrase inhibitors (IIs), (V) (post-)attachment inhibitors (AIs), (VI) CCR5 receptor antagonists, and (VII) fusion inhibitors (FIs). The latter two classes share a similar approach of impeding cell entry. CCR5 antagonists block the cognate co-receptor of CD4<sup>+</sup> T cells. Blocking of CCR5 consequently prevents the initialization of the gp41-TM-mediated membrane fusion [116]. Fusion inhibitors on the other hand directly block the retroviral entry by gp41-TM fusion peptide binding [117]. The recently approved attachment inhibitors Fostemsavir and the therapeutic antibody Ibalizumab-uyk prevent retroviral entry by blocking HIV gp120-SU and the CD4 receptor, respectively [118,119]. Drugs from the other four classes (NRTIs, NNRTIs,

IIs, and PIs) on the contrary do not target retroviral entry but inhibit key enzymes within the replication cycle [13,120,121]. NRTIs and NNRTIs both inhibit provirus synthesis by either leading to chain termination during DNA strand elongation or by directly inhibiting reverse transcriptase activity. Integrase inhibitors, on the other hand, prevent the insertion of the synthesized provirus into the host cell genome. Protease inhibitors block the processing of precursor proteins during assembly and maturation of particles to infectious virions [122].

TABLE 8: Overview of FDA-approved antiretroviral medicines including their mechanism of action, generic names, and approval year amended from HIVinfo.NIH.gov, accessed on 21 October 2021 [115].

Antiretroviral Drug Class	Mechanism of Action	Generic Name, Examples	FDA Approval Year
Nucleoside reverse transcriptase inhibitors (NRTIs)	Incorporation of nucleoside or nucleotide analogues by the reverse transcriptase leads to chain-termination of proviral DNA synthesis [13,120,121]	abacir	1998
		emtricitabine	2003
		lamivudine	1995
		tenofovir disoproxil fumarate	2001
		zidovudine	1987
Non-nucleoside reverse transcriptase inhibitors (NNRTIs)	NNRTIs bind the substrate pocket of the reverse transcriptase, hence reducing polymerase activity and impeding proviral DNA synthesis [13,120,121]	doravirine	2018
		efavirenz	1998
		etravirine	2008
		nevirapine	1996, 2001
		rilpivirine	2011
Protease inhibitors (PIs)	Blocking the active site of the viral protease inhibits the processing of the Gag-Pol polyprotein precursor [13,120–122]	atazanavir	2003
		darunavir	2006
		fosamprenavir	2003
		ritonavir	1996
		saquinavir	1995
Integrase inhibitors (IIs)	Blocking the active site of the viral integrase inhibits insertion of the proviral DNA into host cell genome [13,120,121]	tipranavir	2005
		cabotegravir	2021
		dolutegravir	2013
(Post-)Attachment inhibitors (AIs)	Viral entry is either prevented by binding to gp120-SU (AIs) or by binding the CD4 receptor (post-AIs) [118,119]	raltegravir	2007, 2017
		ibalizumab-uiyk	2018
CCR5 antagonists	Blocking of the co-receptor CCR5 impedes viral entry [116]	fostemsavir	2020
Fusion inhibitors (FIs)	Binding to gp41-TM inhibits viral entry [117]	maraviroc	2007
		enfuvirtide	2003

The use of ART clearly improves the prognosis of HIV-infected individuals since the viral load is suppressed to a steadily low level, preventing progressive CD4+ T cell decline [123,124]. Moreover, the suppression of the plasma viremia to an almost undetectable level decreases the sexual transmission of HIV sustainably, and thus also facilitates prevention of new infections. The risk of acquiring HIV infection within a HIV-discordant relationship is reduced by 96% when ART treatment is initiated immediately or early after HIV diagnosis [125,126]. In addition, a post-exposure

prophylaxis (PEP) treatment with antiretrovirals (tenofovir, emtricitabine, and raltegravir) can reduce the transmission risk by 80%. PEP can be initiated shortly after or ideally within the first 72 h after occupational contact (blood or blood-containing fluid) or after non occupational exposure to the virus [127,128]. ART has to be administered in a stringent and lifelong treatment regimen that requires the variation of different drug combinations to avoid the occurrence of drug resistant viruses quickly emerging during monotherapy [123,129–132]. Since the development and approval of the first antiretroviral drug in 1987, substantial progress in the treatment of HIV infection was achieved [133,134]. The health-related quality of life among HIV-infected individuals has remarkably improved using state-of-the art drugs and advanced dosage schedules [114,123–126]. For example, the recently approved integrase inhibitor cabotegravir and the NNRTI rilpivirine show extended half-life, and thus can be administered on a monthly basis, hence remarkably improving treatment of people living with HIV [135,136]. To reduce the propensity of re-emerging drug resistant variants, promising targets for compound-mediated therapeutic interventions could include conserved mRNA structures such as hairpins, stem-loops, and bulges present in TAR [137–140], RRE [62,141,142], and Psi [143–145], as these structures interact specifically with their cognate viral protein counterparts, namely, Tat, Rev, and the p7-NC of the core protein Gag, respectively. However, these novel approaches are still in the pioneering stage. The use of antiretroviral medicine for pre-exposure prophylaxis (PrEP) became evident as a successful preventive method, despite being associated with high costs and limited access [146]. Positive effects on the reduction of AIDS mortalities resulted from national and global ART campaigns, but in view of slowly decreasing infection numbers and stagnating funding, the ambitious 90-90-90 target is unlikely to be reached [147]. The 90-90-90 target was a strategy based on three pillars, which was announced by the joint United Nations program on HIV/AIDS (UNAIDS) in 2014 claiming that, in 2020 (I) 90% of HIV-infected people will be diagnosed, (II) 90% of those diagnosed will receive ART, and that (III) 90% of those on ART will have a controlled viral load suppression. However, only 5 of more than 40 countries participating in the U.S. President's Emergency Plan for AIDS Relief Countries (PEPFAR) reached this ambitious goal [148]. The U.S. government orchestrates PEPFAR and thereby supports countries with high HIV prevalence in epidemic control such as Uganda, Rwanda, and South Africa [149]. Reaching the global 90-90-90 target expectation remains difficult to meet. The socioeconomic and geopolitical instable situation, e.g., in the Middle East and North Africa present a constant obstacle and complication for achieving the 90-90-90 target [150]. Much alike and in contrast to Western Europe (84-88-90), a strategy progress

monitoring revealed that Eastern Europe (57-45-57) is far away from reaching the target [151]. A quarter of the HIV-infected population worldwide has still no access to ART in 2020, most likely due to infrastructural or financial limitations [111]. Accordingly, HIV treatment in the Western world reveals high lifetime costs of at least USD 326,500 for an individual who acquires HIV at the age of 35 as estimated by a US study from 2015 [152]. The average price of first-line antiretroviral drugs in the US has increased more than 30% since 2012, which is 3.5 times the rate of inflation [153]. Whether the huge financial costs associated with therapy and patient care are manageable in the future appears questionable. A stable health infrastructure is crucial since viral load rapidly rebounds within weeks after ART interruption, supporting the emergence of drug resistant virus variants [154–156].

In view of these obstacles, new global initiatives for HIV prevention are required to tackle the challenges and worldwide financial burden of this epidemic [157]. Ideally, a prophylactic HIV vaccine would be available, enabling global vaccination campaigns in the near future.

## 5.4 VACCINES

### 5.4.1 INTERPLAY OF HIV AND IMMUNE RESPONSE—IMPLICATIONS FOR VACCINE DEVELOPMENT

A financially sustainable alternative to the current ART is necessary to halt the progression of the HIV epidemic. The development of a vaccine followed by a global vaccination campaign is considered the most effective strategy. However, and over the last decades, the development of a potent vaccine has been unsuccessful [158]. The obstacles for the development of a vaccine are rooted in the unique biology of HIV. The high mutation and re-combination rate of the virus generates repeatedly novel immune escape variants [45,46]. In addition, latency facilitates the establishment of viral reservoirs. These two characteristics mainly hamper the design and development of an effective HIV vaccine [159–162]. Besides dendritic cells and macrophages, CD4+ T cells are the main targets of HIV replication. During viremia, infected cells disseminate throughout the body and the viral load increases until hitting a peak after two to four weeks post infection [108]. As part of the cell-mediated immune response, infected CD4+ T cells underlie clearance by CD8+ cytotoxic T lymphocytes (CTLs), which are subsequently activated upon infection and mostly specific for the Gag proteins of HIV [107,108,163]. The following long-term steady state of low viral load is mainly a result of CTL activity limiting HIV replication [164]. Whereas most HIV-producing cells are eradicated by the immune system in the early phase of infection,

small pools of non-activated or naïve infected CD4+ T and T memory cells persist, still containing proviruses [53]. This small pool of cells serves as a viral reservoir that remains dormant until provirus expression is initiated upon antigen- or cytokine-mediated activation [53]. In addition, the CTLs harbor escape variants ensuring that these infected cell pools remain unrecognized by the cellular immune system [46,165]. This way, the viral reservoir represents a genetic archive of numerous HIV variants whose vast majority was generated during viremia [166]. Therefore, vaccination must achieve an early and effective CTL activity in order to control and suppress viremia after infection and hence limit the probability of establishing viral reservoirs. In parallel to the cellular immune response, the humoral immune response is rapidly activated after infection, resulting in the production of HIV-specific antibodies, amongst others, directed against various target epitopes in the Env proteins [167]. However, the vast majority of the Env-binding antibodies target epitopes, not mediating virus neutralization [167,168]. In addition, neutralization-sensitive epitopes are mostly masked by the high density of glycosylation of the Env proteins [169,170]. The resulting glycan shield thus serves as a barrier of virus neutralization by the humoral immune response. Nevertheless, the antibody response still acts as a selection pressure on the virus, leading to the continuous adaptation of Env, and thus the generation of new viral variants evading humoral immune response [168,171]. However, this co-evolution of Env and antibody response also drives the emergence of so-called “broadly neutralizing antibodies” in 20–30% of HIV-1 infected individuals [172]. Broadly neutralizing antibodies (bNAbs) target distinct and highly conserved neutralization-sensitive epitopes on Env trimers [173,174]. BNABs recognize either proteinaceous epitopes or target glycan structures. These bNAbs also mediate the neutralization of a broad range of HIV variants, whereas most induced neutralizing antibodies are variant- or strain-specific [172,175,176]. Highly potent bNAbs were isolated from HIV-infected individuals [177,178]. Noteworthy, a minority of less than 1% of HIV-infected individuals show low viral loads close to the detection limit of very sensitive PCR-mediated diagnostic assays [179,180]. These low viral loads are correlated with a strong CTL response and a decline of infected CD4+ T cells [180]. Individuals exhibiting this trait of spontaneous disease control are summarized under the term “elite controllers” [179,181]. However, the exact mechanism of how elite controllers maintain low viral loads over the years is not yet fully understood despite being of major interest for vaccine design [182]. Some observations point towards an improved Gag-specific T cell response and distinct provirus integration sites [181,183]. This group of HIV-infected individuals therefore represents the closest approximation to how immunity against or control of HIV could be achieved [182,183]. An ideal HIV

vaccine would thus likely consist of two components [184,185]. One component should elicit a bNAb response to combat the large Env diversity of globally circulating HIV variants and consequently prevent infection of new host cells. From the viewpoint of vaccine development, the striking variation of Env represents a particular challenge for the design of potent target antigens [186–189]. Therefore, and to gain a deeper understanding of virus neutralization, the identification and examination of the structure of neutralization-sensitive epitopes became of paramount importance for vaccine development [186,190]. The other component should induce an early and effective T cell response to suppress initial viremia, hence preventing the establishment of viral reservoirs. However, it remains unclear whether a future HIV vaccine will confer sterile immunity or rather facilitate virus replication and viral load suppression, preventing the progression to AIDS and further transmission [191].

#### 5.4.2 HIV CLINICAL VACCINE TRIALS

In 1986, Zagury and colleagues initiated the first HIV vaccine clinical phase I trial in the Democratic Republic of Congo [192]. Since then, numerous further efforts were undertaken to develop a potent HIV vaccine. The scientific challenge of developing a prophylactic vaccine has been pursued now for over three decades and is mainly obstructed by the extremely high variability of HIV and constant immune evasion of new virus variants. The lack of ideal animal models allowing for preclinical testing of vaccine candidates and delivering reliable data predictive for the later desired potency in humans further hampers the development process [193–195]. Three different aims are usually targeted in HIV vaccine development: (I) elicitation of a potent CTL-mediated immunity, (II) induction of a HIV-specific non-neutralizing antibody response, and (III) generation of bNAbs [185]. Several novel approaches to address these assumed “correlates of protection” were already investigated successfully in non-human primate (NHP) studies but revealing limited efficacies in clinical trials in the past years [196]. In this initial regimen, Zagury and colleagues used a vaccinia vector expressing the unprocessed precursor of the HIV envelope protein (gp160). With this approach, it was aimed to induce neutralizing antibodies directed against Env and a parallel potent CTL response [192,197]. The employed vector-based approach was decisive for subsequent vaccination concepts such as the highly anticipated RV144 trial conducted in Thailand in the millennium. In this trial, participants received an attenuated canarypox vector. The regimen comprised prime injections with the canarypox vector vaccine and two booster injections with a recombinant bivalent gp120-SU subunit vaccine derived from HIV subgroup B/E [198,199]. The resulting immune response involved neutralizing antibodies targeting

the V1V2-loop of the gp120-SU and a readily detected CD4<sup>+</sup> T cell response [200–202]. Both were presumably accountable for an observed lower risk of infection [202,203]. The trial demonstrated a 31% efficacy and raised hopes that a prophylactic vaccine could be developed, potentially reaching higher efficacies [198,199]. Due to the moderate success of the RV144 trial in Thailand, the vector and the adjuvanted subunit vaccine components were adapted and applied in different regimens of several follow-up studies such as HVTN 305, HVTN 306, and HVTN 702 [204–206]. Initiated in 2012, HVTN 305 utilized a late boost regimen conducted with 162 HIV-negative RV144 vaccinated recipients aiming at the induction of long-lasting antibody responses. Although immune responses were elevated compared to the initial vaccination series, a durable antibody response was not achieved. In addition, the induced antibodies were barely capable of neutralizing sensitive laboratory-adapted tier 1 HIV strains. Tier 2 strains, representing the circulating viruses, were not neutralized at all [204,207]. The second follow-up study, HVTN 306, started a year later and focused on the effect of less frequent booster injections after the initial vaccination series during the RV144 trial. The prolonged intervals between initial vaccination and boosting showed a positive effect on the magnitude and quality of immune responses [205]. A third follow-up study in South Africa (HVTN 702) was launched in 2016 exchanging the gp120-SU antigens derived from clade B/E with the ones of clade C. The vaccine elicited the desired immune response and reached clinical phase III. However, this new vaccine did not prevent HIV infection in the South African participants [206]. The idea of so-called “mosaic vaccines” was developed to combat the genetic diversity of HIV [208]. Mosaic HIV proteins consist of synthetically shuffled epitopes derived from different HIV variants. Fischer and colleagues disclosed the design of such mosaic HIV vaccines in 2007 and since then research teams around Barouch and Santra picked up the idea and tested mosaic vaccines in rhesus macaques [208–211]. Barouch et al. used a non-replicating adenoviral vector transferring gag, pol, and env mosaic genes. In contrast, Santra et al. administered a DNA vector, containing gag and nef mosaic genes for priming, followed by booster injections with a recombinant vaccinia virus. Despite the use of different mosaic HIV antigens (Gag, Pol, Env, and Nef) in different regimens and vector systems, both studies revealed a similar positive outcome in rhesus macaques. Compared to natural occurring antigens, the mosaic proteins mediated the enhanced T cell epitope recognition of CD8<sup>+</sup> and CD4<sup>+</sup> T cells and the cross-recognition of variants of these epitopes [209–211]. Encouraged by these promising results, an adenovirus serotype 26 (Ad26) vectored vaccine Ad26.Mos.HIV (consisting of Ad26.Mos.1.Env, Ad26.Mos1.Gag-Pol, Ad26.Mos2.Gag-Pol), a modified vaccinia Ankara (MVA)-Mosaic vaccine (MVA.Mos.1.Env, MVA.Mos1.Gag- Pol,



MVA.Mos2.Gag-Pol) and a subsequent protein boost with adjuvanted clade C gp140 proteins (truncated Env precursors) were tested in a clinical trial (APPROACH) and a rhesus monkey challenge study [212]. The envelope glycoproteins were either applied in a membrane-anchored form displayed on the surfaces of Ad26.Mos.1.Env transduced cells or as soluble gp140 proteins used for boosting. The protein boost used in the APPROACH study was thereby composed of stabilized Env trimers of clade C, so called SOSIP trimers, assumed to be crucial for the elicitation of broadly neutralizing antibodies [213,214]. In summary, the vaccine regimen was highly immunogenic in humans and in primates alike. A 67% protection against infection with a Simian-Human Immunodeficiency Virus (SHIV)-SF162P3) was achieved when rhesus monkeys were subjected to six intrarectal virus challenges, raising hopes for the desired potency in humans [212]. In 2017, the vaccine components of the APPROACH study were further used in an efficacy trial in Southern Africa under the study name Imbokodo [212,215]. Imbokodo enrolled 2637 participants in a phase IIb clinical trial. However, the Imbokodo study was recently terminated ahead of schedule due to disappointing efficacy [216]. Yet, there is still hope for the alternative Mosaico trial, started in 2019, which is a related study analyzing the effects of Ad26.Mos.HIV and an adjuvanted clade C gp140 protein vaccination of participants in North America, Latin America, and Europe [217]. Despite advances in the HIV vaccine development, Mosaico and the previously mentioned HVTN 702 were the only two HIV vaccine efficacy trials that enrolled more than 100 participants and reached phase III in the past 10 years. **Table 9** gives a detailed overview of these two trials, including the respective vaccine regimen and trial sites.

TABLE 9: Overview of HIV vaccine phase III clinical trials in the past 10 years with more than 100 participants.

Vaccine Trial	Study ID	Start Year	Vaccine Regimen	Outcome
HVTN 702	NCT 02968849	2016	IM administration of ALVAC-HIV (vCP2438) at months 0 and 1 followed by IM injection of ALVAC-HIV (vCP2438) and bivalent gp120-MF59 adjuvant at a total dose of 200 µg at months 3, 6, and 12	Safe, no serious adverse events were observed, no sufficient protection
Mosaico	NCT 03964415	2019	Priming (IM) with Ad26.Mos4.HIV (Ad26.Mos.1.Env, Ad26.Mos.2S.Env, Ad26.Mos1.Gag-Pol, Ad26.Mos2.Gag-Pol) at months 0 and 3 followed by boosting (IM) with Ad26.Mos4.HIV vaccine and adjuvanted bivalent clade C and mosaic gp140 at months 6 and 12	Results not yet available

Abbreviations: intramuscularly (IM), vCP2438 (canarypox vector 2438), adenoviral vector 26 (Ad26).

## 5.5 OUTLOOK

The extremely high variability of HIV is a challenge for both the further improvement of ART and the development of a prophylactic vaccine. Whereas most current compounds used in ART target viral proteins prone to hyper mutation, mRNA structures such as hairpins and stem-loops can be targeted and due to their conserved structure potentially offer an opportunity to overcome the issue of virus variability. However, ART is cost-intensive, and thus unlikely to be globally applicable and accessible. Therefore, and to fight the global epidemic of HIV, a prophylactic vaccine appears indispensable. An efficient vaccine against HIV infection facilitating future global vaccination campaigns needs to induce a strong and sustainable cellular and humoral immune response including the elicitation of cross-clade neutralizing bNAbs. The concept of using multiple mosaic antigens appears promising in order to cover the high diversity of globally circulating HIV variants. However, and after three decades of conducting clinical trials, it seems likely that the combination of different vaccine platforms will be required to generate an efficient polyvalent vaccine. This will most likely include novel technologies such as mRNA-, HIV-derived virus-like particle (VLP)-based and viral vectored vaccines using a variety of different donor viruses.

**AUTHOR CONTRIBUTIONS:**

Conceptualization, Y.v.H.; writing, Y.v.H., S.S., J.F.R. and J.S.; writing—review and editing, Y.v.H., J.S.; visualization, Y.v.H., S.S. and J.F.R.; supervision, J.S.; funding acquisition, J.S. All authors have read and agreed to the published version of the manuscript.

**FUNDING:**

The APC was funded by the German Federal Ministry of Education and Research, funding program Forschung an Fachhochschulen, contract numbers 13FH242PX6 and 13FH767IA6 to J.S.

**ACKNOWLEDGMENTS:**

Figures created with BioRender.com, accessed on 8 February 2022. Adapted from “HIV replication cycle” and “HIV-1 genome and structure”, by BioRender.com (2022). Retrieved from <https://app.biorender.com/biorender-templates>.

**CONFLICTS OF INTEREST:**

J.S. is listed as a co-inventor on patents describing mosaic HIV vaccines. The other authors declare no conflict of interest.

## 5.6 REFERENCES

1. Woolhouse, M.E.J.; Brierley, L. Epidemiological characteristics of human-infective RNA viruses. *Sci. Data* **2018**, *5*, 1–6, doi:10.1038/sdata.2018.17.
2. Zhang, F.; Chase-Topping, M.; Guo, C.G.; van Bunnik, B.A.D.; Brierley, L.; Woolhouse, M.E.J. Global discovery of human-infective RNA viruses: A modelling analysis. *PLoS Pathog.* **2020**, *16*, 1–18, doi:10.1371/journal.ppat.1009079.
3. Tarantola, A. Four thousand years of concepts relating to rabies in animals and humans, its prevention and its cure. *Trop. Med. Infect. Dis.* **2017**, *2*, 5, doi:10.3390/tropicalmed2020005.
4. Galassi, F.M.; Habicht, M.E.; Rühli, F.J. Poliomyelitis in Ancient Egypt? *Neurol. Sci.* **2017**, *38*, 375, doi:10.1007/s10072-016-2720-9.
5. Dick, O.B.; San Martín, J.L.; Montoya, R.H.; Del Diego, J.; Zambrano, B.; Dayan, G.H. Review: The history of dengue outbreaks in the Americas. *Am. J. Trop. Med. Hyg.* **2012**, *87*, 584–593, doi:10.4269/ajtmh.2012.11-0770.
6. Fields, B.N.; Knipe, D.M.; Howley, P.M. *Fields Virology*; 5th ed.; Wolters Kluwer Health/Lippincott Williams & Wilkins: Philadelphia, **1990**; Vol. 113; ISBN 9781451105636.
7. van Doorn, R.H. The epidemiology of emerging infectious diseases and pandemics. In *Medicine*; **2021**; Vol. 49, pp. 659–662.
8. Gallo RC, M.L. The chronology of AIDS research. *Nature* **1987**, *326*, 435–436, doi:10.1038/326435a0.
9. Barré-Sinoussi, F.; Chermann, J.C.; Rey, F.; Nugeyre, M.T.; Chamaret, S.; Gruest, J.; Dautet, C.; Axler-Blin, C.; Vézinet-Brun, F.; Rouzioux, C.; et al. Isolation of a T-Lymphotropic Retrovirus from a Patient at Risk for Acquired Immune Deficiency Syndrome (AIDS). *Science*. **1983**, *220*, 868–871, doi:10.1126/science.6189183.
10. Murphy, K.; Weaver, C. Das erworbene Immunschwächesyndrom (AIDS). In *Janeway Immunologie*; Springer-Spektrum: Berlin, **2018**; pp. 743–749 ISBN 978-3-662-56003-7.
11. WHO HIV/AIDS Available online: <https://www.who.int/news-room/fact-sheets/detail/hiv-aids> (accessed on Oct 19, 2021).
12. Shaw, G.M.; Hunter, E. HIV transmission. *Cold Spring Harb. Perspect. Med.* **2012**, *2*, 1–24, doi:10.1101/cshperspect.a006965.
13. Arts, E.J.; Hazuda, D.J. HIV-1 antiretroviral drug therapy. *Cold Spring Harb. Perspect. Med.* **2012**, *2*, doi:10.1101/cshperspect.a007161.
14. Cassan, E.; Arigon-Chifolleau, A.M.; Mesnard, J.-M.; Gross, A.; Gascuel, O. Concomitant emergence of the antisense protein gene of HIV-1 and of the pandemic. *Proc. Natl. Acad. Sci. U. S. A.* **2016**, *113*, 11537–11542, doi:10.1073/pnas.1605739113.

15. Sertznig, H.; Hillebrand, F.; Erkelenz, S.; Schaal, H.; Widera, M. Behind the scenes of HIV-1 replication: Alternative splicing as the dependency factor on the quiet. *Virology* **2018**, *516*, 176–188, doi:10.1016/j.virol.2018.01.011.
16. Miller, R.H. Human Immunodeficiency Virus May Encode a Novel Protein on the Genomic DNA Plus Strand. *Science* **1988**, *239*, 1420–1422, doi:10.1126/science.3347840.
17. Churchill, M.J.; Cowley, D.J.; Wesselingh, S.L.; Gorry, P.R.; Gray, L.R. HIV-1 transcriptional regulation in the central nervous system and implications for HIV cure research. *J. Neurovirol.* **2015**, *21*, 290–300, doi:10.1007/s13365-014-0271-5.
18. Barboric, M.; Matija Peterlin, B. A new paradigm in eukaryotic biology: HIV Tat and the control of transcriptional elongation. *PLoS Biol.* **2005**, *3*, e76, doi:10.1371/journal.pbio.0030076.
19. Mbondji-Wonje, C.; Dong, M.; Zhao, J.; Wang, X.; Nanfack, A.; Ragupathy, V.; Sanchez, A.M.; Denny, T.N.; Hewlett, I. Genetic variability of the U5 and downstream sequence of major HIV-1 subtypes and circulating recombinant forms. *Sci. Rep.* **2020**, *10*, doi:10.1038/s41598-020-70083-1.
20. Kirchhoff, F. HIV Life Cycle : Overview. In *Encyclopedia of AIDS*; Springer: New York, NY, USA, **2013**, 1–9, doi:10.1007/978-1-4614-9610-6.
21. Li, L.; Li, H.S.; Pauza, C.D.; Bukrinsky, M.; Zhao, R.Y. Roles of HIV-1 auxiliary proteins in viral pathogenesis and host-pathogen interactions. *Cell Res.* **2005**, *15*, 923–934, doi:10.1038/sj.cr.7290370.
22. Das, A.T.; Harwig, A.; Vrolijk, M.M.; Berkhout, B. The TAR Hairpin of Human Immunodeficiency Virus Type 1 Can Be Deleted When Not Required for Tat-Mediated Activation of Transcription. *J. Virol.* **2007**, *81*, 7742–7748, doi:10.1128/jvi.00392-07.
23. Seitz, R. Human Immunodeficiency Virus (HIV). *Transfus. Med. Hemotherapy* **2016**, *43*, 203–222, doi:10.1159/000445852.
24. Harris, R.S.; Hultquist, J.F.; Evans, D.T. The restriction factors of human immunodeficiency virus. *J. Biol. Chem.* **2012**, *287*, 40875–40883, doi:10.1074/jbc.R112.416925.
25. Malim, M.H.; Bieniasz, P.D. HIV restriction factors and mechanisms of evasion. *Cold Spring Harb. Perspect. Med.* **2012**, *2*, 1–16, doi:10.1101/cshperspect.a006940.
26. Lee, W.J.; Fu, R.M.; Liang, C.; Sloan, R.D. IFITM proteins inhibit HIV-1 protein synthesis. *Sci. Rep.* **2018**, 1–16, doi:10.1038/s41598-018-32785-5.
27. Ramdas, P.; Sahu, A.K.; Mishra, T.; Bhardwaj, V.; Chande, A. From Entry to Egress: Strategic Exploitation of the Cellular Processes by HIV-1. *Front. Microbiol.* **2020**, *11*, 559792, doi:10.3389/fmicb.2020.559792.

28. Neil, S.J.D.; Sandrin, V.; Sundquist, W.I.; Bieniasz, P.D. An Interferon- $\alpha$ -Induced Tethering Mechanism Inhibits HIV-1 and Ebola Virus Particle Release but Is Counteracted by the HIV-1 Vpu Protein. *Cell Host Microbe* **2007**, *2*, 193–203, doi:10.1016/j.chom.2007.08.001.
29. McNatt, M.W.; Zang, T.; Bieniasz, P.D. Vpu Binds Directly to Tetherin and Displaces It from Nascent Virions. **2013**, *9*, 40–44, doi:10.1371/journal.ppat.1003299.
30. Stremlau, M.; Perron, M.; Lee, M.; Li, Y.; Song, B.; Javanbakht, H.; Diaz-griffero, F.; Anderson, D.J.; Sundquist, W.I.; Sodroski, J. Specific recognition and accelerated uncoating of retroviral capsids by the TRIM5 $\alpha$  restriction factor. *Proc. Natl. Acad. Sci. USA* **2006**, *103*, 5514–5519.
31. Turner, B.G.; Summers, M.F. Structural biology of HIV 1 Edited by P. E. Wright. *J. Mol. Biol.* **1999**, *285*, 1–32, doi:10.1006/jmbi.1998.2354.
32. Burnie, J.; Guzzo, C. The incorporation of host proteins into the external HIV-1 envelope. *Viruses* **2019**, *11*, 1–25, doi:10.3390/v11010085.
33. Zhu, P.; Liu, J.; Bess, J.; Chertova, E.; Lifson, J.D.; Grisé, H.; Ofek, G.A.; Taylor, K.A.; Roux, K.H. Distribution and three-dimensional structure of AIDS virus envelope spikes. *Nature* **2006**, *441*, 847–852, doi:10.1038/nature04817.
34. Briggs, J.A.G.; Simon, M.N.; Gross, I.; Kräusslich, H.G.; Fuller, S.D.; Vogt, V.M.; Johnson, M.C. The stoichiometry of Gag protein in HIV-1. *Nat. Struct. Mol. Biol.* **2004**, *11*, 672–675, doi:10.1038/nsmb785.
35. Goodsell, D.S. Viral Zone Expasy Available online: <https://viralzone.expasy.org/5182> (accessed on Sep 29, 2021).
36. Engelman, A.; Cherepanov, P. The structural biology of HIV-1: Mechanistic and therapeutic insights. *Nat. Rev. Microbiol.* **2012**, *10*, 279–290, doi:10.1038/nrmicro2747.
37. Kong, R.; Xu, K.; Zhou, T.; Acharya, P.; Lemmin, T.; Liu, K.; Ozorowski, G.; Soto, C.; Taft, J.D.; Bailer, R.T.; et al. Fusion peptide of HIV-1 as a site of vulnerability to neutralizing antibody. *Science* **2016**, *352*, 828–833, doi:10.1126/science.aae0474.
38. Kwong, P.D.; Wyatt, R.; Robinson, J.; Sweet, R.W.; Sodroski, J.; Hendrickson, W.A. Structure of an HIV gp 120 envelope glycoprotein in complex with the CD4 receptor and a neutralizing human antibody. *Nature* **1998**, *393*, 648–659, doi:10.1038/31405.
39. Gallo, S.A.; Finnegan, C.M.; Viard, M.; Raviv, Y.; Dimitrov, A.; Rawat, S.S.; Puri, A.; Durell, S.; Blumenthal, R. The HIV Env-mediated fusion reaction. *Biochim. et Biophys. Acta (BBA) - Biomembr.* **2003**, *1614*, 36–50, doi:10.1016/S0005-2736(03)00161-5.

40. Zila, V.; Margiotta, E.; Turoňová, B.; Müller, T.G.; Zimmerli, C.E.; Mattei, S.; Allegretti, M.; Börner, K.; Rada, J.; Müller, B.; et al. Cone-shaped HIV-1 capsids are transported through intact nuclear pores. *Cell* **2021**, *184*, 1032–1046.e18, doi:10.1016/j.cell.2021.01.025.
41. Dharan, A.; Bachmann, N.; Talley, S.; Zwickelmaier, V.; Campbell, E.M. Nuclear pore blockade reveals that HIV-1 completes reverse transcription and uncoating in the nucleus. *Nat. Microbiol.* **2020**, *5*, 1088–1095, doi:10.1038/s41564-020-0735-8.
42. Burdick, R.C.; Li, C.; Munshi, M.H.; Rawson, J.M.O.; Nagashima, K.; Hu, W.S.; Pathak, V.K. HIV-1 uncoats in the nucleus near sites of integration. *Proc. Natl. Acad. Sci. U. S. A.* **2020**, *117*, 5486–5493, doi:10.1073/pnas.1920631117.
43. Müller, T.G.; Zila, V.; Peters, K.; Schifferdecker, S.; Stanic, M.; Lucic, B.; Laketa, V.; Lusic, M.; Müller, B.; Kräusslich, H.G. Hiv-1 uncoating by release of viral cDNA from capsid-like structures in the nucleus of infected cells. *Elife* **2021**, *10*, 1–32, doi:10.7554/ELIFE.64776.
44. Davis, A.J.; Carr, J.M.; Bagley, C.J.; Powell, J.; Warrilow, D.; Harrich, D.; Burrell, C.J.; Li, P. Human immunodeficiency virus type-1 reverse transcriptase exists as post-translationally modified forms in virions and cells. *Retrovirology* **2008**, *5*, 1–12, doi:10.1186/1742-4690-5-115.
45. Onafuwa-Nuga, A.; Telesnitsky, A. The Remarkable Frequency of Human Immunodeficiency Virus Type 1 Genetic Recombination. *Microbiol. Mol. Biol. Rev.* **2009**, *73*, 451–480, doi:10.1128/mmbr.00012-09.
46. Ruelas, D.S.; Greene, W.C. An Integrated Overview of HIV-1 Latency. *Cell* **2013**, *155*, 519–529, doi:10.1016/j.cell.2013.09.044.
47. Craigie, R.; Bushman, F.D. HIV DNA integration. *Cold Spring Harb. Perspect. Med.* **2012**, *2*, 1–18, doi:10.1101/cshperspect.a006890.
48. Chiu, T.; Davies, D. Structure and Function of HIV-1 Integrase. *Curr. Top. Med. Chem.* **2004**, *4*, 965–977, doi:10.2174/1568026043388547.
49. Pommier, Y.; Pilon, A.A.; Bajaj, K.; Mazumder, A.; Neamati, N. HIV-1 integrase as a target for antiviral drugs. *Antivir. Chem. Chemother.* **1997**, *8*, 463–483, doi:10.1177/095632029700800601.
50. Karn, J.; Stoltzfus, C.M. Transcriptional and Posttranscriptional Regulation of HIV-1 Gene Expression. *Cold Spring Harb. Perspect. Med.* **2012**, *2*, a006916, doi:10.1101/cshperspect.a006916.
51. Dutilleul, A.; Rodari, A.; Van Lint, C. Depicting HIV-1 Transcriptional Mechanisms: A Summary of What We Know. *Viruses* **2020**, *12*, 1385, doi:10.3390/v12121385.

52. Verdikt, R.; Hernalsteens, O.; Van Lint, C. Epigenetic Mechanisms of HIV-1 Persistence. *Vaccines* **2021**, *9*, 514, doi:10.3390/vaccines9050514.
53. Shukla, A.; Ramirez, N.G.P.; D'Orso, I. HIV-1 Proviral Transcription and Latency in the New Era. *Viruses* **2020**, *12*, 555, doi:10.3390/v12050555.
54. Hokello, J.; Lakhikumar Sharma, A.; Tyagi, M. AP-1 and NF- $\kappa$ B synergize to transcriptionally activate latent HIV upon T-cell receptor activation. *FEBS Lett.* **2021**, *595*, 577–594, doi:10.1002/1873-3468.14033.
55. Kharytonchyk, S.; Monti, S.; Smaldino, P.J.; Van, V.; Bolden, N.C.; Brown, J.D.; Russo, E.; Swanson, C.; Shuey, A.; Telesnitsky, A.; et al. Transcriptional start site heterogeneity modulates the structure and function of the HIV-1 genome. *Proc. Natl. Acad. Sci. U. S. A.* **2016**, *113*, 13378–13383, doi:10.1073/pnas.1616627113.
56. Schier, A.C.; Taatjes, D.J. Structure and mechanism of the RNA polymerase II transcription machinery. *Genes Dev.* **2020**, *34*, 465–488, doi:10.1101/gad.335679.119.
57. González-Jiménez, A.; Campos, A.; Navarro, F.; Clemente-Blanco, A.; Calvo, O. Regulation of Eukaryotic RNAPs Activities by Phosphorylation. *Front. Mol. Biosci.* **2021**, *8*, 681865, doi:10.3389/fmolb.2021.681865.
58. Quaresma, A.J.C.; Bugai, A.; Barboric, M. Cracking the control of RNA polymerase II elongation by 7SK snRNP and P-TEFb. *Nucleic Acids Res.* **2016**, *44*, 7527–7539, doi:10.1093/nar/gkw585.
59. Bengal, E.; Aloni, Y. Transcriptional elongation by purified RNA polymerase II is blocked at the trans-activation-responsive region of human immunodeficiency virus type 1 in vitro. *J. Virol.* **1991**, *65*, 4910–4918, doi:10.1128/jvi.65.9.4910-4918.1991.
60. Kao, S.-Y.; Calman, A.F.; Luciw, P.A.; Peterlin, B.M. Anti-termination of transcription within the long terminal repeat of HIV-1 by tat gene product. *Nature* **1987**, *330*, 489–493, doi:10.1038/330489a0.
61. McNamara, R.P.; McCann, J.L.; Gudipaty, S.A.; D'Orso, I. Transcription factors mediate the enzymatic disassembly of promoter-bound 7SK snRNP to locally recruit P-TEFb for transcription elongation. *Cell Rep.* **2013**, *5*, 1256–1268, doi:10.1016/j.celrep.2013.11.003.
62. Li, Y.; Liu, M.; Chen, L.F.; Chen, R. P-TEFb: Finding its ways to release promoter-proximally paused RNA polymerase II. *Transcription* **2018**, *9*, 88–94, doi:10.1080/21541264.2017.1281864.
63. Barboric, M.; Yik, J.H.N.; Czudnochowski, N.; Yang, Z.; Chen, R.; Contreras, X.; Geyer, M.; Peterlin, B.M.; Zhou, Q. Tat



- competes with HEXIM1 to increase the active pool of P-TEFb for HIV-1 transcription. *Nucleic Acids Res.* **2007**, *35*, 2003–2012, doi:10.1093/nar/gkm063.
64. Tantale, K.; Garcia-Oliver, E.; Robert, M.C.; L’Hostis, A.; Yang, Y.; Tsanov, N.; Topno, R.; Gostan, T.; Kozulic-Pirher, A.; Basu-Shrivastava, M.; et al. Stochastic pausing at latent HIV-1 promoters generates transcriptional bursting. *Nat. Commun.* **2021**, *12*, 4508, doi:10.1038/s41467-021-24462-5.
65. Nguyen Quang, N.; Goudey, S.; Ségéral, E.; Mohammad, A.; Lemoine, S.; Blugeon, C.; Versapuech, M.; Paillart, J.C.; Berlioz-Torrent, C.; Emiliani, S.; et al. Dynamic nanopore long-read sequencing analysis of HIV-1 splicing events during the early steps of infection. *Retrovirology* **2020**, *17*, 25, doi:10.1186/s12977-020-00533-1.
66. Emery, A.; Swanstrom, R. HIV-1: To Splice or Not to Splice, That Is the Question. *Viruses* **2021**, *13*, 181, doi:10.3390/v13020181.
67. Bohne, J.; Wodrich, H.; Kräusslich, H.G. Splicing of human immunodeficiency virus RNA is position-dependent suggesting sequential removal of introns from the 5' end. *Nucleic Acids Res.* **2005**, *33*, 825–837, doi:10.1093/nar/gki185.
68. D’Souza, V.; Summers, M.F. How retroviruses select their genomes. *Nat. Rev. Microbiol.* **2005**, *3*, 643–655, doi:10.1038/nrmicro1210.
69. Obayashi, C.M.; Shinohara, Y.; Masuda, T.; Kawai, G. Influence of the 5'-terminal sequences on the 5'-UTR structure of HIV-1 genomic RNA. *Sci. Rep.* **2021**, *11*, 10920, doi:10.1038/s41598-021-90427-9.
70. Esquiaqui, J.M.; Kharytonchuk, S.; Drucker, D.; Telesnitsky, A. HIV-1 spliced RNAs display transcription start site bias. *RNA* **2020**, *26*, 708–714, doi:10.1261/rna.073650.119.
71. Toro-Ascuy, D.; Rojas-Araya, B.; Valiente-Echeverría, F.; Soto-Rifo, R. Interactions between the HIV-1 unspliced mRNA and host mRNA decay machineries. *Viruses* **2016**, *8*, 320, doi:10.3390/v8110320.
72. Bresson, S.; Tollervey, D. Surveillance-ready transcription: Nuclear RNA decay as a default fate. *Open Biol.* **2018**, *8*, 170270, doi:10.1098/rsob.170270.
73. Nawroth, I.; Mueller, F.; Basyuk, E.; Beerens, N.; Rahbek, U.L.; Darzacq, X.; Bertrand, E.; Kjems, J.; Schmidt, U. Stable assembly of HIV-1 export complexes occurs cotranscriptionally. *RNA* **2014**, *20*, 1–8, doi:10.1261/rna.038182.113.
74. Malim, M.H.; Emerman, M. HIV-1 Accessory Proteins—Ensuring Viral Survival in a Hostile Environment. *Cell Host Microbe* **2008**, *3*, 388–398, doi:10.1016/j.chom.2008.04.008.
75. Faust, T.B.; Binning, J.M.; Gross, J.D.; Frankel, A.D. Making Sense of Multifunctional Proteins: Human Immunodeficiency Virus Type 1 Accessory and Regulatory Proteins and Connections to Transcription. *Annu. Rev. Virol.*

- 2017, 4, 241–260, doi:10.1146/annurev-virology-101416-041654.
76. Li, G.; De Clercq, E. HIV Genome-Wide Protein Associations: a Review of 30 Years of Research. *Microbiol. Mol. Biol. Rev.* **2016**, *80*, 679–731, doi:10.1128/MMBR.00065-15.
77. Jacks, T.; Powert, M.D.; Masiarz, F.R.; Luciw, P.A.; Barr, P.J.; Varmus, H.E. Characterization of ribosomal frameshifting in HIV-1 gag-pol expression. *Nature* **1988**, *331*, 280–283, doi:10.1038/331280a0.
78. Murphy, R.E.; Saad, J.S. The interplay between HIV-1 Gag binding to the plasma membrane and Env incorporation. *Viruses* **2020**, *12*, 548, doi:10.3390/v12050548.
79. Brown, J.D.; Kharytonchyk, S.; Chaudry, I.; Iyer, A.S.; Carter, H.; Becker, G.; Desai, Y.; Glang, L.; Choi, S.H.; Singh, K.; et al. Structural basis for transcriptional start site control of HIV-1 RNA fate. *Science*. **2020**, *368*, 413–417, doi:10.1126/science.aaz7959.
80. Ding, P.; Kharytonchyk, S.; Kuo, N.; Cannistraci, E.; Flores, H.; Chaudhary, R.; Sarkar, M.; Dong, X.; Telesnitsky, A.; Summers, M.F. 5'-Cap sequestration is an essential determinant of HIV-1 genome packaging. *Proc. Natl. Acad. Sci. U. S. A.* **2021**, *118*, e2112475118, doi:10.1073/pnas.2112475118.
81. Mouhand, A.; Pasi, M.; Catala, M.; Zargarian, L.; Belfetmi, A.; Barraud, P.; Mauffret, O.; Tisné, C. Overview of the nucleic-acid binding properties of the HIV-1 nucleocapsid protein in its different maturation states. *Viruses* **2020**, *12*, 1109, doi:10.3390/v12101109.
82. Zhao, H.; Datta, S.A.K.; Kim, S.H.; To, S.C.; Chaturvedi, S.K.; Rein, A.; Schuck, P. Nucleic acid-induced dimerization of HIV-1 Gag protein. *J. Biol. Chem.* **2019**, *294*, 16480–16493, doi:10.1074/jbc.RA119.010580.
83. Sarni, S.; Biswas, B.; Liu, S.; Olson, E.D.; Kitzrow, J.P.; Rein, A.; Wysocki, V.H.; Musier-Forsyth, K. HIV-1 Gag protein with or without p6 specifically dimerizes on the viral RNA packaging signal. *J. Biol. Chem.* **2020**, *295*, 14391–14401, doi:10.1074/jbc.RA120.014835.
84. Murray, P.S.; Li, Z.; Wang, J.; Tang, C.L.; Honig, B.; Murray, D. Retroviral matrix domains share electrostatic homology: Models for membrane binding function throughout the viral life cycle. *Structure* **2005**, *13*, 1521–1531, doi:10.1016/j.str.2005.07.010.
85. Alfadhli, A.; Still, A.; Barklis, E. Analysis of Human Immunodeficiency Virus Type 1 Matrix Binding to Membranes and Nucleic Acids. *J. Virol.* **2009**, *83*, 12196–12203, doi:10.1128/jvi.01197-09.
86. Gaines, C.R.; Tkacik, E.; Rivera-Oven, A.; Somani, P.; Achimovich, A.; Alabi, T.; Zhu, A.; Getachew, N.; Yang, A.L.; McDonough, M.; et al. HIV-1 Matrix Protein Interactions with tRNA:

- Implications for Membrane Targeting. *J. Mol. Biol.* **2018**, *430*, 2113–2127, doi:10.1016/j.jmb.2018.04.042.
87. Datta, S.A.K.; Heinrich, F.; Raghunandan, S.; Krueger, S.; Curtis, J.E.; Rein, A.; Nanda, H. HIV-1 Gag extension: Conformational changes require simultaneous interaction with membrane and nucleic acid. *J. Mol. Biol.* **2011**, *406*, 205–214, doi:10.1016/j.jmb.2010.11.051.
  88. Chen, S.; Xu, J.; Liu, M.; Rao, A.L.N.; Zandi, R.; Gill, S.S.; Mohideen, U. Investigation of HIV-1 Gag binding with RNAs and lipids using Atomic Force Microscopy. *PLoS One* **2020**, *15*, e0228036, doi:10.1371/journal.pone.0228036.
  89. Mateu, M.G. The capsid protein of human immunodeficiency virus: Intersubunit interactions during virus assembly. *FEBS J.* **2009**, *276*, 6098–6109, doi:10.1111/j.1742-4658.2009.07313.x.
  90. Kondo, E.; Mammano, F.; Cohen, E.A.; Göttlinger, H.G. The p6gag domain of human immunodeficiency virus type 1 is sufficient for the incorporation of Vpr into heterologous viral particles. *J. Virol.* **1995**, *69*, 2759–2764, doi:10.1128/jvi.69.5.2759-2764.1995.
  91. Hurley, J.H.; Cada, A.K. Inside job: How the ESCRTs release HIV-1 from infected cells. *Biochem. Soc. Trans.* **2018**, *46*, 1029–1036, doi:10.1042/BST20180019.
  92. Kleinpeter, A.B.; Freed, E.O. HIV-1 maturation: Lessons learned from inhibitors. *Viruses* **2020**, *12*, 940, doi:10.3390/v12090940.
  93. Pornillos, O.; Ganser-Pornillos, B.K. Maturation of retroviruses. *Curr. Opin. Virol.* **2019**, *36*, 47–55, doi:10.1016/j.coviro.2019.05.004.
  94. Blakemore, R.J.; Burnett, C.; Swanson, C.; Kharytonchuk, S.; Telesnitsky, A.; Munro, J.B. Stability and conformation of the dimeric HIV-1 genomic RNA 5'UTR. *Biophys. J.* **2021**, *120*, 1–17, doi:10.1016/j.bpj.2021.09.017.
  95. Murakami, T.; Ablan, S.; Freed, E.O.; Tanaka, Y. Regulation of Human Immunodeficiency Virus Type 1 Env-Mediated Membrane Fusion by Viral Protease Activity. *J. Virol.* **2004**, *78*, 1026–1031, doi:10.1128/jvi.78.2.1026-1031.2004.
  96. Elcheva, I.A.; Spiegelman, V.S. The role of cis- and trans-acting RNA regulatory elements in leukemia. *Cancers (Basel)*. **2020**, *12*, 1–30, doi:10.3390/cancers12123854.
  97. Ranum, L.P.W.; Cooper, T.A. RNA-mediated neuromuscular disorders. *Annu. Rev. Neurosci.* **2006**, *29*, 259–277, doi:10.1146/annurev.neuro.29.051605.113014.
  98. Mirkin, S.M. Expandable DNA repeats and human disease. *Nature* **2007**, *447*, 932–940, doi:10.1038/nature05977.
  99. Heinz, A.; Nabariya, D.K.; Krauss, S. Huntingtin and Its Role in Mechanisms of RNA-Mediated Toxicity. *Toxins (Basel)*. **2021**, *13*,

- 487, doi:10.3390/toxins13070487.
100. Kim, W.; Kim, D.Y.; Lee, K.H. Rna-binding proteins and the complex pathophysiology of als. *Int. J. Mol. Sci.* **2021**, *22*, 1–18, doi:10.3390/ijms22052598.
  101. Garcia-Moreno, M.; Noerenberg, M.; Ni, S.; Järvelin, A.I.; González-Almela, E.; Lenz, C.E.; Bach-Pages, M.; Cox, V.; Avolio, R.; Davis, T.; et al. System-wide Profiling of RNA-Binding Proteins Uncovers Key Regulators of Virus Infection. *Mol. Cell* **2019**, *74*, 196–211.e11, doi:10.1016/j.molcel.2019.01.017.
  102. Das, A.T.; Vrolijk, M.M.; Harwig, A.; Berkhout, B. Opening of the TAR hairpin in the HIV-1 genome causes aberrant RNA dimerization and packaging. *Retrovirology* **2012**, *9*, 1–12, doi:10.1186/1742-4690-9-59.
  103. Fernandes, J.D.; Jayaraman, B.; Frankel, A.D. The HIV-1 Rev response element. *RNA Biol.* **2012**, *9*, 6–11, doi:10.4161/rna.9.1.18178.
  104. Ajasin, D.; Eugenin, E.A. HIV-1 Tat: Role in Bystander Toxicity. *Front. Cell. Infect. Microbiol.* **2020**, *10*, 1–15, doi:10.3389/fcimb.2020.00061.
  105. Fujii, R.; Okamoto, M.; Aratani, S.; Oishi, T.; Ohshima, T.; Taira, K.; Baba, M.; Fukamizu, A.; Nakajima, T. A Role of RNA Helicase A in cis-Acting Transactivation Response Element-mediated Transcriptional Regulation of Human Immunodeficiency Virus Type 1. *J. Biol. Chem.* **2001**, *276*, 5445–5451, doi:10.1074/jbc.M006892200.
  106. Gerena, Y.; Menéndez-Delmestre, R.; Delgado-Nieves, A.; Vélez, J.; Méndez-Álvarez, J.; Sierra-Pagan, J.E.; Skolasky, R.L.; Henderson, L.; Nath, A.; Wojna, V. Release of Soluble Insulin Receptor From Neurons by Cerebrospinal Fluid From Patients With Neurocognitive Dysfunction and HIV Infection. *Front. Neurol.* **2019**, *10*, 1–9, doi:10.3389/fneur.2019.00285.
  107. Moir, S.; Chun, T.-W.; Fauci, A.S. Pathogenic Mechanisms of HIV Disease. *Annu. Rev. Pathol. Mech. Dis.* **2011**, *6*, 223–248, doi:10.1146/annurev-pathol-011110-130254.
  108. Deeks, S.G.; Overbaugh, J.; Phillips, A.; Buchbinder, S. HIV infection. *Nat. Rev. Dis. Prim.* **2015**, *1*, 15035, doi:10.1038/nrdp.2015.35.
  109. Cesarman, E.; Damania, B.; Krown, S.E.; Martin, J.; Bower, M.; Whitby, D. Kaposi sarcoma. *Nat. Rev. Dis. Prim.* **2019**, *5*, doi:10.1038/s41572-019-0060-9.
  110. Justiz Vaillant, A.A.; Naik, R. HIV-1 Associated Opportunistic Infections Available online: <http://www.ncbi.nlm.nih.gov/pubmed/30969609> (accessed on Oct 21, 2021).
  111. U.S. Department of Health & Human Services Global Statistics Available online: <https://www.hiv.gov/hiv-basics/overview/data-and-trends/global-statistics> (accessed on Oct 21, 2021).

112. Maenza, J.; Flexner, C. Combination antiretroviral therapy for HIV infection. *Am. Fam. Physician* **1998**, *57*, 2789–98.
113. Warnke, D.; Barreto, J.; Temesgen, Z. Therapeutic review: Antiretroviral drugs. *J. Clin. Pharmacol.* **2007**, *47*, 1570–1579, doi:10.1177/0091270007308034.
114. Panel on Antiretroviral Guidelines for Adults and Adolescents. Guidelines for the Use of Antiretroviral Agents in Adults and Adolescents with HIV. Accessed [2021 Oct 25]. *Dep. Heal. Hum. Serv.*
115. U.S. Department of Health & Human Services FDA-Approved HIV Medicines Available online: <https://hivinfo.nih.gov/understanding-hiv/fact-sheets/fda-approved-hiv-medicines> (accessed on Oct 21, 2021).
116. Qi, B.; Fang, Q.; Liu, S.; Hou, W.; Li, J.; Huang, Y.; Shi, J. Advances of CCR5 antagonists: From small molecules to macromolecules. *Eur. J. Med. Chem.* **2020**, *208*, 112819, doi:10.1016/j.ejmech.2020.112819.
117. Jamjian, M.C.; McNicholl, I.R. Enfuvirtide: First fusion inhibitor for treatment of HIV infection. *Am. J. Heal. Pharm.* **2004**, *61*, 1242–1247, doi:10.1093/ajhp/61.12.1242.
118. Meanwell, N.A.; Krystal, M.R.; Nowicka-Sans, B.; Langley, D.R.; Conlon, D.A.; Eastgate, M.D.; Grasela, D.M.; Timmins, P.; Wang, T.; Kadow, J.F. Inhibitors of HIV-1 Attachment: The Discovery and Development of Teme savir and its Prodrug Fostemsavir. *J. Med. Chem.* **2018**, *61*, 62–80, doi:10.1021/acs.jmedchem.7b01337.
119. Beccari, M. V.; Mogle, B.T.; Sidman, E.F.; Mastro, K.A.; Asiago-Reddy, E.; Kufel, W.D. Ibalizumab, a Novel Monoclonal Antibody for the Management of Multidrug-Resistant HIV-1 Infection. *Antimicrob. Agents Chemother.* **2019**, *63*, 1–12, doi:10.1128/AAC.00110-19.
120. Kemnic, T.R.; Gulick, P.G. HIV Antiretroviral Therapy Available online: <http://www.ncbi.nlm.nih.gov/pubmed/30020680> (accessed on Oct 21, 2021).
121. Ghosh, R.K.; Ghosh, S.M.; Chawla, S. Recent advances in antiretroviral drugs. *Expert Opin. Pharmacother.* **2011**, *12*, 31–46, doi:10.1517/14656566.2010.509345.
122. Adamson, C.S. Protease-Mediated Maturation of HIV: Inhibitors of Protease and the Maturation Process. *Mol. Biol. Int.* **2012**, *2012*, 604261, doi:10.1155/2012/604261.
123. Palella, F.J.; Delaney, K.M.; Moorman, A.C.; Loveless, M.O.; Fuhrer, J.; Satten, G.A.; Aschman, D.J.; Holmberg, S.D. Declining Morbidity and Mortality among Patients with Advanced Human Immunodeficiency Virus Infection. *N. Engl. J. Med.* **1998**, *338*, 853–860, doi:10.1056/NEJM199803263381301.
124. Moore, R.D.; Chaisson, R.E. Natural history of HIV infection in the era of combination

- antiretroviral therapy. *Aids* **1999**, *13*, 1933–1942, doi:10.1097/00002030-199910010-00017.
125. Cohen, M.S.; Chen, Y.Q.; McCauley, M.; Gamble, T.; Hosseinipour, M.C.; Kumarasamy, N.; Hakim, J.G.; Kumwenda, J.; Grinsztejn, B.; Pilotto, J.H.S.; et al. Prevention of HIV-1 Infection with Early Antiretroviral Therapy. *N. Engl. J. Med.* **2011**, *365*, 493–505, doi:10.1056/NEJMoa1105243.
126. Cohen, M.S.; Chen, Y.Q.; McCauley, M.; Gamble, T.; Hosseinipour, M.C.; Kumarasamy, N.; Hakim, J.G.; Kumwenda, J.; Grinsztejn, B.; Pilotto, J.H.S.; et al. Antiretroviral Therapy for the Prevention of HIV-1 Transmission. *N. Engl. J. Med.* **2016**, *375*, 830–839, doi:10.1056/nejmoa1600693.
127. Thomas, R.; Galanakis, C.; Vézina, S.; Longpré, D.; Boissonnault, M.; Huchet, E.; Charest, L.; Murphy, D.; Trottier, B.; Machouf, N. Adherence to Post-Exposure Prophylaxis (PEP) and Incidence of HIV Seroconversion in a Major North American Cohort. *PLoS One* **2015**, *10*, e0142534, doi:10.1371/journal.pone.0142534.
128. Rey, D. Post-exposure prophylaxis for HIV infection. *Expert Rev. Anti. Infect. Ther.* **2011**, *9*, 431–442, doi:10.1586/eri.11.20.
129. Mohri, H.; Singh, M.K.; Ching, W.T.W.; Ho, D.D. Quantitation of zidovudine-resistant human immunodeficiency virus type 1 in the blood of treated and untreated patients. *Proc. Natl. Acad. Sci.* **1993**, *90*, 25–29, doi:10.1073/pnas.90.1.25.
130. Kirschner, D.E.; Webb, G.F. Understanding drug resistance for monotherapy treatment of HIV infection. *Bull. Math. Biol.* **1997**, *59*, 763–785, doi:10.1007/BF02458429.
131. Pennings, P.S. HIV drug resistance: problems and perspectives. *Infect. Dis. Rep.* **2013**, *5*, 5, doi:10.4081/idr.2013.s1.e5.
132. Richman, D.D. HIV drug resistance. *Annu. Rev. Pharmacol. Toxicol.* **1993**, *33*, 149–164, doi:10.1146/annurev.pharmtox.33.1.149.
133. Dau, B.; Holodniy, M. Novel targets for antiretroviral therapy: Clinical progress to date. *Drugs* **2009**, *69*, 31–50, doi:10.2165/00003495-200969010-00003.
134. Cunha, R.F.; Simões, S.; Carvalheiro, M.; Pereira, J.M.A.; Costa, Q.; Ascenso, A. Novel Antiretroviral Therapeutic Strategies for HIV. *Molecules* **2021**, *26*, 5305, doi:10.3390/molecules26175305.
135. Cutrell, A.G.; Schapiro, J.M.; Perno, C.F.; Kuritzkes, D.R.; Quercia, R.; Patel, P.; Polli, J.W.; Dorey, D.; Wang, Y.; Wu, S.; et al. Exploring predictors of HIV-1 virologic failure to long-acting cabotegravir and rilpivirine: a multivariable analysis. *AIDS* **2021**, *35*, 1333–1342, doi:10.1097/QAD.0000000000000283.

136. Rizzardini, G.; Overton, E.T.; Orkin, C.; Swindells, S.; Arasteh, K.; Górgolas Hernández-Mora, M.; Pokrovsky, V.; Girard, P.-M.; Oka, S.; Andrade-Villanueva, J.F.; et al. Long-Acting Injectable Cabotegravir + Rilpivirine for HIV Maintenance Therapy: Week 48 Pooled Analysis of Phase 3 ATLAS and FLAIR Trials. *JAIDS J. Acquir. Immune Defic. Syndr.* **2020**, *85*, 498–506, doi:10.1097/QAI.0000000000002466.
137. Li, X.-D.; Liu, L.; Cheng, L. Identification of thienopyridine carboxamides as selective binders of HIV-1 trans Activation Response (TAR) and Rev Response Element (RRE) RNAs. *Org. Biomol. Chem.* **2018**, *16*, 9191–9196, doi:10.1039/C8OB02753F.
138. Chavali, S.S.; Mali, S.M.; Jenkins, J.L.; Fasan, R.; Wedekind, J.E. Co-crystal structures of HIV TAR RNA bound to lab-evolved proteins show key roles for arginine relevant to the design of cyclic peptide TAR inhibitors. *J. Biol. Chem.* **2020**, *295*, 16470–16486, doi:10.1074/jbc.RA120.015444.
139. Melidis, L.; Styles, I.B.; Hannon, M.J. Targeting structural features of viral genomes with a nano-sized supramolecular drug. *Chem. Sci.* **2021**, *12*, 7174–7184, doi:10.1039/D1SC00933H.
140. Sobic, A.; Olivato, G.; Carraro, C.; Göttlich, R.; Fabris, D.; Gatto, B. Bis-3-Chloropiperidines Targeting TAR RNA as A Novel Strategy to Impair the HIV-1 Nucleocapsid Protein. *Molecules* **2021**, *26*, 1874, doi:10.3390/molecules26071874.
141. Dai, Y.; Wynn, J.E.; Peralta, A.N.; Sherpa, C.; Jayaraman, B.; Li, H.; Verma, A.; Frankel, A.D.; Le Grice, S.F.; Santos, W.L. Discovery of a Branched Peptide That Recognizes the Rev Response Element (RRE) RNA and Blocks HIV-1 Replication. *J. Med. Chem.* **2018**, *61*, 9611–9620, doi:10.1021/acs.jmedchem.8b01076.
142. Medina-Trillo, C.; Sedgwick, D.M.; Herrera, L.; Beltrán, M.; Moreno, Á.; Barrio, P.; Bedoya, L.M.; Alcamí, J.; Fustero, S.; Gallego, J. Nucleic acid recognition and antiviral activity of 1,4-substituted terphenyl compounds mimicking all faces of the HIV-1 Rev protein positively-charged  $\alpha$ -helix. *Sci. Rep.* **2020**, *10*, 7190, doi:10.1038/s41598-020-64120-2.
143. Dietz, J.; Koch, J.; Kaur, A.; Raja, C.; Stein, S.; Grez, M.; Pustowka, A.; Mensch, S.; Ferner, J.; Möller, L.; et al. Inhibition of HIV-1 by a Peptide Ligand of the Genomic RNA Packaging Signal  $\Psi$ . *ChemMedChem* **2008**, *3*, 749–755, doi:10.1002/cmdc.200700194.
144. Warui, D.M.; Baranger, A.M. Identification of specific small molecule ligands for stem loop 3 ribonucleic acid of the packaging signal  $\Psi$  of human immunodeficiency virus-1. *J. Med. Chem.* **2009**, *52*, 5462–5473, doi:10.1021/jm900599v.
145. Ingemarsdotter, C.K.; Zeng, J.; Long, Z.; Lever, A.M.L.; Kenyon, J.C. An RNA-binding compound

- that stabilizes the HIV-1 gRNA packaging signal structure and specifically blocks HIV-1 RNA encapsidation. *Retrovirology* **2018**, *15*, 25, doi:10.1186/s12977-018-0407-4.
146. Eakle, R.; Venter, F.; Rees, H. Pre-exposure prophylaxis (PrEP) in an era of stalled HIV prevention: Can it change the game? *Retrovirology* **2018**, *15*, 1–10, doi:10.1186/s12977-018-0408-3.
  147. Frank, T.D.; Carter, A.; Jahagirdar, D.; Biehl, M.H.; Douwes-Schultz, D.; Larson, S.L.; Arora, M.; Dwyer-Lindgren, L.; Steuben, K.M.; Abbastabar, H.; et al. Global, regional, and national incidence, prevalence, and mortality of HIV, 1980–2017, and forecasts to 2030, for 195 countries and territories: a systematic analysis for the Global Burden of Diseases, Injuries, and Risk Factors Study 2017. *Lancet HIV* **2019**, *6*, e831–e859, doi:10.1016/S2352-3018(19)30196-1.
  148. Assessing Global HIV Targets in PEPFAR Countries: A Dashboard Available online: <https://www.kff.org/global-health-policy/issue-brief/assessing-global-hiv-targets-in-pepfar-countries-a-dashboard/#> (accessed on Oct 21, 2021).
  149. UNAIDS Joint United Nations Programme on HIV/AIDS 90-90-90 An ambitious treatment target to help end the AIDS epidemic. *United Nations* **2014**, 40.
  150. Joulaei, H.; Shooshtarian, S.; Dianatinasab, M. Is UNAIDS 90-90-90 Target a Dream or a Reality for Middle East and North Africa Region on Ending the AIDS Epidemic? A Review Study. *Aids Rev.* **2019**, *20*, 83–93, doi:10.24875/AIDSRev.M18000020.
  151. Porter, K.; Gourlay, A.; Attawell, K.; Hales, D.; Supervie, V.; Touloumi, G.; Rosinska, M.; Vourli, G.; van Sighem, A.; Pharris, A.; et al. Substantial Heterogeneity in Progress Toward Reaching the 90-90-90 HIV Target in the WHO European Region. *JAIDS J. Acquir. Immune Defic. Syndr.* **2018**, *79*, 28–37, doi:10.1097/QAI.0000000000001761.
  152. Schackman, B.R.; Fleishman, J.A.; Su, A.E.; Berkowitz, B.K.; Moore, R.D.; Walensky, R.P.; Becker, J.E.; Voss, C.; Paltiel, A.D.; Weinstein, M.C.; et al. The lifetime medical cost savings from preventing HIV in the United States. *Med. Care* **2015**, *53*, 293–301, doi:10.1097/MLR.0000000000000308.
  153. McCann, N.C.; Horn, T.H.; Hyle, E.P.; Walensky, R.P. HIV Antiretroviral Therapy Costs in the United States, 2012–2018. *JAMA Intern. Med.* **2020**, *180*, 601–603, doi:10.1001/jamainternmed.2019.7108.
  154. Davey, R.T.; Bhat, N.; Yoder, C.; Chun, T.-W.; Metcalf, J.A.; Dewar, R.; Natarajan, V.; Lempicki, R.A.; Adelsberger, J.W.; Miller, K.D.; et al. HIV-1 and T cell dynamics after interruption of highly active



- antiretroviral therapy (HAART) in patients with a history of sustained viral suppression. *Proc. Natl. Acad. Sci.* **1999**, *96*, 15109–15114, doi:10.1073/pnas.96.26.15109.
155. Hamers, R.L.; Rinke de Wit, T.F.; Holmes, C.B. HIV drug resistance in low-income and middle-income countries. *Lancet HIV* **2018**, *5*, e588–e596, doi:10.1016/S2352-3018(18)30173-5.
  156. Bandera, A.; Gori, A.; Clerici, M.; Sironi, M. Phylogenies in ART: HIV reservoirs, HIV latency and drug resistance. *Curr. Opin. Pharmacol.* **2019**, *48*, 24–32, doi:10.1016/j.coph.2019.03.003.
  157. Tran, H.; Saleem, K.; Lim, M.; Chow, E.P.F.; Fairley, C.K.; Terris-Prestholt, F.; Ong, J.J. Global estimates for the lifetime cost of managing HIV. *AIDS* **2021**, *35*, 1273–1281, doi:10.1097/QAD.00000000000002887.
  158. Robinson, H.L. HIV/AIDS Vaccines: 2018. *Clin. Pharmacol. Ther.* **2018**, *104*, 1062–1073, doi:10.1002/cpt.1208.
  159. Cohn, L.B.; Chomont, N.; Deeks, S.G. The Biology of the HIV-1 Latent Reservoir and Implications for Cure Strategies. *Cell Host Microbe* **2020**, *27*, 519–530, doi:10.1016/j.chom.2020.03.014.
  160. Douek, D.C.; Kwong, P.D.; Nabel, G.J. The rational design of an AIDS vaccine. *Cell* **2006**, *124*, 677–681, doi:10.1016/j.cell.2006.02.005.
  161. Larijani MS, Sadat SM, R.A. HIV-1 Immune evasion: The main obstacle toward a successful vaccine. *Arch. Asthma, Allergy Immunol.* **2018**, *2*, 013–015, doi:10.29328/journal.aaai.1001013.
  162. Rolland, M. HIV-1 immune evasion—a threat to effective vaccines? *Nat. Med.* **2016**, *22*, 580–581, doi:10.1038/nm.4119.
  163. Perez, C.L.; Milush, J.M.; Buggert, M.; Eriksson, E.M.; Larsen, M. V.; Liegler, T.; Hartogensis, W.; Bacchetti, P.; Lund, O.; Hecht, F.M.; et al. Targeting of Conserved Gag-Epitopes in Early HIV Infection Is Associated with Lower Plasma Viral Load and Slower CD4 + T Cell Depletion. *AIDS Res. Hum. Retroviruses* **2013**, *29*, 602–612, doi:10.1089/aid.2012.0171.
  164. Kiepiela, P.; Ngumbela, K.; Thobakgale, C.; Ramduth, D.; Honeyborne, I.; Moodley, E.; Reddy, S.; De Pierres, C.; Mncube, Z.; Mkhwanazi, N.; et al. CD8+ T-cell responses to different HIV proteins have discordant associations with viral load. *Nat. Med.* **2007**, *13*, 46–53, doi:10.1038/nm1520.
  165. Guha, D.; Ayyavoo, V. Innate Immune Evasion Strategies by Human Immunodeficiency Virus Type 1. *ISRN AIDS* **2013**, *2013*, 1–10, doi:10.1155/2013/954806.
  166. Blankson, J.N.; Persaud, D.; Siliciano, R.F. The Challenge of Viral Reservoirs in HIV-1 Infection. *Annu. Rev. Med.* **2002**, *53*, 557–593, doi:10.1146/annurev.med.53.082901.104024.

167. Tomaras, G.D.; Haynes, B.F. HIV-1-specific antibody responses during acute and chronic HIV-1 infection. *Curr. Opin. HIV AIDS* **2009**, *4*, 373–379, doi:10.1097/COH.0b013e32832f00c0.
168. Overbaugh, J.; Morris, L. The Antibody Response against HIV-1. *Cold Spring Harb. Perspect. Med.* **2012**, *2*, a007039–a007039, doi:10.1101/cshperspect.a007039.
169. Wyatt, R.; Kwong, P.D.; Desjardins, E.; Sweet, R.W.; Robinson, J.; Hendrickson, W.A.; Sodroski, J.G. The antigenic structure of the HIV gp120 envelope glycoprotein. *Nature* **1998**, *393*, 705–711, doi:10.1038/31514.
170. Ward, A.B.; Wilson, I.A. The HIV-1 envelope glycoprotein structure: nailing down a moving target. *Immunol. Rev.* **2017**, *275*, 21–32, doi:10.1111/imr.12507.
171. Harada, S.; Yoshimura, K. Driving HIV-1 into a Vulnerable corner by taking advantage of viral adaptation and evolution. *Front. Microbiol.* **2017**, *8*, 390, doi:10.3389/fmicb.2017.00390.
172. Hraber, P.; Seaman, M.S.; Bailer, R.T.; Mascola, J.R.; Montefiori, D.C.; Korber, B.T. Prevalence of broadly neutralizing antibody responses during chronic HIV-1 infection. *AIDS* **2014**, *28*, 163–169, doi:10.1097/QAD.0000000000000106.
173. Doores, K.J. The HIV glycan shield as a target for broadly neutralizing antibodies. *FEBS J.* **2015**, *282*, 4679–4691, doi:10.1111/febs.13530.
174. Sok, D.; Burton, D.R. Recent progress in broadly neutralizing antibodies to HIV. *Nat. Immunol.* **2018**, *19*, 1179–1188, doi:10.1038/s41590-018-0235-7.
175. Binley, J.M.; Wrin, T.; Korber, B.; Zwick, M.B.; Wang, M.; Chappey, C.; Stiegler, G.; Kunert, R.; Zolla-Pazner, S.; Katinger, H.; et al. Comprehensive Cross-Clade Neutralization Analysis of a Panel of Anti-Human Immunodeficiency Virus Type 1 Monoclonal Antibodies. *J. Virol.* **2004**, *78*, 13232–13252, doi:10.1128/JVI.78.23.13232-13252.2004.
176. Gray, E.S.; Moore, P.L.; Choge, I.A.; Decker, J.M.; Bibollet-Ruche, F.; Li, H.; Leseka, N.; Treurnicht, F.; Mlisana, K.; Shaw, G.M.; et al. Neutralizing Antibody Responses in Acute Human Immunodeficiency Virus Type 1 Subtype C Infection. *J. Virol.* **2007**, *81*, 6187–6196, doi:10.1128/JVI.00239-07.
177. Gorny, M.K.; Conley, A.J.; Karwowska, S.; Buchbinder, A.; Xu, J.Y.; Emini, E.A.; Koenig, S.; Zolla-Pazner, S. Neutralization of diverse human immunodeficiency virus type 1 variants by an anti-V3 human monoclonal antibody. *J. Virol.* **1992**, *66*, 7538–7542, doi:10.1128/jvi.66.12.7538-7542.1992.
178. Walker, L.M.; Phogat, S.K.; Chan-Hui, P.-Y.; Wagner, D.; Phung, P.; Goss, J.L.; Wrin, T.; Simek, M.D.; Fling, S.; Mitcham, J.L.; et al. Broad

- and Potent Neutralizing Antibodies from an African Donor Reveal a New HIV-1 Vaccine Target. *Science*. **2009**, *326*, 285–289, doi:10.1126/science.1178746.
179. Woldemeskel, B.A.; Kwaa, A.K.; Blankson, J.N. Viral reservoirs in elite controllers of HIV-1 infection: Implications for HIV cure strategies. *EBioMedicine* **2020**, *62*, 103118, doi:10.1016/j.ebiom.2020.103118.
  180. Deeks, S.G.; Walker, B.D. Human Immunodeficiency Virus Controllers: Mechanisms of Durable Virus Control in the Absence of Antiretroviral Therapy. *Immunity* **2007**, *27*, 406–416, doi:10.1016/j.immuni.2007.08.010.
  181. Walker, B.D.; Yu, X.G. Unravelling the mechanisms of durable control of HIV-1. *Nat. Rev. Immunol.* **2013**, *13*, 487–498, doi:10.1038/nri3478.
  182. Baker, B.; Block, B.; Rothchild, A.; Walker, B. Elite control of HIV infection: implications for vaccine design. *Expert Opin. Biol. Ther.* **2009**, *9*, 55–69, doi:10.1517/14712590802571928.
  183. Jiang, C.; Lian, X.; Gao, C.; Sun, X.; Einkauf, K.B.; Chevalier, J.M.; Chen, S.M.Y.; Hua, S.; Rhee, B.; Chang, K.; et al. Distinct viral reservoirs in individuals with spontaneous control of HIV-1. *Nature* **2020**, *585*, 261–267, doi:10.1038/s41586-020-2651-8.
  184. Barouch, D.H. Challenges in the development of an HIV-1 vaccine. *Nature* **2008**, *455*, 613–619, doi:10.1038/nature07352.
  185. Cohen, K.W.; Frahm, N. Current views on the potential for development of a HIV vaccine. *Expert Opin. Biol. Ther.* **2017**, *17*, 295–303, doi:10.1080/14712598.2017.1282457.
  186. Zolla-Pazner, S. Identifying epitopes of HIV-1 that induce protective antibodies. *Nat. Rev. Immunol.* **2004**, *4*, 199–210, doi:10.1038/nri1307.
  187. Pantophlet, R.; Burton, D.R. GP120: Target for Neutralizing HIV-1 Antibodies. *Annu. Rev. Immunol.* **2006**, *24*, 739–769, doi:10.1146/annurev.immunol.24.021605.090557.
  188. Mascola, J.R.; Montefiori, D.C. The Role of Antibodies in HIV Vaccines. *Annu. Rev. Immunol.* **2010**, *28*, 413–444, doi:10.1146/annurev-immunol-030409-101256.
  189. Burton, D.R.; Hangartner, L. Broadly Neutralizing Antibodies to HIV and Their Role in Vaccine Design. *Annu. Rev. Immunol.* **2016**, *34*, 635–659, doi:10.1146/annurev-immunol-041015-055515.
  190. Saphire, E.O.; Parren, P.W.H.I.; Pantophlet, R.; Zwick, M.B.; Morris, G.M.; Rudd, P.M.; Dwek, R.A.; Stanfield, R.L.; Burton, D.R.; Wilson, I.A. Crystal Structure of a Neutralizing Human IgG Against HIV-1: A Template for Vaccine Design. *Science*. **2001**, *293*, 1155–1159, doi:10.1126/science.1061692.
  191. Ghosn, J.; Taiwo, B.; Seedat, S.; Autran, B.; Katlama, C. HIV. *Lancet* **2018**, *392*, 685–697,

- doi:10.1016/S0140-6736(18)31311-4.
192. Zagury D, Léonard R, Fouchard M, Réveil B, Bernard J, Ittelé D, Cattan A, Zirimwabagabo L, Kalumbu M, Justin W, et al. Immunization against AIDS in humans. *Nature* **1987**, *326*, 249–250, doi:10.1038/326249a0.
  193. Hatzioannou, T.; T. Evans, D. Animal models for HIV/AIDS research. *Nat Rev Microbiol.* **2015**, *10*, 852–867, doi:10.1038/nrmicro2911.Animal.
  194. Policicchio, B.B.; Pandrea, I.; Apetrei, C. Animal Models for HIV Cure Research. *Front. Immunol.* **2016**, *7*, 1–15, doi:10.3389/fimmu.2016.00012.
  195. Van Rompay, K.K.A. Tackling HIV and AIDS: Contributions by non-human primate models. *Lab Anim. (NY)*. **2017**, *46*, 259–270, doi:10.1038/labani.1279.
  196. Ng'uni, T.; Chasara, C.; Ndhlovu, Z.M. Major Scientific Hurdles in HIV Vaccine Development: Historical Perspective and Future Directions. *Front. Immunol.* **2020**, *11*, 1–17, doi:10.3389/fimmu.2020.590780.
  197. Esparza, J. A brief history of the global effort to develop a preventive HIV vaccine. *Vaccine* **2013**, *31*, 3502–3518, doi:10.1016/j.vaccine.2013.05.018.
  198. Rerks-Ngarm, S.; Pitisuttithum, P.; Nitayaphan, S.; Kaewkungwal, J.; Chiu, J.; Paris, R.; Premisri, N.; Namwat, C.; de Souza, M.; Adams, E.; et al. Vaccination with ALVAC and AIDSVAX to Prevent HIV-1 Infection in Thailand. *N. Engl. J. Med.* **2009**, *361*, 2209–2220, doi:10.1056/NEJMoa0908492.
  199. Pitisuttithum, P.; Rerks-Ngarm, S.; Bussaratid, V.; Dhitavat, J.; Maekanantawat, W.; Pungpak, S.; Suntharasamai, P.; Vanijanonta, S.; Nitayapan, S.; Kaewkungwal, J.; et al. Safety and Reactogenicity of Canarypox ALVAC-HIV (vCP1521) and HIV-1 gp120 AIDSVAX B/E Vaccination in an Efficacy Trial in Thailand. *PLoS One* **2011**, *6*, e27837, doi:10.1371/journal.pone.0027837.
  200. Zolla-Pazner, S.; DeCamp, A.; Gilbert, P.B.; Williams, C.; Yates, N.L.; Williams, W.T.; Howington, R.; Fong, Y.; Morris, D.E.; Soderberg, K.A.; et al. Vaccine-Induced IgG Antibodies to V1V2 Regions of Multiple HIV-1 Subtypes Correlate with Decreased Risk of HIV-1 Infection. *PLoS One* **2014**, *9*, e87572, doi:10.1371/journal.pone.0087572.
  201. Karasavvas, N.; Billings, E.; Rao, M.; Williams, C.; Zolla-Pazner, S.; Bailer, R.T.; Koup, R.A.; Madnote, S.; Arworn, D.; Shen, X.; et al. The Thai Phase III HIV Type 1 Vaccine Trial (RV144) Regimen Induces Antibodies That Target Conserved Regions Within the V2 Loop of gp120. *AIDS Res. Hum. Retroviruses* **2012**, *28*, 1444–1457, doi:10.1089/aid.2012.0103.
  202. Lin, L.; Finak, G.; Ushey, K.; Seshadri, C.; Hawn, T.R.; Frahm, N.; Scriba, T.J.; Mahomed, H.; Hanekom, W.; Bart, P.A.; et al. COMPASS identifies T-cell subsets

- correlated with clinical outcomes. *Nat. Biotechnol.* **2015**, *33*, 610–616, doi:10.1038/nbt.3187.
203. Haynes, B.F.; Gilbert, P.B.; McElrath, M.J.; Zolla-Pazner, S.; Tomaras, G.D.; Alam, S.M.; Evans, D.T.; Montefiori, D.C.; Karnasuta, C.; Sutthent, R.; et al. Immune-Correlates Analysis of an HIV-1 Vaccine Efficacy Trial. *N. Engl. J. Med.* **2012**, *366*, 1275–1286, doi:10.1056/NEJMoa1113425.
204. Rerks-Ngarm, S.; Pitisuttithum, P.; Excler, J.-L.; Nitayaphan, S.; Kaewkungwal, J.; Prensri, N.; Kunasol, P.; Karasavvas, N.; Schuetz, A.; Ngauy, V.; et al. Randomized, Double-Blind Evaluation of Late Boost Strategies for HIV-Uninfected Vaccine Recipients in the RV144 HIV Vaccine Efficacy Trial. *J. Infect. Dis.* **2017**, *215*, 1255–1263, doi:10.1093/infdis/jix099.
205. Pitisuttithum, P.; Nitayaphan, S.; Chariyalertsak, S.; Kaewkungwal, J.; Dawson, P.; Dhitavat, J.; Phonrat, B.; Akapirat, S.; Karasavvas, N.; Wiczorek, L.; et al. Late boosting of the RV144 regimen with AIDSVAX B/E and ALVAC-HIV in HIV-uninfected Thai volunteers: a double-blind, randomised controlled trial. *Lancet HIV* **2020**, *7*, e238–e248, doi:10.1016/S2352-3018(19)30406-0.
206. Gray, G.E.; Bekker, L.-G.; Laher, F.; Malahleha, M.; Allen, M.; Moodie, Z.; Grunenber, N.; Huang, Y.; Grove, D.; Prigmore, B.; et al. Vaccine Efficacy of ALVAC-HIV and Bivalent Subtype C gp120–MF59 in Adults. *N. Engl. J. Med.* **2021**, *384*, 1089–1100, doi:10.1056/NEJMoa2031499.
207. Seaman, M.S.; Janes, H.; Hawkins, N.; Grandpre, L.E.; Devoy, C.; Giri, A.; Coffey, R.T.; Harris, L.; Wood, B.; Daniels, M.G.; et al. Tiered Categorization of a Diverse Panel of HIV-1 Env Pseudoviruses for Assessment of Neutralizing Antibodies. *J. Virol.* **2010**, *84*, 1439–1452, doi:10.1128/JVI.02108-09.
208. Fischer, W.; Perkins, S.; Theiler, J.; Bhattacharya, T.; Yusim, K.; Funkhouser, R.; Kuiken, C.; Haynes, B.; Letvin, N.L.; Walker, B.D.; et al. Polyvalent vaccines for optimal coverage of potential T-cell epitopes in global HIV-1 variants. *Nat. Med.* **2007**, *13*, 100–106, doi:10.1038/nm1461.
209. Corey, L.; McElrath, M.J. HIV vaccines: Mosaic approach to virus diversity. *Nat. Med.* **2010**, *16*, 268–270, doi:10.1038/nm0310-268.
210. Barouch, D.H.; O'Brien, K.L.; Simmons, N.L.; King, S.L.; Abbink, P.; Maxfield, L.F.; Sun, Y.H.; La Porte, A.; Riggs, A.M.; Lynch, D.M.; et al. Mosaic HIV-1 vaccines expand the breadth and depth of cellular immune responses in rhesus monkeys. *Nat. Med.* **2010**, *16*, 319–323, doi:10.1038/nm.2089.
211. Santra, S.; Liao, H.X.; Zhang, R.; Muldoon, M.; Watson, S.; Fischer, W.; Theiler, J.; Szinger, J.; Balachandran, H.; Buzby, A.; et al. Mosaic vaccines elicit CD8<sup>+</sup> T lymphocyte responses that confer enhanced immune coverage of diverse HIV strains in monkeys.

- Nat. Med.* **2010**, *16*, 324–328, doi:10.1038/nm.2108.
212. Barouch, D.H.; Tomaka, F.L.; Wegmann, F.; Stieh, D.J.; Alter, G.; Robb, M.L.; Michael, N.L.; Peter, L.; Nkolola, J.P.; Borducchi, E.N.; et al. Evaluation of a mosaic HIV-1 vaccine in a multicentre, randomised, double-blind, placebo-controlled, phase 1/2a clinical trial (APPROACH) and in rhesus monkeys (NHP 13-19). *Lancet* **2018**, *392*, 232–243, doi:10.1016/S0140-6736(18)31364-3.
213. Sanders, R.W.; Derking, R.; Cupo, A.; Julien, J.-P.; Yasmeen, A.; de Val, N.; Kim, H.J.; Blattner, C.; de la Peña, A.T.; Korzun, J.; et al. A Next-Generation Cleaved, Soluble HIV-1 Env Trimer, BG505 SOSIP.664 gp140, Expresses Multiple Epitopes for Broadly Neutralizing but Not Non-Neutralizing Antibodies. *PLoS Pathog.* **2013**, *9*, e1003618, doi:10.1371/journal.ppat.1003618.
214. Sanders, R.W.; Van Gils, M.J.; Derking, R.; Sok, D.; Ketas, T.J.; Burger, J.A.; Ozorowski, G.; Cupo, A.; Simonich, C.; Goo, L.; et al. HIV-1 neutralizing antibodies induced by native-like envelope trimers. *Science*. **2015**, *349*, doi:10.1126/science.aac4223.
215. A Study to Assess the Efficacy of a Heterologous Prime/Boost Vaccine Regimen of Ad26.Mos4.HIV and Aluminum Phosphate-Adjuvanted Clade C gp140 in Preventing Human Immunodeficiency Virus (HIV) -1 Infection in Women in Sub-Saharan Africa [NCT03060629] Available online: <https://clinicaltrials.gov/ct2/show/NCT03060629> (accessed on Oct 21, 2021).
216. Johnson & Johnson and Global Partners Announce Results from Phase 2b Imbokodo HIV Vaccine Clinical Trial in Young Women in Sub-Saharan Africa Available online: <https://www.janssen.com/johnson-johnson-and-global-partners-announce-results-phase-2b-imbokodo-hiv-vaccine-clinical-trial> (accessed on Oct 21, 2021).
217. A Study of Heterologous Vaccine Regimen of Adenovirus Serotype 26 Mosaic4 Human Immunodeficiency Virus(Ad26.Mos4.HIV), Adjuvanted Clade C gp140 and Mosaic gp140 to Prevent HIV-1 Infection Among Cis-gender Men and Transgender Individuals Who Have Sex With Available online: <https://clinicaltrials.gov/ct2/show/NCT03964415> (accessed on Oct 29, 2021).

## 6 SUMMARY & OUTLOOK

The optimization of biotechnological processes to produce gene therapeutics consists of many laborious, cost- and time-intensive developmental steps. Currently a more streamlined upstreaming process from transient to stable productions is urgently needed. In a first proof-of-concept study and to advance the previous published work of Berg et al. 2019 [93], suspension 293-F cells were co-transfected using a SB100X transposase-encoding plasmid and hybrid transposon-MLV/MSCV-derived packaging, envelope and transfer vector components. After only three weeks of selection, the polyclonal suspension VPC, called VPC-MSCV-EGFP, stably produced ecotropic MLV-based retroviral vectors in serum-free medium. The transduction efficiencies of the vectors were successfully tested in mouse fibroblasts, myeloblasts as well as in preclinical relevant murine bone marrow-derived HSPCs. Functional titers were tenfold higher than previously reported titers of ecotropic MLV vectors produced in stable suspension WIL-2 cells, reaching up to  $1.4 \times 10^7$  TU/mL [94]. In addition, the transduction efficiency of up to 37 % in murine HSPCs at an MOI of 6 after one round of transduction was comparable or even higher to transduction efficiencies of ecotropic MLV vectors transiently produced in adherent Phoenix-Eco cells [95]. For stability testing and larger-scale productions, the VPC culture volume was successfully scaled up to 100 mL in shake flasks and vector harvests were concentrated 20-fold using ultrafiltration devices. Although a first-generation transfer vector was utilized, no generation of RCRs was detected employing RT- and marker rescue-assays. After stable transfection of the transfer vector however, a homologous recombination event within the genomes of the transduced target cells was detected. The utilized transfer vector contained an untranslated region of the *gag* sequence downstream of  $\Psi$  sharing homology with the *gag* sequence of the packaging construct. Thus, full length *gag* sequences were packaged and stably transduced at low frequencies into the target cells within a range of 10–100 copies per 10,000 cell genomes. The removal or codon optimization of the *gag* sequence will be of utility for future transfer vector designs [96]. This study was published in collaboration with the Paul-Ehrlich-Institute in Langen in the *Journal of Virological Methods* in 2021. In addition, to prepare for a fully automated production in a bioreactor, the VPC was successfully scaled up in collaboration with the Max-Planck-Institute for Dynamic of complex technical systems in Magdeburg in an automated perfusion high-density reactor, holding promise for future industrial scale productions (the manuscript is presently under review with the Springer Journal: *Applied Microbiology and Biotechnology* and not published yet).

In a second study the transposition technology using the SB100X transposase was optimized. Therefore, the plasmid-based transposase construct was exchanged with an *in vitro* transcribed transposase mRNA-transcript. A key technical step was the co-transfection of the transposase-encoding mRNA into the packaging cells using PEI at optimized ratios [97]. Since no plasmid-based transposase was co-transfected and possibly stably integrated within the host cell genome, the risk of potential remobilization events of the transposon-viral donor vectors within the genome of the VPC was greatly reduced. In addition, the transposase could be used as an mRNA transcript in a 1:1 ratio (transposase to donor vector) without risking overproduction inhibition (OPI) resulting from long-term expression of the transposase [98]. Here, three stable ecotropic MLV-based VPCs were compared. The stable MLV-Gag-, Pol- and ecotropic MLV (PVC-211) Env-expressing suspension VPC, called MuPACK.e was established and stably transfected with (1) a plasmid-based *egfp* and *neo<sup>R</sup>* encoding transfer vector, (2) a plasmid-encoding transposase and the transposon-based transfer vector encoding the same genes (3) a mRNA-encoding transposase and the transposon-based transfer vector. The latter polyclonal VPC was named MuPACK.e.SB-LEGFP-N1<sub>mRNA</sub> and was able to generate 10-fold higher functional titers as compared to the two other VPCs and five-fold higher to communicated titers of the VPC-MSCV-EGFP. Functional titers in NIH/3T3 cells reached up to  $5 \times 10^7$  TU/mL. The produced functional titers were also tenfold superior to previously communicated vector titers produced by VPCs generated with comparable technologies using a hybrid MLV-*piggyBac* transposon system [99,100].

To prepare for a high cell density experiment in an STR in collaboration with the Max-Planck-Institute for Dynamic of complex technical systems in Magdeburg, the VPC was successfully expanded to  $1.5 \times 10^7$  cells/mL in an adapted culture medium called Dynamis™, being four times higher than in Freestyle™ expression medium. This finding led to a first STR cultivation over 10 days resulting in satisfactory VPC viabilities and functional titers in NIH/3T3 target cells as well as in stable production parameters, such as pH and osmolality. In summary, the described application of the SB100X transposase as mRNA transcripts in combination with transposon-viral donor plasmids was demonstrated superior to simple plasmid transfections or plasmid-based transposase transpositions. This should allow a more streamlined and rapid production of different kinds of pseudotyped viral vectors harboring different transfer vectors or envelope proteins of choice within only three weeks. In addition, the Dynamis™ medium should facilitate future high-density productions of viral vectors under current good manufacturing practice (cGMP) in fully automated bioreactors. Today's production of clinical grade RVVs in adherent and transient transfected VPCs



only allows the production of gene therapeutics at single doses. Using STRs instead, many doses could be collected over a period of months, thus massively lowering the costs [82]. The here described suspension-based VPC provided scalability from laboratory size to an industrial STR size and should also foster the acceleration of the subsequent downstream processes to purify the continuously harvested viral vectors using for example perfusion filtration systems [101,102]. This study was published in *Frontiers in Bioengineering and Biotechnology* in 2023.

In future applications the choice and design of the transfer vector will be of great importance as the viral LTRs as well as strong promoters are mainly responsible for activation of neighboring genes, especially proto-oncogenes. In this thesis, a first generation transfer vector was utilized without SIN-LTRs, resulting in homologous recombination of the *psi-gag* sequences within the VPC and bearing the risk of RCR formation. For future transfer vector designs, the remaining *gag* sequences next to the viral packaging signal should be codon-optimized or removed to eliminate homologous recombination [96]. Moreover, SIN-LTRs should be employed, lowering the risk of RCR formation within the VPC, as well as eliminating the risk of LTR enhancer activities inducing proto-oncogenes [103–105]. Next to the utilization of SIN-transfer vectors, a safer integration site away from proto-oncogenes within the host cell genome should be preferred.  $\gamma$ -RVs preferentially integrate close to transcriptional start sites (TSS), e.g., gene regulatory elements such as promoters and enhancers. The genomic integration sites of RVs as well as LVs are mainly dependent on host-cell cofactors. These proteins, known as tetherin restriction factors, bind to the viral integrase as well as chromatin target sites [9]. To target a safer integration site, the viral integrase can be modified. The interaction site of a tethering cofactor within the C-terminal domain of the viral integrase can be removed and replaced with chromatin-binding peptides targeting integrations sites distant to gene regulatory elements. In previous studies, viral productivities as well as transgene expressions were not hampered and no genotoxic effects in hematopoietic stem cells were observed [106]. Recent *in vitro* and *in vivo* pre-clinical studies however implicate that retroviral vectors with altered IN do not fully exclude TSS integration sites. Future pre-clinical studies must evaluate this risk [9,107].

Apart from the utilization of a safer transfer vector and packaging construct, pseudotyping of future clinical grade vectors is key for efficient transgene delivery into different kinds of human target cells. Different envelope proteins show altered gene transfer efficacies depending on the target cell population. The envelope proteins of MLV-4070A, RD114 or GaLV would be of first choice for a stable suspension VPC

[56,87,104,108,109]. These envelope proteins are known to efficiently pseudotype the retroviral particles providing stability in human sera and during ultracentrifugation, ultrafiltration or freeze-thaw cycles and being non-cytotoxic. Using these envelopes, high VPC productivities and high functional titers can be achieved in clinically relevant human target cells [77,87,109]. These pseudotyped RVVs could then be used to deliver clinically relevant transgenes (e.g., functional genes, CARs, tumor-associated antigens (TAAs) or suicide genes) into appropriate patient-derived target cells such as HSPCs and human lymphocytes [2,110].

For effective long-term gene therapy, three essential points need to be fulfilled: (1) stable and efficient delivery of the transgene into the specific target cells, (2) long-term expression of the transgene and (3) minimal secondary side effects caused by the viral vector due to immune reactions or proto-oncogene activations [10]. RVVs still play a key role in many gene therapy applications and researchers are evaluating novel safety measures, e.g., better vector designs, conditional gene expressions, selectable and/or inducible gene expression, insulator elements or weaker promoters to reduce the risk of surrounding promoter/enhancer effects of neighboring genes and the use of LTR or IN mutations [29,37]. This thesis helped to get one step forward to optimize rapid stable VPC establishments and respective upstreaming in serum-free media. However, further studies with clinically relevant RV-, Ad-, AAV- and LV-based vectors are needed to proof its applicability [111].

## 7 REFERENCES

1. Shahryari, A.; Burtscher, I.; Nazari, Z.; Lickert, H. Engineering Gene Therapy: Advances and Barriers. *Adv Ther (Weinh)* **2021**, *4*, 2100040, doi:10.1002/ADTP.202100040.
2. Bulcha, J.T.; Wang, Y.; Ma, H.; Tai, P.W.L.; Gao, G. Viral Vector Platforms within the Gene Therapy Landscape. *Signal Transduct Target Ther* **2021**, *6*.
3. Landhuis, E. The Definition of Gene Therapy Has Changed. *Nature* **2021**, doi:10.1038/d41586-021-02736-8.
4. Ramamoorth, M.; Narvekar, A. Non Viral Vectors in Gene Therapy - An Overview. *Journal of Clinical and Diagnostic Research* **2015**, *9*, GE01–GE06, doi:10.7860/JCDR/2015/10443.5394.
5. Stephen, S.L.; Montini, E.; Sivanandam, V.G.; Al-Dhalimy, M.; Kestler, H.A.; Finegold, M.; Grompe, M.; Kochanek, S. Chromosomal Integration of Adenoviral Vector DNA In Vivo . *J Virol* **2010**, *84*, 9987–9994, doi:10.1128/jvi.00751-10.
6. Baum, C.; Düllmann, J.; Li, Z.; Fehse, B.; Meyer, J.; Williams, D.A.; Von Kalle, C. Side Effects of Retroviral Gene Transfer into Hematopoietic Stem Cells. *Blood* **2003**, *101*, 2099–2114.
7. Verdera, H.C.; Kuranda, K.; Mingozi, F. AAV Vector Immunogenicity in Humans: A Long Journey to Successful Gene Transfer. *Molecular Therapy* **2020**, *28*, 723, doi:10.1016/J.YMTHE.2019.12.010.
8. Howarth, J.L.; Lee, Y.B.; Uney, J.B. Using Viral Vectors as Gene Transfer Tools (Cell Biology and Toxicology Special Issue: ETCS-UK 1 Day Meeting on Genetic Manipulation of Cells). *Cell Biol Toxicol* **2010**, *26*, 1–20, doi:10.1007/s10565-009-9139-5.
9. Yoder, K.E.; Rabe, A.J.; Fishel, R.; Larue, R.C. Strategies for Targeting Retroviral Integration for Safer Gene Therapy: Advances and Challenges. *Front Mol Biosci* **2021**, *8*.
10. Lundstrom, K. Viral Vectors in Gene Therapy: Where Do We Stand in 2023? **2023**, doi:10.3390/v15030698.
11. Mann, R.; Mulligan, R.C.; Baltimore, D. Construction of a Retrovirus Packaging Mutant and Its Use to Produce Helper-Free Defective Retrovirus. *Cell* **1983**, *33*, 153–159, doi:10.1016/0092-8674(83)90344-6.
12. Wei, C.M.; Gibson, M.; Spear, P.G.; Scolnick, E.M. Construction and Isolation of a Transmissible Retrovirus Containing the Src Gene of Harvey Murine Sarcoma Virus and the Thymidine Kinase Gene of Herpes Simplex Virus Type 1. *J Virol* **1981**, *39*, 935–944, doi:10.1128/jvi.39.3.935-944.1981.
13. Shimotohno, K.; Temin, H.M. Formation of Infectious Progeny Virus after Insertion of Herpes Simplex Thymidine Kinase Gene into DNA of an Avian Retrovirus. *Cell* **1981**, *26*, 67–77, doi:10.1016/0092-8674(81)90034-9.
14. Hwang, L.H.; Gilboa, E. Expression of Genes Introduced into Cells by Retroviral Infection Is More Efficient than That of Genes Introduced into Cells by DNA Transfection. *J Virol* **1984**, *50*, 417–424, doi:10.1128/jvi.50.2.417-424.1984.
15. Sinn, P.L.; Sauter, S.L.; McCray, P.B. Gene Therapy Progress and Prospects: Development of Improved Lentiviral and Retroviral Vectors – Design, Biosafety, and Production. *Gene Ther*

- 2005, 12, 1089–1098, doi:10.1038/sj.gt.3302570.
16. Modlich, U.; Bohne, J.; Schmidt, M.; Von Kalle, C.; Knöss, S.; Schambach, A.; Baum, C. Cell-Culture Assays Reveal the Importance of Retroviral Vector Design for Insertional Genotoxicity. *Blood* **2006**, *108*, 2545, doi:10.1182/BLOOD-2005-08-024976.
  17. Thomas, C.E.; Ehrhardt, A.; Kay, M.A. Progress and Problems with the Use of Viral Vectors for Gene Therapy. *Nature Reviews Genetics* **2003**, *4*, 346–358, doi:10.1038/nrg1066.
  18. Barquinero, J.; Eixarch, H.; Pérez-Melgosa, M. Retroviral Vectors: New Applications for an Old Tool. *Gene Ther* **2004**, *11*, S3–S9, doi:10.1038/sj.gt.3302363.
  19. MacLachlan, N.J.; Dubovi, E.J.; Barthold, S.W.; Swayne, D.E.; Winton, J.R. *Fenner's Veterinary Virology: Fifth Edition*; Elsevier Inc., 2016; ISBN 9780128009468.
  20. Kurth, R.; Bannert, N. *Retroviruses*; Kurth, R., Bannert, N., Eds.; Caister Academic Press: Norfolk, UK, 2010; ISBN 978-1-904455-55-4.
  21. Rosenberg, S.A.; Aebersold, P.; Cornetta, K.; Kasid, A.; Morgan, R.A.; Moen, R.; Karson, E.M.; Lotze, M.T.; Yang, J.C.; Topalian, S.L.; et al. Gene Transfer into Humans – Immunotherapy of Patients with Advanced Melanoma, Using Tumor-Infiltrating Lymphocytes Modified by Retroviral Gene Transduction. *New England Journal of Medicine* **1990**, *323*, 570–578, doi:10.1056/NEJM199008303230904.
  22. Anderson, W.F. Human Gene Therapy. *Science (1979)* **1992**, *256*, 808–813, doi:10.1126/science.256.5058.808.
  23. Blaese, R.M.; Culver, K.W.; Miller, A.D.; Carter, C.S.; Fleisher, T.; Clerici, M.; Shearer, G.; Chang, L.; Chiang, Y.; Tolstoshev, P.; et al. T Lymphocyte-Directed Gene Therapy for ADA-SCID: Initial Trial Results after 4 Years. *Science (1979)* **1995**, *270*, 475–480, doi:10.1126/science.270.5235.475.
  24. Li, Z.; Düllmann, J.; Schiedlmeier, B.; Schmidt, M.; Von Kalle, C.; Meyer, J.; Forster, M.; Stocking, C.; Wahlers, A.; Frank, O.; et al. Murine Leukemia Induced by Retroviral Gene Marking. *Science (1979)* **2002**, *296*, 497, doi:10.1126/SCIENCE.1068893.
  25. Hacein-Bey-Abina, S.; Von Kalle, C.; Schmidt, M.; McCormack, M.P.; Wulffraat, N.; Leboulch, P.; Lim, A.; Osborne, C.S.; Pawliuk, R.; Morillon, E.; et al. *LMO2-Associated Clonal T Cell Proliferation in Two Patients after Gene Therapy for SCID-X1*; 2003;
  26. Hacein-Bey-Abina, S.; Garrigue, A.; Wang, G.P.; Soulier, J.; Lim, A.; Morillon, E.; Clappier, E.; Caccavelli, L.; Delabesse, E.; Beldjord, K.; et al. Insertional Oncogenesis in 4 Patients after Retrovirus-Mediated Gene Therapy of SCID-X1. *J Clin Invest* **2008**, *118*, 3132–3142, doi:10.1172/JCI35700.
  27. Howe, S.J.; Mansour, M.R.; Schwarzwaelder, K.; Bartholomae, C.; Hubank, M.; Kempinski, H.; Brugman, M.H.; Pike-Overzet, K.; Chatters, S.J.; De Ridder, D.; et al. Insertional Mutagenesis Combined with Acquired Somatic Mutations Causes Leukemogenesis Following Gene Therapy of SCID-X1 Patients. *Journal of Clinical Investigation* **2008**, *118*, 3143–3150, doi:10.1172/JCI35798.
  28. Cavazzana-Calvo, M.; Hacein-Bey, S.; De Saint Basile, G.; Gross, F.; Yvon, E.; Nusbaum, P.; Selz, F.; Hue, C.; Certain, S.; Casanova, J.L.; et al. Gene Therapy of

- Human Severe Combined Immunodeficiency (SCID)-X1 Disease. *Science (1979)* **2000**, *288*, 669–672, doi:10.1126/science.288.5466.669.
29. Sinn, P.L.; Sauter, S.L.; McCray, P.B. Gene Therapy Progress and Prospects: Development of Improved Lentiviral and Retroviral Vectors - Design, Biosafety, and Production. *Gene Ther* **2005**, *12*, 1089–1098.
  30. Volkova, N.A.; Fomina, E.G.; Smolnikova, V. V.; Zinovieva, N.A.; Fomin, I.K. The U3 Region of Moloney Murine Leukemia Virus Contains Position-Independent Cis-Acting Sequences Involved in the Nuclear Export of Full-Length Viral Transcripts. *J Biol Chem* **2014**, *289*, 20158, doi:10.1074/JBC.M113.545855.
  31. Hacein-Bey-Abina, S.; Pai, S.-Y.; Gaspar, H.B.; Armant, M.; Berry, C.C.; Blanche, S.; Bleesing, J.; Blondeau, J.; de Boer, H.; Buckland, K.F.; et al. A Modified  $\gamma$ -Retrovirus Vector for X-Linked Severe Combined Immunodeficiency. *New England Journal of Medicine* **2014**, *371*, 1407–1417, doi:10.1056/NEJMoa1404588.
  32. Cavazzana, M.; Six, E.; Lagresle-Peyrou, C.; André-Schmutz, I.; Hacein-Bey-Abina, S. Gene Therapy for X-Linked Severe Combined Immunodeficiency: Where Do We Stand? *Hum Gene Ther* **2016**, *27*, 108–116, doi:10.1089/hum.2015.137.
  33. Lee, M.Y.H.; Khoury, G.; Olshansky, M.; Sonza, S.; Carter, G.P.; McMahon, J.; Stinear, T.P.; Turner, S.J.; Lewin, S.R.; Purcell, D.F.J. Detection of Chimeric Cellular: HIV MRNAs Generated Through Aberrant Splicing in HIV-1 Latently Infected Resting CD4+ T Cells. *Front Cell Infect Microbiol* **2022**, *12*, 467, doi:10.3389/FCIMB.2022.855290/BIBTEX .
  34. Moiani, A.; Paleari, Y.; Sartori, D.; Mezzadra, R.; Miccio, A.; Cattoglio, C.; Cocchiarella, F.; Lidonnici, M.R.; Ferrari, G.; Mavilio, F. Lentiviral Vector Integration in the Human Genome Induces Alternative Splicing and Generates Aberrant Transcripts. *Journal of Clinical Investigation* **2012**, *122*, 1653–1666, doi:10.1172/JCI61852.
  35. Themis, M.; Waddington, S.N.; Schmidt, M.; von Kalle, C.; Wang, Y.; Al-Allaf, F.; Gregory, L.G.; Nivsarkar, M.; Themis, M.; Holder, M. V.; et al. Oncogenesis Following Delivery of a Nonprimate Lentiviral Gene Therapy Vector to Fetal and Neonatal Mice. *Molecular Therapy* **2005**, *12*, 763–771, doi:10.1016/J.YMTHE.2005.07.358.
  36. Modlich, U.; Navarro, S.; Zychlinski, D.; Maetzig, T.; Knoess, S.; Brugman, M.H.; Schambach, A.; Charrier, S.; Galy, A.; Thrasher, A.J.; et al. Insertional Transformation of Hematopoietic Cells by Self-Inactivating Lentiviral and Gammaretroviral Vectors. *Mol Ther* **2009**, *17*, 1919–1928, doi:10.1038/MT.2009.179.
  37. Zychlinski, D.; Schambach, A.; Modlich, U.; Maetzig, T.; Meyer, J.; Grassman, E.; Mishra, A.; Baum, C. Physiological Promoters Reduce the Genotoxic Risk of Integrating Gene Vectors. *Molecular Therapy* **2008**, *16*, 718–725, doi:10.1038/MT.2008.5.
  38. Hendrie, P.C.; Huo, Y.; Stolitenko, R.B.; Russell, D.W. A Rapid and Quantitative Assay for Measuring Neighboring Gene Activation by Vector Proviruses. *Molecular Therapy* **2008**, *16*, 534–540, doi:10.1038/SJ.MT.6300398.
  39. Vargas, J.E.; Chicaybam, L.; Stein, R.T.; Tanuri, A.; Delgado-Cañedo, A.; Bonamino, M.H. Retroviral Vectors and Transposons for Stable Gene Therapy: Advances, Current Challenges and

- Perspectives. *J Transl Med* **2016**, *14*, 1–15, doi:10.1186/s12967-016-1047-x.
40. John Wileys and Sons LTD Gene Therapy Clinical Trials Worldwide Available online: <https://a873679.fmphost.com/fmi/webd/GTCT> (accessed on 20 April 2023).
  41. Aiuti, A.; Slavin, S.; Aker, M.; Ficara, F.; Deola, S.; Mortellaro, A.; Morecki, S.; Andolfi, G.; Tabucchi, A.; Carlucci, F.; et al. Correction of ADA-SCID by Stem Cell Gene Therapy Combined with Nonmyeloablative Conditioning. *Science (1979)* **2002**, *296*, 2410–2413, doi:10.1126/science.1070104.
  42. Gaspar, H.B.; Thrasher, A.J. Gene Therapy for Severe Combined Immunodeficiencies. *Expert Opin Biol Ther* **2005**, *5*, 1175–1182, doi:10.1517/14712598.5.9.1175.
  43. Howe, S.J.; Mansour, M.R.; Schwarzwaelder, K.; Bartholomae, C.; Hubank, M.; Kempinski, H.; Brugman, M.H.; Pike-Overzet, K.; Chatters, S.J.; De Ridder, D.; et al. Insertional Mutagenesis Combined with Acquired Somatic Mutations Causes Leukemogenesis Following Gene Therapy of SCID-X1 Patients. *Journal of Clinical Investigation* **2008**, *118*, 3143–3150, doi:10.1172/JCI35798.
  44. Boztug, K.; Schmidt, M.; Schwarzer, A.; Banerjee, P.P.; Díez, I.A.; Dewey, R.A.; Böhm, M.; Nowrouzi, A.; Ball, C.R.; Glimm, H.; et al. Stem-Cell Gene Therapy for the Wiskott–Aldrich Syndrome. *New England Journal of Medicine* **2010**, *363*, 1918–1927, doi:10.1056/NEJMoa1003548.
  45. Braun, C.J.; Boztug, K.; Paruzynski, A.; Witzel, M.; Schwarzer, A.; Rothe, M.; Modlich, U.; Beier, R.; Göhring, G.; Steinemann, D.; et al. Gene Therapy for Wiskott–Aldrich Syndrome—Long-Term Efficacy and Genotoxicity. *Sci Transl Med* **2014**, *6*, doi:10.1126/scitranslmed.3007280.
  46. Hacein-Bey Abina, S.; Gaspar, H.B.; Blondeau, J.; Caccavelli, L.; Charrier, S.; Buckland, K.; Picard, C.; Six, E.; Himoudi, N.; Gilmour, K.; et al. Outcome Following Gene Therapy in Patients with Severe Wiskott–Aldrich Syndrome HHS Public Access Author Manuscript. *JAMA* **2015**, *313*, 1550–1563, doi:10.1001/jama.2015.3253.Outcome.
  47. Ferrua, F.; Cicalese, M.P.; Galimberti, S.; Giannelli, S.; Dionisio, F.; Barzaghi, F.; Migliavacca, M.; Bernardo, M.E.; Calbi, V.; Assanelli, A.A.; et al. Lentiviral Haemopoietic Stem/Progenitor Cell Gene Therapy for Treatment of Wiskott–Aldrich Syndrome: Interim Results of a Non-Randomised, Open-Label, Phase 1/2 Clinical Study. *Lancet Haematol* **2019**, *6*, e239–e253, doi:10.1016/S2352-3026(19)30021-3.
  48. Gordon, E.M.; Hall, F.L. Rixin-G, a Targeted Genetic Medicine for Cancer. *Expert Opin Biol Ther* **2010**, *10*, 819–832, doi:10.1517/14712598.2010.481666.
  49. Aiuti, A.; Roncarolo, M.G.; Naldini, L. Gene Therapy for ADA-SCID, the First Marketing Approval of an Ex Vivo Gene Therapy in Europe: Paving the Road for the next Generation of Advanced Therapy Medicinal Products. *EMBO Mol Med* **2017**, *9*, 737–740, doi:10.15252/EMMM.201707573.
  50. Lu, J.; Jiang, G. The Journey of CAR-T Therapy in Hematological Malignancies. *Mol Cancer* **2022**, *21*.
  51. Thompson, A.A.; Walters, M.C.; Kwiatkowski, J.; Rasko, J.E.J.; Ribeil, J.-A.; Hongeng, S.; Magrin, E.; Schiller, G.J.; Payen, E.; Semeraro, M.; et al. Gene Therapy in Patients with Transfusion-Dependent  $\beta$ -Thalassemia. *New England*

- Journal of Medicine* **2018**, *378*, 1479–1493, doi:10.1056/nejmoa1705342.
52. Shahryari, A.; Jazi, M.S.; Mohammadi, S.; Nikoo, H.R.; Nazari, Z.; Hosseini, E.S.; Burtscher, I.; Mowla, S.J.; Lickert, H. Development and Clinical Translation of Approved Gene Therapy Products for Genetic Disorders. *Front Genet* **2019**, *10*, 868, doi:10.3389/FGENE.2019.00868/BIBTEX.
  53. Kurian, K.M.; Watson, C.J.; Wyllie, A.H. Retroviral Vectors. *J Clin Pathol* **2000**, *53*, 173–176, doi:10.1515/9783110808636-002.
  54. Miller, A.D. Retrovirus Packaging Cells. **1990**, *14*, 5–14.
  55. Gammaretrovirus ~ ViralZone Available online: <https://viralzone.expasy.org/67> (accessed on 2 June 2023).
  56. Cone, R.D.; Mulligan, R.C. High-Efficiency Gene Transfer into Mammalian Cells: Generation of Helper-Free Recombinant Retrovirus with Broad Mammalian Host Range. **1984**, *81*, 6349–6353.
  57. Miller, A.D.; Buttimore, C. Redesign of Retrovirus Packaging Cell Lines To Avoid Recombination Leading to Helper Virus Production. *Mol Cell Biol* **1986**, *6*, 2895–2902.
  58. Danos, O.; Mulligan, R.C. Safe and Efficient Generation of Recombinant Retroviruses with Amphotropic and Ecotropic Host Ranges. *Proc Natl Acad Sci U S A* **1988**, *85*, 6460–6464, doi:10.1073/pnas.85.17.6460.
  59. Coroadinha, A.S.; Gama-Norton, L.; Amaral, A.I.; Hauser, H.; Alves, P.M.; Cruz, P.E. *Production of Retroviral Vectors: Review*; 2010; Vol. 10;.
  60. Maetzig, T.; Galla, M.; Baum, C.; Schambach, A. Gammaretroviral Vectors: Biology, Technology and Application. *Viruses* **2011**, *3*, 677–713, doi:10.3390/v3060677.
  61. Brenner, S.; Malech, H.L. Current Developments in the Design of Onco-Retrovirus and Lentivirus Vector Systems for Hematopoietic Cell Gene Therapy. *Biochim Biophys Acta Mol Cell Res* **2003**, *1640*, 1–24, doi:10.1016/S0167-4889(03)00024-7.
  62. Martinez-Salas, E.; Francisco-Velilla, R.; Fernandez-Chamorro, J.; Embarek, A.M. Insights into Structural and Mechanistic Features of Viral IRES Elements. *Front Microbiol* **2018**, *8*, 2629, doi:10.3389/FMICB.2017.02629/BIBTEX.
  63. Higashimoto, T.; Urbinati, F.; Perumbeti, A.; Jiang, G.; Zarzuela, A.; Chang, L.J.; Kohn, D.B.; Malik, P. The Woodchuck Hepatitis Virus Post-Transcriptional Regulatory Element Reduces Readthrough Transcription from Retroviral Vectors. *Gene Therapy* **2007**, *14*, 1298–1304, doi:10.1038/sj.gt.3302979.
  64. Suomalainen, M.; Garoff, H. Incorporation of Homologous and Heterologous Proteins into the Envelope of Moloney Murine Leukemia Virus. *J Virol* **1994**, *68*, 4879–4889, doi:10.1128/jvi.68.8.4879-4889.1994.
  65. Albritton, L.M.; Tseng, L.; Scadden, D.; Cunningham, J.M. A Putative Murine Ecotropic Retrovirus Receptor Gene Encodes a Multiple Membrane-Spanning Protein and Confers Susceptibility to Virus Infection. *Cell* **1989**, *57*, 659–666, doi:10.1016/0092-8674(89)90134-7.
  66. Kozak, C.A. The Mouse “Xenotropic” Gammaretroviruses and Their XPR1 Receptor. *Retrovirology* **2010**, *7*, 101, doi:10.1186/1742-4690-7-101.

67. Van Hoeven, N.S.; Miller, A.D. Use of Different but Overlapping Determinants in a Retrovirus Receptor Accounts for Non-Reciprocal Interference between Xenotropic and Polytopic Murine Leukemia Viruses. *Retrovirology* **2005**, *2*, 76, doi:10.1186/1742-4690-2-76.
68. Schneiderman, R.D.; Farrell, K.B.; Wilson, C.A.; Eiden, M. V The Japanese Feral Mouse Pit1 and Pit2 Homologs Lack an Acidic Residue at Position 550 but Still Function as Gibbon Ape Leukemia Virus Receptors: Implications for Virus Binding Motif. *J Virol* **1996**, *70*, 6982, doi:10.1128/JVI.70.10.6982-6986.1996.
69. Eiden, M. V; Farrell, K.B.; Wilson, C.A. Substitution of a Single Amino Acid Residue Is Sufficient to Allow the Human Amphotropic Murine Leukemia Virus Receptor to Also Function as a Gibbon Ape Leukemia Virus Receptor. *J Virol* **1996**, *70*, 1080–1085, doi:10.1128/JVI.70.2.1080-1085.1996.
70. Livingston, D.M.; Todaro, G.J. Endogenous Type C Virus from a Cat Cell Clone with Properties Distinct from Previously Described Feline Type C Virus. *Virology* **1973**, *53*, 142–151, doi:10.1016/0042-6822(73)90473-X.
71. Wilson, C.A.; Farrell, K.B.; Eiden, M. V Properties of a Unique Form of the Murine Amphotropic Leukemia Virus Receptor Expressed on Hamster Cells. *J Virol* **1994**, *68*, 7697–7703, doi:10.1128/jvi.68.12.7697-7703.1994.
72. Miller, D.G.; Miller, A.D. A Family of Retroviruses That Utilize Related Phosphate Transporters for Cell Entry. *J Virol* **1994**, *68*, 8270–8276, doi:10.1128/jvi.68.12.8270-8276.1994.
73. Barrette, S.; Douglas, J.; Orlic, D.; Anderson, S.M.; Seidel, N.E.; Miller, A.D.; Bodine, D.M. Superior Transduction of Mouse Hematopoietic Stem Cells with 10A1 and VSV-G Pseudotyped Retrovirus Vectors. *Molecular Therapy* **2000**, *1*, 330–338, doi:10.1006/MTHE.2000.0052.
74. Han, J.Y.; Cannon, P.M.; Lai, K.M.; Zhao, Y.; Eiden, M. V; Anderson, W.F. Identification of Envelope Protein Residues Required for the Expanded Host Range of 10A1 Murine Leukemia Virus. *J Virol* **1997**, *71*, 8103–8108, doi:10.1128/jvi.71.11.8103-8108.1997.
75. Nikolic, J.; Belot, L.; Raux, H.; Legrand, P.; Gaudin, Y.; Albertini, A.A. Structural Basis for the Recognition of LDL-Receptor Family Members by VSV Glycoprotein. *Nature Communications* **2018**, *9:1* **2018**, *9*, 1–12, doi:10.1038/s41467-018-03432-4.
76. Tailor, C.S.; Nouri, A.; Lee, C.G.; Kozak, C.; Kabat, D. Cloning and Characterization of a Cell Surface Receptor for Xenotropic and Polytopic Murine Leukemia Viruses. *Proc Natl Acad Sci U S A* **1999**, *96*, 927, doi:10.1073/PNAS.96.3.927.
77. Park, J.; Inwood, S.; Kruthiventi, S.; Jenkins, J.; Shiloach, J.; Betenbaugh, M. Progressing from Transient to Stable Packaging Cell Lines for Continuous Production of Lentiviral and Gammaretroviral Vectors. *Curr Opin Chem Eng* **2018**, *22*, 128–137, doi:10.1016/j.coche.2018.09.007.
78. Ginn, S.L.; Amaya, A.K.; Alexander, I.E.; Edelstein, M.; Abedi, M.R. Gene Therapy Clinical Trials Worldwide to 2017: An Update. *Journal of Gene Medicine* **2018**, *20*.
79. Przybylowski, M.; Hakakha, A.; Stefanski, J.; Hodges, J.; Sadelain, M.; Rivière, I. Production Scale-up and Validation of Packaging Cell Clearance



- of Clinical-Grade Retroviral Vector Stocks Produced in Cell Factories. *Gene Ther* **2006**, *13*, 95–100, doi:10.1038/sj.gt.3302648.
80. Feldman, S.A.; Goff, S.L.; Xu, H.; Black, M.A.; Kochenderfer, J.N.; Johnson, L.A.; Yang, J.C.; Wang, Q.; Parkhurst, M.R.; Cross, S.; et al. Rapid Production of Clinical-Grade Gammaretroviral Vectors in Expanded Surface Roller Bottles Using a “Modified” Step-Filtration Process for Clearance of Packaging Cells. *Hum Gene Ther* **2011**, *22*, 107, doi:10.1089/HUM.2010.064.
  81. Ausubel, L.J.; Hall, C.; Sharma, A.; Shakeley, R.; Lopez, P.; Quezada, V.; Couture, S.; Laderman, K.; McMahon, R.; Huang, P.; et al. Production of CGMP-Grade Lentiviral Vectors. *Bioprocess Int* **2012**, *10*, 32.
  82. van der Loo, J.C.M.; Wright, J.F. Progress and Challenges in Viral Vector Manufacturing. *Hum Mol Genet* **2016**, *25*, R42, doi:10.1093/HMG/DDV451.
  83. Wagner, D.L.; Koehl, U.; Chmielewski, M.; Scheid, C.; Stripecke, R. Review: Sustainable Clinical Development of CAR-T Cells – Switching From Viral Transduction Towards CRISPR-Cas Gene Editing. *Front Immunol* **2022**, *13*, doi:10.3389/fimmu.2022.865424.
  84. Kinsella, T.M.; Nolan, G.P. Episomal Vectors Rapidly and Stably Produce High-Titer Recombinant Retrovirus. *Hum Gene Ther* **1996**, *7*, 1405–1413, doi:10.1089/HUM.1996.7.12-1405.
  85. Doty, R.T.; Sabo, K.M.; Chen, J.; Miller, A.D.; Abkowitz, J.L. An All-Feline Retroviral Packaging System for Transduction of Human Cells. <https://home.liebertpub.com/hum> **2010**, *21*, 1019–1027, doi:10.1089/HUM.2010.032.
  86. Ghani, K.; Cottin, S.; Kamen, A.; Caruso, M. Generation of a High-Titer Packaging Cell Line for the Production of Retroviral Vectors in Suspension and Serum-Free Media. *Gene Ther* **2007**, *14*, 1705–1711, doi:10.1038/sj.gt.3303039.
  87. Ghani, K.; Wang, X.; de Campos-Lima, P.O.; Olszewska, M.; Kamen, A.; Rivière, I.; Caruso, M. Efficient Human Hematopoietic Cell Transduction Using RD114- and GALV-Pseudotyped Retroviral Vectors Produced in Suspension and Serum-Free Media. *Hum Gene Ther* **2009**, *20*, 966–974, doi:10.1089/hum.2009.001.
  88. McClintock, B. Controlling Elements and the Gene. *Cold Spring Harb Symp Quant Biol* **1956**, *21*, 197–216, doi:10.1101/SQB.1956.021.01.017.
  89. Cordaux, R.; Batzer, M.A. The Impact of Retrotransposons on Human Genome Evolution. *Nat Rev Genet* **2009**, *10*, 691, doi:10.1038/NRG2640.
  90. Izsvák, Z.; Ivics, Z. Sleeping Beauty Transposition: Biology and Applications for Molecular Therapy. **2003**, doi:10.1016/j.yymthe.2003.11.009.
  91. Ivics, Z.; Hackett, P.B.; Plasterk, R.H.; Izsvák, Z. Molecular Reconstruction of Sleeping Beauty, a Tc1-like Transposon from Fish, and Its Transposition in Human Cells. *Cell* **1997**, *91*, 501–510, doi:10.1016/S0092-8674(00)80436-5.
  92. Mátés, L.; Chuah, M.K.L.; Belay, E.; Jerchow, B.; Manoj, N.; Acosta-Sanchez, A.; Grzela, D.P.; Schmitt, A.; Becker, K.; Matrai, J.; et al. Molecular Evolution of a Novel Hyperactive Sleeping Beauty Transposase Enables Robust Stable Gene Transfer in Vertebrates. *Nat Genet* **2009**, *41*, 753–761, doi:10.1038/ng.343.
  93. Berg, K.; Schäfer, V.N.; Bartnicki, N.; Eggenschwiler, R.; Cantz, T.; Stütz, J. Rapid Establishment of Stable Retroviral Packaging Cells and Recombinant Susceptible Target Cell Lines

- Employing Novel Transposon Vectors Derived from Sleeping Beauty. *Virology* **2019**, *531*, 40–47, doi:10.1016/j.virol.2019.02.014.
94. Chan, L.M.C.; Coutelle, C.; Themis, M. A Novel Human Suspension Culture Packaging Cell Line for Production of High-Titre Retroviral Vectors. *Gene Ther* **2001**, *8*, 697–703, doi:10.1038/sj.gt.3301456.
95. Li, Z.; Schwieger, M.; Lange, C.; Kraunus, J.; Sun, H.; Van Den Akker, E.; Modlich, U.; Serinsöz, E.; Will, E.; Von Laer, D.; et al. Predictable and Efficient Retroviral Gene Transfer into Murine Bone Marrow Repopulating Cells Using a Defined Vector Dose. *Exp Hematol* **2003**, *31*, 1206–1214, doi:10.1016/j.exphem.2003.08.008.
96. Tareen, S.U.; Nicolai, C.J.; Campbell, D.J.; Flynn, P.A.; Slough, M.M.; Vin, C.D.; Kelley-Clarke, B.; Odegard, J.M.; Robbins, S.H. A Rev-Independent Gag/Pol Eliminates Detectable Psi-Gag Recombination in Lentiviral Vectors. *Biores Open Access* **2013**, *2*, 421, doi:10.1089/BIORES.2013.0037.
97. Tschorn, N.; van Heuvel, Y.; Stitz, J. Transgene Expression and Transposition Efficiency of Two-Component Sleeping Beauty Transposon Vector Systems Utilizing Plasmid or mRNA Encoding the Transposase. *Mol Biotechnol* **2022**, doi:10.1007/s12033-022-00642-6.
98. Grabundzija, I.; Irgang, M.; Mátés, L.; Belay, E.; Matrai, J.; Gogol-Döring, A.; Kawakami, K.; Chen, W.; Ruiz, P.; Chuah, M.K.L.; et al. Comparative Analysis of Transposable Element Vector Systems in Human Cells. *Molecular Therapy* **2010**, *18*, 1200–1209, doi:10.1038/mt.2010.47.
99. Troyanovsky, B.; Bitko, V.; Fouty, B.; Solodushko, V. Simple Viral/Minimal PiggyBac Hybrid Vectors for Stable Production of Self-Inactivating Gamma-Retroviruses. *BMC Res Notes* **2015**, *8*, 379, doi:10.1186/s13104-015-1354-y.
100. Feldman, S.A.; Xu, H.; Black, M.A.; Park, T.S.; Robbins, P.F.; Kochenderfer, J.N.; Morgan, R.A.; Rosenberg, S.A. Use of the Piggy Bac Transposon to Create Stable Packaging Cell Lines for the Production of Clinical-Grade Self-Inactivating  $\gamma$ -Retroviral Vectors. *Hum Gene Ther Methods* **2014**, *25*, 253–260, doi:10.1089/hgtb.2014.071.
101. Wolf, M.W.; Reichl, U. Downstream Processing of Cell Culture-Derived Virus Particles. *Expert Rev Vaccines* **2011**, *10*, 1451, doi:10.1586/ERV.11.111.
102. Hein, M.D.; Chawla, A.; Cattaneo, M.; Kupke, S.Y.; Genzel, Y.; Reichl, U. Cell Culture-Based Production of Defective Interfering Influenza A Virus Particles in Perfusion Mode Using an Alternating Tangential Flow Filtration System. *Appl Microbiol Biotechnol* **2021**, *105*, 7251–7264, doi:10.1007/s00253-021-11561-y.
103. Zufferey, R.; Dull, T.; Mandel, R.J.; Bukovsky, A.; Quiroz, D.; Naldini, L.; Trono, D. Self-Inactivating Lentivirus Vector for Safe and Efficient In Vivo Gene Delivery. *J Virol* **1998**, *72*, 9873, doi:10.1128/JVI.72.12.9873-9880.1998.
104. Morgan, M.A.; Galla, M.; Grez, M.; Fehse, B.; Schambach, A. Retroviral Gene Therapy in Germany with a View on Previous Experience and Future Perspectives. *Gene Ther* **2021**, *28*, 494–512, doi:10.1038/s41434-021-00237-x.
105. Cavazza, A.; Cocchiarella, F.; Bartholomae, C.; Schmidt, M.; Pincelli, C.; Larcher, F.; Mavilio, F. Self-Inactivating MLV Vectors Have a Reduced Genotoxic Profile in Human

- Epidermal Keratinocytes. *Gene Ther* **2013**, *20*, 949–957, doi:10.1038/gt.2013.18.
106. El Ashkar, S.; Van Looveren, D.; Schenk, F.; Vranckx, L.S.; Demeulemeester, J.; De Rijck, J.; Debysen, Z.; Modlich, U.; Gijssbers, R. Engineering Next-Generation BET-Independent MLV Vectors for Safer Gene Therapy. *Mol Ther Nucleic Acids* **2017**, *7*, 231–245, doi:10.1016/j.omtn.2017.04.002.
  107. Loyola, L.; Achuthan, V.; Gilroy, K.; Borland, G.; Kilbey, A.; MacKay, N.; Bell, M.; Hay, J.; Aiyer, S.; Fingerma, D.; et al. Disrupting MLV Integrase: BET Protein Interaction Biases Integration into Quiescent Chromatin and Delays but Does Not Eliminate Tumor Activation in a MYC/Runx2 Mouse Model. *PLoS Pathog* **2019**, *15*, doi:10.1371/journal.ppat.1008154.
  108. Tomás, H.A.; Rodrigues, A.F.; Carrondo, M.J.T.; Coroadinha, A.S. LentiPro26: Novel Stable Cell Lines for Constitutive Lentiviral Vector Production. *Sci Rep* **2018**, *8*, 1–11, doi:10.1038/s41598-018-23593-y.
  109. Sandrin, V.; Boson, B.; Salmon, P.; Gay, W.; Nègre, D.; Le Grand, R.; Trono, D.; Cosset, F.L. Lentiviral Vectors Pseudotyped with a Modified RD114 Envelope Glycoprotein Show Increased Stability in Sera and Augmented Transduction of Primary Lymphocytes and CD34+ Cells Derived from Human and Nonhuman Primates. *Blood* **2002**, *100*, 823–832, doi:10.1182/BLOOD-2001-11-0042.
  110. Sterner, R.C.; Sterner, R.M. CAR-T Cell Therapy: Current Limitations and Potential Strategies. *Blood Cancer J* **2021**, *11*, doi:10.1038/s41408-021-00459-7.
  111. Barquintero, J.; Eixarch, H.; Pérez-Melgosa, M. Retroviral Vectors: New Applications for an Old Tool. *Gene Therapy* **2004**, *11*:1 **2004**, *11*, S3–S9, doi:10.1038/sj.gt.3302363.

## **8 CONFERENCES & POSTER**

### **30<sup>th</sup> Annual Meeting of the Society for Virology; 24<sup>th</sup>-26<sup>th</sup> of March 2021**

#### **Poster Presentation based on the publication:**

**van Heuvel, Y.; Berg, K.; Hirsch, T.; Winn, K.; Modlich, U.; Stitz, J.** Establishment of a novel stable human suspension packaging cell line producing ecotropic retroviral MLV(PVC-211) vectors efficiently transducing murine hematopoietic stem and progenitor cells. *J. Virol. Methods* **2021**, 297, 114243, doi:10.1016/j.jviromet.2021.114243.

### **32<sup>nd</sup> Annual Meeting of the Society for Virology; 28<sup>th</sup>-31<sup>st</sup> of March 2023**

#### **Poster Presentation based on the publication:**

**van Heuvel, Y.; Schatz, S.; Hein, M.; Dogra, T.; Kazenmaier, D.; Tschorn, N.; Genzel, Y.; Stitz, J.** Novel Suspension Retroviral Packaging Cells Generated by Transposition Using Transposase Encoding mRNA Advance Vector Yields and Enable Production in Bioreactors. *Front Bioeng Biotechnol* **2023**, 11, doi:10.3389/fbioe.2023.1076524.

## 9 CURRICULUM VITAE

Name: Yasemin van Heuvel

Birthplace: Hamburg

### EDUCATION

Oct. 2013 – Aug. 2016	Master studies in biology, RWTH Aachen, Germany and ETH Zurich, Switzerland
Oct. 2010 – Oct. 2013	Bachelor studies in biology, RWTH Aachen, Germany
2001 – 2010	High School Diploma, Burgau-Gymnasium Dueren, Germany

### Work Experience

Feb. 2019 – Sep. 2023	Doctorate at Gottfried Wilhelm Leibniz University Hannover, Germany; Prof. Dr. Thomas Scheper in cooperation with TH Koeln, Germany; Prof. Dr. Jörn Stitz
Oct. 2016 – Jan. 2019	Medical Project Coordinator, SYNLAB International GmbH, Munich, Germany
Mar. 2015 – Sep. 2015	Internship at Fraunhofer Center for Molecular Biotechnology (CMB), Newark Delaware, USA

## 10 LIST OF PUBLICATIONS

1. Hein, M.D.; Kazenmaier, D.; **van Heuvel, Y.** (10 %); Dogra, T.; Cattaneo, M.; Kupke, S.; Stitz, J.; Genzel, Y.; Reichl, U. Production of retroviral vectors in continuous high cell density culture. *Applied Microbiology and Biotechnology* 2023, doi: 10.1007/s00253-023-12689-9.
2. **van Heuvel, Y.** (75 %); Schatz, S.; Hein, M.; Dogra, T.; Kazenmaier, D.; Tschorn, N.; Genzel, Y.; Stitz, J. Novel Suspension Retroviral Packaging Cells Generated by Transposition Using Transposase Encoding mRNA Advance Vector Yields and Enable Production in Bioreactors. *Front Bioeng Biotechnol* 2023, 11, doi:10.3389/fbioe.2023.1076524.
3. Tschorn, N.; **van Heuvel, Y.** (20 %); Stitz, J. Transgene Expression and Transposition Efficiency of Two-Component Sleeping Beauty Transposon Vector Systems Utilizing Plasmid or mRNA Encoding the Transposase. *Mol Biotechnol.* 2022, doi: 10.1007/s12033-022-00642-6.
4. **van Heuvel, Y.** (75 %); Schatz, S.; Rosengarten, J.F.; Stitz, J. Infectious RNA: Human Immunodeficiency Virus (HIV) Biology, Therapeutic Intervention, and the Quest for a Vaccine. *Toxins (Basel)*. 2022, 14, doi:10.3390/toxins14020138.
5. **van Heuvel, Y.** (80 %); Berg, K.; Hirsch, T.; Winn, K.; Modlich, U.; Stitz, J. Establishment of a novel stable human suspension packaging cell line producing ecotropic retroviral MLV(PVC-211) vectors efficiently transducing murine hematopoietic stem and progenitor cells. *J. Virol. Methods* 2021, 297, 114243, doi:10.1016/j.jviromet.2021.114243.

### Prior publications to this thesis:

6. Kombrink, A.; Tayyrov, A.; Essig, A.; Stöckli, M.; Micheller, S.; Hintze, J.; **van Heuvel, Y.** (5 %); Dürig, N.; Lin, C.-W.; Kallio, P.T.; et al. Induction of antibacterial proteins and peptides in the coprophilous mushroom *Coprinopsis cinerea* in response to bacteria. *ISME J.* 2019, 13, doi:10.1038/s41396-018-0293-8.
7. Fischbach, F.; Nedelcu, J.; Leopold, P.; Zhan, J.; Clarner, T.; Nellesen, L.; Beißel, C.; **van Heuvel, Y.** (5 %); Goswami, A.; Weis, J.; et al. Cuprizone-induced graded oligodendrocyte vulnerability is regulated by the transcription factor DNA damage-inducible transcript 3. *Glia* 2019, 67, doi:10.1002/glia.23538.
8. Franzoi, M.; **van Heuvel, Y.** (20 %); Thomann, S.; Schürch, N.; Kallio, P.T.; Venier, P.; Essig, A. Structural Insights into the Mode of Action of the Peptide Antibiotic Copsin. *Biochemistry* 2017, 56, doi:10.1021/acs.biochem.7b00697.
9. Goldberg, J.; Daniel, M.; **van Heuvel, Y.** (10 %); Victor, M.; Beyer, C.; Clarner, T.; Kipp, M. Short-term cuprizone feeding induces selective amino acid deprivation with concomitant activation of an integrated stress response in oligodendrocytes. *Cell. Mol. Neurobiol.* 2013, 33, doi:10.1007/s10571-013-9975-y.